NON-INVASIVE PERMEABILITY ASSESSMENT OF HIGH-PERFORMANCE CONCRETE BRIDGE DECK MIXTURES

By

James W. Bryant, Jr

Dissertation submitted to the Faculty of

Virginia Polytechnic Institute and State University

in partial fulfillment of the requirements for the degree of

Doctorate of Philosophy

in

Civil Engineering

APPROVED

Dr. Jesus M. de la Garza	Dr. Richard E. Weyers
(Co-Chairperson)	(Co-Chairperson)

Dr. Richard M. Barker

Dr. William Reynolds

Mr. James Lefter

Keywords: High-Performance Concrete; Concrete Resistivity; Chloride Ion Penetrability; Initial current; Permeability; In-Place Testing

April 2001

Non-Invasive Permeability Assessment of High-Performance Concrete Bridge Deck Mixtures

James W. Bryant, Jr.

Abstract

Concrete construction methods and practices influence the final in-place quality of concrete. A low permeability concrete mixture does not alone ensure quality in-place concrete. If the concrete mixture is not transported, placed and cured properly, it may not exhibit the desired durability and mechanical properties.

This study investigates the in-place permeation properties of low permeability concrete bridge decks mixtures used in the Commonwealth of Virginia. Permeation properties were assessed in both the laboratory and in the field using 4-point Wenner array electrical resistivity, surface air flow (SAF), and chloride ion penetrability (ASTM C 1202-97).

Laboratory test specimens consisted of two concrete slabs having dimensions of 280 x 280 x 102-mm (11 x 11 x 4-in) and twelve 102 x 204-mm (4 x 8-in) cylinders per concrete mixture. Specimens were tested at 7, 28 and 91-days. Thirteen cylinder specimens per concrete mixture underwent standard curing in a saturated limewater bath. The simulated field-curing regimes used wet burlap and plastic sheeting for 3 (3B) and 7 days (7B) respectively and was applied to both slabs and cylinder specimens.

Slab specimen were tested on finished surface using the SAF at 28 and 91 days, and 4-point electrical resistivity measurements at 1, 3, 7, 14, 28 and 91 days. Compressive strength (CS) tests were conducted at 7 and 28 days. Chloride ion penetrability tests were performed at 7, 28, and 91 days.

Statistical analyses were performed to assess the significance of the relationships for the following: Total charge passed and initial current (ASTM C 1202-97); 3B resistivity and 7B resistivity; Slab and cylinder resistivity; Slab resistivity and ASTM C-1202-97 (Total Charge and Initial current); and Surface Air Flow and ASTM C-1202-97.

Field cast specimens, test slabs and cylinders, were cast on-site during concrete bridge deck construction. The slab dimensions were 30.5 x 40.6 x 10.2-cm (12 x 16 x 4 in.), and the cylinders were 10.2 x 20.4-cm (4 x 8-in). In-situ SAF and resistivity measurements were taken on the bridge deck at 14, 42 and 91 days. In-place SAF and resistivity measurements on laboratory field cast slabs were taken at 7, 14 and 28-days. ASTM C 1202-97 specimens were prepared from field cast cylinders and tested at 7 and 28 and 42-days. The relationship between in-place permeation measures from field specimens was compared to laboratory data.

Results indicated no difference in chloride ion penetrability (Figures 7.4 and 7.5) and 28-day compressive strength (Figure 7.2) with regard to differing simulated field curing regimes, for same age testing. There was no significant difference at the 95 % confidence

level between 3B resistivity and 7B resistivity specimens tested at the same age (Figures 7.9 and 7.10).

A well defined relationship was observed between total charge passed and initial current (Figure 7-6). An inverse power function was found to describe the relationship between charge passed/initial current and electrical resistivity for all laboratory mixtures used in this study (Figure 7.17 – 7.22). Field data was used to validate laboratory established models for charge passed/initial current and electrical resistivity. Laboratory established models were able to predict 30 to 50% of the field data (Figures 7.31 – 7.34). Results indicate that the SAF lacked the sensitivity to classify the range of concretes used in this study (Figure 7.24).

Acknowledgements

I thank GOD for guiding me through this doctoral process. I am extremely grateful to my Committee Chairpersons, Dr. Jesus M. de la Garza and Dr. Richard E. Weyers, for all of their guidance over the past 3 years. I want to especially thank Dr. Richard E. Weyers for treating me as a peer, and working side-by-side with me at the laboratory during the experimental phase of this research. I would also like to thank the other committee members, Dr. Richard Barker, Dr. William Reynolds, and Mr. James Lefter, for their comments and support.

I would like to thank the National Science Foundation for providing financial support during my tenure as a NSF Graduate Trainee in Civil Infrastructure Systems. I would also like to thank Michael Sprinkel, Mike Burton, and William Ordel of the Virginia Transportation Research Council (VTRC) for all of their assistance in conducting the ASTM C 1202-97 tests. I would like to thank Mr. William Payne of Concorr inc. for use of the SAF device.

I would like to thank the Commonwealth of Virginia Department of Transportation as well as PCL Civil Constructors, Inc. and Project Engineer, Sean Bush for giving me access to the Wilson Creek Bridge project.

I would like to thank my family and friends who have been there for me through this entire process. This work is dedicated to my mother Charlotte A. Bryant and in memory of my father, James W. Bryant, Sr.

Table of Contents

List of Figures

List of Tables

CHAPTER 1. INTRODUCTION AND BACKGROUND

1.1 INTRODUCTION

When concrete is properly designed and carefully produced with good quality control it is an inherently durable material. Five factors that may affect the durability of concrete are constituent materials, construction practices, physical properties, environmental exposure conditions, and type of loads. Once the concrete is in-place, prolonged exposure to adverse conditions may lead to deleterious attacks including corrosion of reinforcing steel, freezing and thawing action, sulfate attack, alkali-silica and alkali-carbonate reaction. In each case, the concrete degradation process involves the penetration and subsequent movement of water or other fluids transporting aggressive agents into the concrete pore system. The rate of deterioration may be accelerated by poor quality concrete, which is influenced by the inadequate selection of materials and/or poor concrete construction practices. High performance concrete (HPC) has been suggested to increase the resistance of concrete to aggressive forces from the environment, which has positive implications of long-term durability (Roy D M et al. 1993).

A definition of HPC is both difficult and somewhat elusive. Early definitions of HPC were associated with its high-strength capacities. The Federal Highway Administration (FHWA) proposed to define HPC using long-term performance criteria (Goodspeed C H et al. 1996). The proposed definition consists of the following strength and durability parameters (1) compressive strength, (2) elastic modulus, (3) freezing and thawing, (4) chloride permeability, (5) abrasion resistance, (6) scaling resistance, (7) shrinkage, and (8) creep. Table 1-1 presents the performance criteria for each parameter along with the designated test procedure.

Foster (1994) defines HPC as concrete made with appropriate materials combined according to a selected mixture proportions, properly mixed, transported, placed, consolidated and cured so that the resulting concrete will “perform” in its’ intended environment throughout its design life (Foster S W 1994).

Table 1-1. Definition of HPC proposed by FHWA (Goodspeed C H et al. 1996).

Performance Characteristics	Standard test method	FHWA HPC performance grade			
		1	2	3	4
Freeze-thaw durability (X_{ft} = relative dynamic modulus of elasticity after 300 cycles)	AASHTO T 161 ASTM C 666 Procedure A	60%≤X<80%	80%≤X		
Scaling resistance (X_s = visual rating of the surface after after 50 cycles)	ASTM C 672	X=4, 5	X=2, 3	X=0, 1	
Abrasion resistance (X_w = avg. depth of wear in mm)	ASTM C 944	2.0>X≥1.0	1.0>X≥0.5	0.5>X	
Chloride penetration (X_{CL} = coulombs)	AASHTO T 277 ASTM C 1202	3000≥X>2000	2000≥X>800	800≥X	
Strength (X_{CS} = compressive strength)	AASHTO T 2 ASTM C 39	41≤X<55 Mpa (6≤X<8 ksi)	55≤X<69 Mpa (8≤X<10 ksi)	69≤X<97 Mpa (10≤X<14 ksi)	97 =Mpa≤X (14 ksi≤X)
Elasticity (X_E = modulus)	ASTM C 469	28≤X<40 GPa ($4\leq X<6x10^6$psi)	40≤X<50 GPa ($6\leq X<7.5x10^6$psi)	50 GPa≤X ($7.5x10^6$psi≤X)	
Shrinkage (X_ε = microstrain)	ASTM C 157	800>X≥600	600>X≥400	400>X	
Specific creep (X_{SC} = microstrain per Mpa)	ASTM C 512	75≥X>60/MPa (0.52≥X>0.41/psi	60≥X>45/MPa (0.41≥X>0.31/psi	45≥X>30/MPa (0.31≥X>0.21/psi)	30/MPa≥X (0.21/psi≥X)

* A given performance concrete mix design is specified by a grade for each desired performance characteristic. For example a concrete may perform at Grade 4 in strength and elasticity, Grade 3 in shrinkage and scaling resistance and Grade 2 in all other categories.

The American Concrete Institute International (ACI) defines HPC as concrete meeting special combinations of performance and uniformity requirements that cannot always be achieved routinely using conventional constituents and normal mixing, placing and curing practices (Russell HG 1999). Furthermore, it is concrete in which certain properties are developed for a particular application and environment. The critical HPC properties as identified by ACI are long-term mechanical properties, early age strength, permeability, long life in severe environments, density, rate of placement, heat of hydration, compaction without segregation, toughness, and volume stability. High Performance Concrete can only be defined with reference to the performance requirements of its intended use.

1.2 CONCRETE PERFORMANCE

In the use of HPC, one major question of concern is: Can HPC reliably be achieved in the field? Constructability concerns include workability, safety, flowability, construction site maneuverability, rate of slump loss, equipment availability, uniformity, and construction loads including equipment, formwork and shoring/reshoring schedule.

Shilstone *et al.*, (1993) states that "Only when a material becomes usable in [the] construction [of a concrete element] is it truly a product." Reinforcement details, section size and shape, obstructions to casting, and other limitations to access may affect concrete placement (Shilstone JM et al. 1993). A concrete mixture is defined constructible if it can be properly installed.

It is well recognized that concrete construction methods and practices influence the final quality of in-place concrete (Rasheeduzzafar A.S et al. 1989). The placement of concrete includes transporting the concrete to the jobsite delivery point, discharging into formwork, consolidating and providing proper curing conditions to insure adequate durability, serviceability, structural integrity and appearance in accordance to design specifications. Figure 1.1 presents a summary of the affects that construction practices may have on concrete performance.

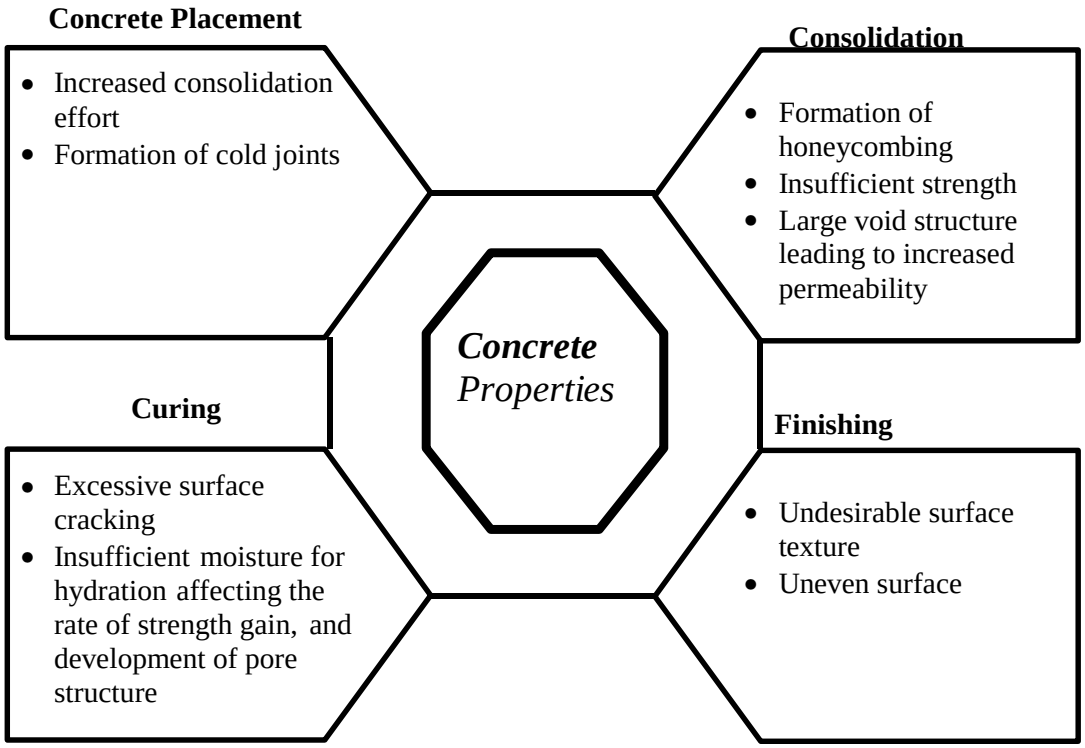

Figure 1.1. The effect of concrete construction practices on the final quality of concrete.

A concrete mixture design is just a proportion of ingredients. If the concrete mixture is not transported, placed and cured properly it will not exhibit the desired performance qualities. The philosophy of Professor J. M. de la Garza of Virginia Tech is "Construction is the last phase of design. In other words, design is not what is represented by calculations or drawings but design is what is actually built in-place." This philosophy is represented by Figure 1.2.

There is a need to quantify the in-place performance of concrete structures since the design performance expectations may differ from actual as-built properties. As the definition of HPC extends to parameters including modulus, shrinkage, and permeability there is a need to develop a methodology to measure these properties in the field.

In-situ performance qualification can be an early indicator of long-term durability and/or give an indication of the present quality of the concrete. Swamy (1996) states that the key to concrete durability and therefore its performance is to enable concrete to attain a tight and highly impermeable pore structure (Swamy RN 1996). The pore structure is essentially a network of conduits that connect the exterior of the concrete to its interior. Aggressive

substances transport into the concrete matrix via the pore system. The long-term durability of concrete is controlled by its ability to impede the ingress of deleterious substances into the concrete pore structure. Therefore when considering long-term durability of concrete, permeation properties are of utmost significance.

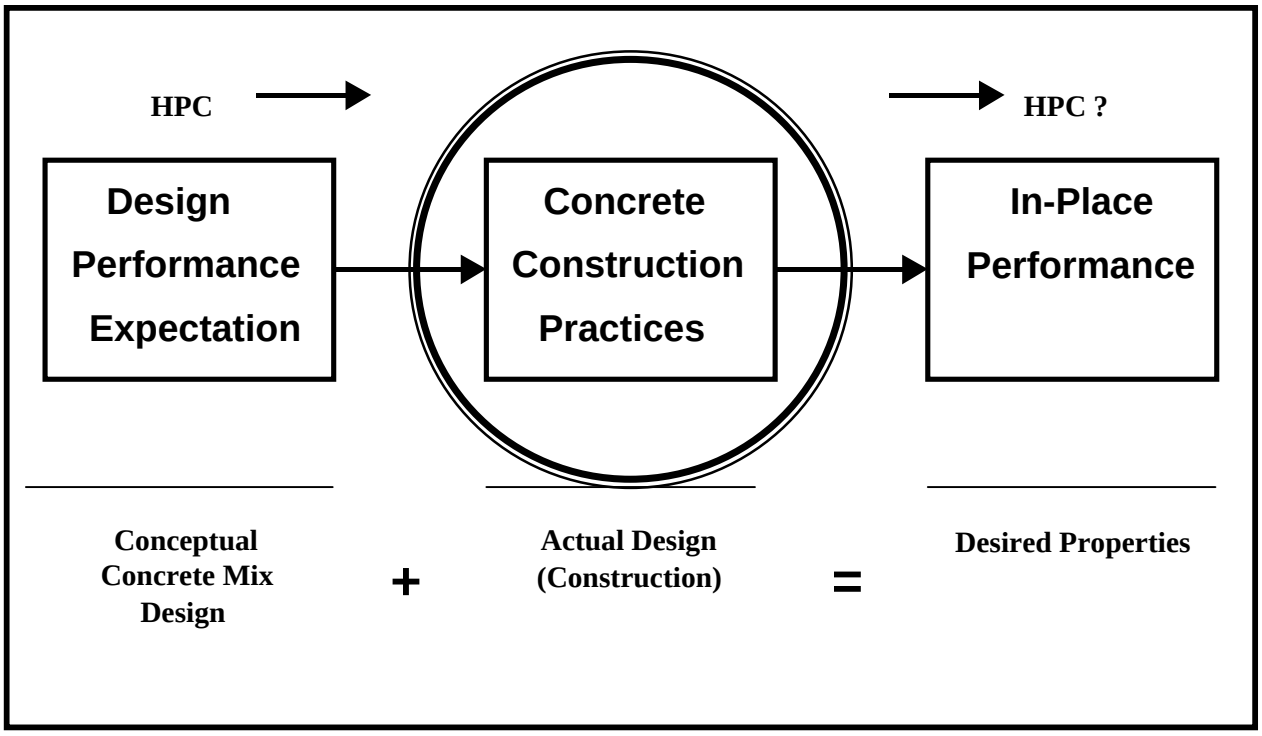

Figure 1.2. "Construction is the last phase of design"

1.3 PERMEABILITY MEASURES

There is no one universally accepted standard test method for measuring the permeation properties of concrete. The most widely used method, in the United States, for assessing the permeation properties is ASTM C 1202-97 (AASHTO T-277), which is based on chloride ion diffusion. Electrical properties of concrete are dependent on the amount of free water within the concrete, the type of cementitious materials, the degree of hydration, water/cm ratio and the proportion of aggregate present. These same factors play a large role in the development of strength and durability.

In addition to ASTM C 1202, electrical resistivity has been used to characterize the electrical properties of concrete. Several researchers have reported a relationship between

electrical resistivity and concrete properties including compressive strength, water content, total charge passed (ASTM C 1202-97), and porosity (Hughes B P et al. 1985); (Rengaswamy N S et al. 1986); (Tashiro C et al. 1987); (Wilson J G et al. 1985). However, there is no quantification of permeation measures based on resistivity measurements.

1.3.1 Overview of In-Place Permeability Measures

In-place permeability testing methods lie within two broad categories: (1) hydraulic permeability (surface absorption and water permeability); and (2) gas permeability (change in pressure and forced pressure methods). A number of researchers have proposed various techniques and procedures for measuring the in-place permeation properties of concrete (Table 1-2). Recently many of these in-place permeation measurement devices have become commercially available. There are still questions as to how well the in-place tests characterize the permeation properties of the concrete.

In the United States the Surface Air Flow (SAF) method proposed by Whiting and Cady (1993) has been promoted as an effective measure of relative concrete permeability. In this method a vacuum is created on an approximately 4-in diameter surface of the concrete using a vacuum plate. The pressure inside the vacuum plate is reduced due to flow of air through the concrete. This change is vacuum pressure is monitored with respect to time. The relative permeability of the concrete is determined by the amount of air flow in ml/minute that occurs when the vacuum pressure stabilizes.

Good correlations were found between the SAF measurements and laboratory air permeability results, water permeability and chloride diffusion constants determined from 90-day ponding tests (Whiting D. et. al, 1992). It is suggested that the SAF can be used as a qualitative measure of chloride diffusion coefficients or permeabilities of the surface layer of concrete.

Table 1-2. In-situ permeability test methods (Basheer PAM 1993)

Transport Mechanism	Test Methods	Principle Investigators
Absorption	**Absorptivity** • *Surface:* (1) ISAT (2) Standpipe test • *Drilled Hole* (1) Figg water test (2) Covercrete absorption • *Sorptivity* (1) Aotuclam sorptivity	 BSI (1970) Meyer A. (1987) (Figg J 1989) (Dhir R K et al. 1987) (Basheer PAM 1993)
Permeability	**Gas Permeability** • *Pressure differential tests*: (1) Figg air test (2) Surface Air Flow (SAF) (3) Surface pressure inflow (autoclam test) **Water Permeability** (1) Autoclam water permeability (2) Field Permeability Test (Drilled Hole)	 (Figg J 1989) (Whiting D, et al, 1992) (Basheer PAM 1993) (Basheer PAM 1993)) (Meletiou Constantine A et al. 1992)

1.4 RESEARCH SCOPE AND OBJECTIVES

There has been little investigation into the effectiveness of the SAF device in characterizing the permeation properties of concrete, other than the initial research conducted by Whiting and Cady (1993). Although researchers have established that a relationship exist between the electrical resistivity and permeation properties little work has been done on field applications.

In-place permeability is a controlling factor when considering the durability of concrete bridge decks. In the Commonwealth of Virginia, ASTM C 1202-97 is used to assess the permeation properties of concrete bridge mixtures. Concrete construction practices affect the in-place quality of concrete (Figure 1.1). Therefore, the as-built properties of a concrete structure may differ from the desired design expectations (Figure 1.2). There is need to determine the relationship between in-place permeability

measurements and ASTM C 1202 for concrete bridge elements in the Commonwealth of Virginia, if either of these methods are to be used to assess in-place permeability.

This study investigated the in-place permeability of a broad range of class 35 (A4) bridge deck mixtures used in the Commonwealth of Virginia. Permeation properties were assessed using the SAF, ASTM C 1202, and electrical resistivity. The effect of concrete initial curing time on the long-term permeation properties was also investigated.

The objectives of this research are:

- To evaluate the effectiveness of in-place testing methods in assessing the present quality of concrete as determined by laboratory test methods (ASTM C 1202).
- To investigate the effect of initial moist curing period on the development of strength and long-term permeability.

This dissertation contains 8 chapters including Chapter 1 Introduction and Background, the remaining 7 chapters are as follows: Chapter 2 Concrete Transport Mechanisms; Chapter 3 Permeability of Concrete; Chapter 4 Concrete Resistivity; Chapter 5 Methods and Materials; Chapter 6 Results; Chapter 7 Analysis and Discussion; and Chapter 8 Conclusion and Recommendations.

CHAPTER 2. CONCRETE TRANSPORT MECHANISMS

2.1 INTRODUCTION

The functional service life on a concrete element is strongly dependent on its transport properties (Martys, 1995). The ingress of deleterious substances into concrete takes place through the pore system in the cement matrix or micro-cracks. There are several mechanisms that determine the rate at which a substance is able to flow through the concrete matrix, including porosity, pore size distribution, pore connectivity, environmental conditions, and the degree of pore saturation.

The principal ways through which an aggressive substance may transport through the concrete matrix are diffusion, permeation (gas permeability and water permeability), capillary action and absorption. Diffusion refers to the movement of fluids under a differential concentration. The transport of a fluid caused by a pressure differential refers to permeability. Sorption is the result of capillary action in the pore system exposed to the ambient medium (Neville, 1995). The transport of aggressive substances into the concrete matrix may not be due to any single mechanism, but several mechanisms acting simultaneously (Kropp et al., 1995). This chapter provides a summary of above transport mechanisms.

2.2 DIFFUSION

Diffusion is the process by which a fluid can pass through concrete under the action of a concentration gradient (Concrete Society, 1987). It is defined as the "transfer of mass by random motion of free molecules or ions in the pore solution resulting in a net flow from regions of higher concentration to regions of lower concentration of the diffusing substance (Kropp et al., 1995).

The mass transfer rate through unit area of a substance is given by

$$J = \frac{dm}{dt}\frac{1}{A}$$ **Equation 2-1**

where, J = mass flux (kg/m^{2}s)

m = mass of flowing media (kg)

t = time (s)

A = area (m^2)

The rate of mass transfer is proportional to the concentration gradient d*c*/d*L* and the diffusion coefficient *D*. This relationship is expressed by Fick's first law of diffusion:

$$J = -D\frac{dc}{dL}$$ **Equation 2-2**

where D = diffusion coefficient (m^2/s)

dc/d*L* = concentration gradient (kg/m^4)

L = distance or thickness of sample (m)

J = mass transport rate (kg/m^2)

The diffusion coefficient is a characteristic material property describing the transfer ability of a given substance. D may vary with the local concentration of free ions or molecules, concrete age, and temperature.

2.3 PERMEATION

Permeability can be defined as the ease with which a fluid can flow through a solid. The flow through a media is caused by a pressure differential. The coefficient of permeability is the material characteristic describing the permeation of fluids through a porous material due to a pressure head (Kropp et al., 1995).

2.3.1 Gas Permeability

The most direct method to measure gas permeability is by application of a pressure gradient across a concrete specimen and measurement of the flow rate at steady-state conditions. The coefficient of gas permeability is expressed by equation 2-3.

$$K_g = \eta\frac{QL}{tA}\frac{2p}{(p_1 - p_2)(p_1 + p_2)}$$ **Equation 2-3**

where

K_g = coefficient of permeability (m^2)

η = viscosity of the gas (Ns/m^2)

Q = volume of gas flowing (m^3)

L = penetration depth (m)

A = penetrated area (m^2)

p = pressure at which the volume Q is measured (N/m^2)

p_1 = entry pressure of the gas (N/m^2)

p_2 = exit gas pressure (N/m^2)

Equation (2-3) is only valid for laminar flow. The transport of gases through the pore system does not always follow this assumption due to the wide range of pore sizes.

2.3.2 Water Permeability

Water is perhaps the most importance fluid that flows through concrete. Water is considered to be incompressible, therefore equation (2-3) may be expressed as:

$$\frac{dq}{dt}\frac{1}{A} = \frac{K_w \rho g}{\eta}\frac{\Delta h}{L}$$ **Equation 2-4**

K_w = the coefficient of permeability

dq/dt = rate of flow of water (m^3/s)

A = cross-sectional area of the sample (m^2)

Δh = decrease in hydraulic head through the sample (m)

L = thickness of sample (m)

η = dynamic viscosity of the fluid ($N\ s/m^2$)

ρ = density of the fluid (kg/m^3)

g = acceleration due to gravity

The coefficient of permeability in this case is solely a function of the material through which the water is flowing. The water flow in a saturated pore system follows Darcy's law for laminar flow through a porous material.

2.4 CAPILLARY ACTION

Capillary action transports liquids through a porous solid by way of surface tension acting in the capillary pores. Capillary action is affected by the characteristics of both the liquid and the porous medium. The characteristics of the liquid that influence capillary action are viscosity, density, and surface tension. The influencing characteristics of the solid include pore structure (radius, tortuosity and capillary continuity) and surface energy.

Steady state capillary suction of water in a pore system is given by Darcy's law modified for non-saturated water flow:

$$F = -\frac{k_p}{\eta}\frac{dp_w}{dx} \qquad \textbf{Equation 2-5}$$

where

dp_w/dx = Pore water pressure gradient (N/m^2)

k_p = The coefficient of moisture permeability (kg/m)

Equation (2-6) presents the pore pressure in terms of air pressure p_a, radius of the water meniscus r_m and surface tension, σ.

$$p_w = p_a - \frac{2\sigma}{r_m} \qquad \textbf{Equation 2-6}$$

In cases of continuous drying only small pores are filled with water and the pore water pressure p_w is extremely low ($p_w << 0$). If a continuous liquid path is present capillary suction occurs in those areas.

The pore pressure can also be written it terms of water vapor pressure at saturation, p_s, and pore relative humidity φ:

$$p_w = p_s + \frac{RT\rho}{M_w}\ln\varphi \qquad \textbf{Equation 2-7}$$

where

R = The universal gas constant

T = Temperature in degree Kelvin

M_w = The molar weight of water

ρ = The density of water

It follows that at a relative humidity slightly under 100 % negative pore water pressure will occur, causing partially saturated pores. If the relative humidity (RH) is maintained capillary suction will occur only in the wetter portion of the pore system.

The effect of gravity must be taken into account when considering the larger pore spaces. Equation (2-8) presents the flow due to capillary suction in the larger pores,

$$F = \frac{k_p}{\eta}\frac{d}{dx}\left(p_w + \rho g h(x)\right) \qquad \textbf{Equation 2-8}$$

where $h(x)$ is the vertical distance between the point x and a water table (Kropp et al., 1995).

CHAPTER 3. PERMEABILITY OF CONCRETE

3.1 INTRODUCTION

Permeability can be defined as the ease with which a fluid can flow through a solid. It is well recognized that the permeability of hardened cement paste greatly affects the durability of concrete and in turn is strongly affected by the pore structure (Mehta K P 1990). Permeability of concrete is a function of the w/c ratio, aggregate particle size, pore size and distribution.

The pore structure is formed during the hydration process. The void spaces between the cement particles start to fill up with hydration products. The w/c ratio and the degree of hydration determine the total capillary porosity. Generally the capillary porosity increases or decreases as w/c ratio increases or decreases. At a w/c ratio of approximately 0.6, the capillary voids become connected, causing a rapid increase in the coefficient of permeability (Mehta K P 1990).

The particle size of the aggregate also plays an important role in the permeability of concrete, the larger the aggregate size, the greater the coefficient of permeability. The aggregate size directly affects the transition zone. There are micro-cracks present in the transition zone between the aggregate and the cement paste. During the initial stages of hydration the transition zone is weak and cracking may occur due to differential strains between the cement paste and the aggregate, which are caused by drying and shrinking, thermal shrinkage, and externally applied loads. The micro-cracks that occur in the transition zone are larger in width than most capillary cavities present in the cement paste matrix. These voids (micro-cracks) help to establish interconnections in the pore structure, which lead to increased permeability of the system.

This chapter includes the following sections: (3.2) Factors Influencing Permeability; and (3.3) Permeability Measures.

3.2 FACTORS INFLUENCING PERMEABILITY

3.2.1 Concrete Microstructure

Concrete permeability is determined, in part, by its microstructure (pore and crack structure). Concrete has a very complex microstructure comprised of a variety of phases with diverse material properties (Martys, N S, 1995). Transportation of fluids through concrete occurs through the network of continuous pores, which exist in the concrete's cementious matrix, as well as the porosity that exist in the interfacial regions with the aggregate. Fluids may transport into the pore system by diffusion, permeation, capillary action, and absorption. These transport mechanisms were briefly discussed in Chapter 2.

There is a close relation between the transport of deleterious substances into the cement matrix and the porosity of the cement. The interconnected porosity governs the transport of material and therefore the kinetics of the cement degradation. The permeability of concrete is determined by both the total porosity and its distribution (Roy D M et al. 1993). Porosity is a volume property representing the total void space. Porosity is a function of the original packing of the cement, mineral admixtures, and the aggregate particles, as well as the water-to-solids ratio, the reheology, which is related to the degree of dispersion of the solids originally present, and the curing conditions (Roy D M et al. 1993).

There are several sources of porosity in concrete including: (1) gel pores; (2) smaller capillary pores; (3) larger capillary pores; (4) large voids, which may include air entrained voids; (5) porosity associated with the paste-aggregate interfacial zones; (6) discontinuities and microcracks associated with dimensional instabilities that occur during curing; and (7) aggregate porosity. Pore diameters within the concrete matrix span over many decades, ranging from nanometers for capillary voids to millimeters for entrapped air.

3.2.2 Concrete Construction Practices

Factors needed to ensure low permeability concrete include selection of proper constituent materials, proper proportioning of the selected ingredients to achieve desired fresh and hardened properties, careful quality control in every phase of concrete production, and the selection and implementation of the proper concrete placement methods.

Several researchers have discussed the importance of concrete placement practices in the development of durable concrete. The ways in which concrete construction practices affect the in-place quality of concrete were briefly discussed in Chapter 1. Improper construction practices may lead to the formation of a larger void structure than originally intended in the "design," leading to high permeability concretes. Adequate curing and the use of supplementary cementious materials have been found to be affective in producing low permeable concretes.

3.2.2.1 Concrete Curing

Concrete curing may be defined as procedures employed to provide an environment in which adequate hydration of cementious materials occur. The object of curing is to keep the concrete near saturation, sealing the moisture in, until the voids that were filled with water are filled with sufficient hydration products to achieve the desired properties. The two major categories used to describe concrete curing methods include membrane curing and wet or moist curing. Membrane curing seals the concrete surface by the application of membrane-forming chemical compounds. Moist curing requires that the surface of the concrete is in continuous contact with water and may be achieved by ponding or flooding, covering wet concrete with earth or straw, or the use of a wet burlap blanket. The type of curing method used is dependent upon several factors including water availability, environmental conditions and geometric constraints.

Curing time is also a major factor when using the moist curing method. The length of curing is depended upon the severity of the drying conditions and the desired hardened concrete properties. Proper curing is essential for long-term durability of concrete (Haque, et al, 1990).

Several investigators have discussed the effect of concrete curing time on the development of strength and permeability (Haque MN 1990); (Ewertson C et al. 1993); (Saricimen H et al. 1995); (Marusin S L 1986). These researchers found that strength increases and permeability decrease with increased moist curing times.

The specification of curing durations is usually dependent on the compressive strength requirements. ACI recommends a minimum curing duration of 7-days or the time necessary to attain 70 percent of the compressive strength (ACI 308-92). Sufficient strength may be achieved in a concrete element without proper curing durations but the durability may be insufficient (Tabor 1993). The cover concrete, which is directly exposed to the ambient environment, is more susceptible to the influences of curing durations than the core concrete. The near surface concrete may develop a large pore structure due to insufficient moisture for hydration, which directly affects the permeability of the structure.

3.2.3 Supplementary Cementious Materials

The three most common supplementary cementious materials used are silica fume (microsilica), ground granulated blast furnace slag, and fly ash. The use of supplementary materials for enhancing concrete durability is well documented (Khatri R P et al. 1995).

3.3 PERMEABILITY MEASURES

There is no universally accepted standard test method for measuring the permeation properties of concrete. Permeation procedures may be categorized by their respective transport mechanisms: (1) absorption, (2) permeability (flow), and (3) ionic flow. The most widely used method for measuring permeation properties in the United States is ASTM C 1202-97 (AASHTO T-277), which is based on chloride ion diffusion. Section 3.3.1 provides a summary of the Chloride Ion Penetrability Test, known as the Rapid Chloride-ion Penetrability Test (RCPT).

3.3.1 Chloride Ion Penetrability Test

ASTM C1202-97 “Electrical Indication of Concrete’s Ability to Resist Chloride Ion Penetration," was originally designated by the American Association of State Highway Officials (AASHTO) as AASHTO T 277 in 1983. The RCPT was the first test proposed for a rapid qualitative assessment of chloride ion permeability in ordinary portland cement concretes. David Whiting et al. (1983) correlated total charge passed (coulombs) results from RCPT to depth of chloride penetration results from AASHTO T 259, the 90-day salt ponding test (Whiting et al., 1983).

ASTM C1202-97 measures the movement of chloride ions through concrete. The test specimen consists of 50-mm (2-in.) thick slices of 100mm (4-in.) nominal diameter cylinders of cores. Once the specimen is conditioned for testing, one end is immersed in a sodium chloride solution and the other in a sodium hydroxide solution. A 60 V potential is maintained across both ends. The amount of current passing through the test specimen is measured for 6 hours. The plot of current versus time is integrated, yielding the total charge passed. The total charge passed, in coulombs, is to be related to the chloride ion penetrability of the specimen. Table 3-1 presents chloride ion penetrability ratings for ASTM C1202.

Table 3-1. Chloride Ion Penetrability Based on Charge Passed

Chloride Ion Penetrability	Charge Passed (coulombs)
High	> 4000
Moderate	2000 – 4000
Low	1000 –2000
Very Low	100 – 1000
Negligible	<100

Permeability specifications based on ASTM C 1202 or AASHTO T 277 are common in the concrete construction industry (Shi C et al. 1998). Several researchers have expressed concerns about the ability of the RCPT to assess the chloride ion penetrability of concretes containing supplementary cementitious materials including pozzolanic materials and slag (Berke et al. 1988); (Feldman Rolf F et al. 1994); (Wee T H et al. 2000). The main criticism surrounds the severity of the test conditions, which causes large increases in the temperature of the test specimen due to polarization (Feldman et al. 2000). The polarization effect may cause chemical and physical changes to the pore structure.

The use of the initial current results has been found to correlate well with total charge passed (Feldman et al., 2000); (Zia et al., 1993). Total charge passed and initial current are both measured during the ASTM C 1202-97 test. The initial current is an instantaneous result usually obtained in the first 10 minutes of the test, while the total charge passed is the integration of current over time. The use of initial current measurements prevents changes to

the pore system due to the measurements shorter testing time. There is no penetrability rating based on initial charge measurements.

3.3.2 **In-Place Permeability Measurements**

3.3.2.1 Gas Permeability

There is no standard test method for the measurement of gas (air) permeability. Figg (1993) proposed an on-site method for measuring the air permeability of the surface layer of concrete. In this method a hole, 10-mm (0.4-in.) diameter by 40-mm (1.6-in.) deep, is cast in-place or drilled into the concrete surface and plunged with silicone rubber to half its depth. A hypodermic needle is then pressed through the plug into the small test cavity. The test cavity is then evacuated to a pressure of 55-kPa (8-psi) below the atmospheric pressure and the time in seconds for a pressure increase of 5-kPa (.7-psi) is taken as a measure of the concrete permeability. Permeation properties for cover concrete based on the Figg method are show in Table 3-2.

Schonlin and Hilsdorf (1988) proposed a method for measuring air permeability using a small suction chamber, which is adhered to the concrete surface by creating a partial vacuum inside the chamber. The vacuum inside the chamber is reduced due to the decreased flow of air through the concrete into the chamber. The change in vacuum pressure is monitored with respect to time. The permeability index of the concrete is determined from the change of pressure in the chamber within a given time period.

Basheer et al. (1993) developed the "Autoclam" permeability system for measuring the in-place permeation properties of concrete by applying a pressure over the concrete surface to force in air. The base ring of the “Autoclam” is fastened to the concrete surface by mechanical anchors or strong adhesives. The flow lines are located within 40-mm (1.6-in.) from the test surface. The rate of decay of air pressure in the cell is recorded for the air permeability test. A mean of three tests was found to provide statistically satisfactory results. It was also shown that reliable data could be collected by drying the surface even if the test surface was initially wet. The test variables were w/c ratio, aggregate/cement ratio, and

number of days of wet curing. Table 3-3 presents the permeation ratings for concrete based on the Autoclam indices.

Table 3-2. Concrete permeability ratings based on Figg method (after Basheer, 1993).

Concrete Category	Protective Quality	Permeability Index	
		Measured Time (s)	Air Flow (ml/s)
0	Poor	< 30	< 8
1	Not very good	30 – 100	8 – 25
2	Fair	100 – 300	25 – 75
3	Good	300 – 1000	75 – 250
4	Excellent	> 1000	> 250

Whiting and Cady (1992) developed a device for measuring the surface air flow (SAF) of concrete as part of a SHRP project. This method is similar to the method proposed by Schonlin and Hilsdorf (1988). A linear relationship was found between results obtained on the same specimens using the laboratory and field versions of the method. A series of field trials were also conducted to evaluate the device's field performance. The results showed that there exists a general relationship between the readings taken in the field and the air permeability values determined from cores. This device is portable, can take measurements on overhead and vertical surfaces, has a short testing time, and is easy to operate. However, the device has an effective depth of measurement of only approximately 12.5 mm (0.5 in.). The permeability ratings for concrete based on this method is presented in Table 3-4.

Table 3-3. Protective Quality based on Autoclam permeation indices (Basheer et al., 1993)

Protective Quality	Clam air permeability index (In (pressure/min)
Very good	≤ 10
Good	$10 > x \leq 50$
Poor	$50 > x \leq 90$
Very poor	$x > 90$

Table 3-4. Permeability ratings based on SAF measurements (Whiting et al, 1992).

Relative Permeability	Surface Air Flow (ml/min)
Low	$x \leq 30$
Moderate	$30 < x \leq 80$
High	$x > 80$

Torrent, R. J. (1992) proposed an air permeability method using a two chamber vacuum cell. A regulator balances the pressure in the inner (measuring) chamber and in the outer (guard ring) chamber. Spurious lateral airflow is eliminated and unidirectional airflow into the measuring chamber is achieved. A vacuum is produced in both chambers for 1 min then the increase in pressure in the inner chamber is recorded. The coefficient of air permeability can be calculated and the depth of effective penetration can be estimated.

3.3.2.2 Hydraulic Permeability

Hydraulic permeability is a measure of absorption, the liquid transport mechanism due to capillary suction in the concrete pore system. The most noted method for measuring water permeability is the Initial Surface Absorption Test (ISAT). This method has been standardized as BS 1881 Part 5-1970 (British Standards Institute, 1970). A gasketed cap is either clamped or adhered to the concrete surface. Water is poured into the inlet until the outlet runs clear. A capillary tube is then affixed to the outlet tube, an initial reading is taken and subsequent readings are obtained at 10, 30, 60 and 120 minutes. Concrete absorption indices based on ISAT are presented in table 3-5.

Table 3-5 Typical ISAT results (Basheer, 1993).

Concrete absorption	ISAT results: ml/m^2			
	Time after starting test			
	10 min	30 min	60 min	120 min
High	> 50	> 35	> 20	> 15
Average	25 – 50	17 – 35	10 – 20	7 – 15
Low	< 25	< 17	< 10	< 7

The air permeability method proposed by Figg (1992) can also be used for testing water permeability. The drilled cavity is filled with water at a hydrostatic head to 100 ml and

the time for 0.1 ml to be absorbed by the concrete is measured. The permeability is expressed as a function of time (seconds), the longer the time the more impermeable the concrete. The apparatus proposed by Basheer et al. (1993) can also be adapted to measure water permeability

Meletiou and Bloomquist (1992) proposed a method for measuring the water permeability of concrete in-place. A 22 mm (0.875 in) diameter by 152 mm (6-in) in length hole is drilled perpendicular to the surface of the concrete. A field permeability test (FTP) probe is inserted into the hole. The hole opening is sealed with two rubber o-rings when the probe is in its final position. The vacuum is applied to the FTP for 5 to 10 minutes, injecting water into the hole at a pressure of 1.0 to 3.4 Mpa (150 to 5000 psi). After steady state flow is achieved, the flow rate of the water is recorded and the coefficient of water permeability is calculated according to Darcy's law.

The initial moisture content and the degree of saturation of the concrete was found to have a significant effect on this test method, therefore the specimen under investigation should be pre-saturated prior to testing.

Armaghani et al. 1994 investigated the use of the FTP for durability specifications and ratings in Florida. Specimen where tested for water permeability (in the lab and in the field) and AASHTO T 277. A correlation was established between all three test methods. Table 3-6 presents the permeability classification proposed by Armaghani *et al.*, 1994.

Table 3-6. Permeability Classification System (Armaghani et al. 1994).

Concrete Permeability Classification	**Permeability range**		
	K-Chloride (AASHTO 277 & ASTM C 1202)	**K-Water (Lab) cm/s (10^{-12})**	**K-Water (Field) cm/s (10^{-12})**
Negligible	< 100	< 0.25	< 25
Very Low	100 – 1000	.025 – 2.5	25 – 150
Low	1000 –2000	2.5 – 25	150 – 750
Moderate	2000 – 4000	25 – 250	750 – 1500
High	> 4000	250 – 2500	1500 – 5000
Very High	N/A	> 2500	> 5000

There is a need to investigate the relationships between in-place permeation measurements and the most widely used method for measuring permeation properties in the United States, ASTM C 1202-97. Comparisons between in-place permeation measures and, ASTM-C 1202-97, are not available, with the exception of the study by Armaghani et al. 1994 correlating water permeability to ASTM C 1202-97 results.

CHAPTER 4. CONCRETE RESISTIVITY

4.1 INTRODUCTION

"Concrete resistivity is a geometry-independent material property that describes the electrical resistance, that is the ratio between applied voltage and resulting current in a unit cell (Polder 2000, pp. 126)." The resistivity of concrete is affected by the temperature, relative humidity (moisture condition), type of cementitious material (e.g. cement, supplementary cementitious material), water/cementitious (w/cm) ratio and degree of hydration. The total porosity and the concentration of ions are influenced by the w/cm ratio (Hughes B P et al. 1985). The reciprocal of resistivity is conductivity. Resistivity measurements are typically used in concrete applications because the applied voltage and the resulting current are known.

Electrical current is initially carried by the free migration of ions across the cement pore system. Ions of a particular sign accumulate on one side of a pore and ions of the opposite sign accumulate on the other side to create an opposing electric field and contribute to the decrease in current. The magnitude of the electric field and the mobility of ions in the pore water solution determine the rate of this process (Hughes B P et al. 1985).

The electrical resistivity of cement paste is generally much smaller than that of aggregate, with values on the order of 13 Ω–m and 1000 Ω–m respectively. "In terms of its electrical properties, concrete can be regarded as being made up of large numbers of relatively small volume particles of insulating material embedded in a conducting matrix of cement paste (Wilson J G et al. 1985, pp. 79)." The resistivity is therefore a function of the distribution of these volumes throughout the system.

Figure 4.1 presents two models that describe resistivity as a function of the volume distribution of the bulk material proposed by Wilson et al, 1986. Model A assumes that the volume of aggregate fills the entire cross-section of the conduction path, similarly to a solid rock. This system is modeled as two electrical resistances connected in series. The two resistances R_a and R_c represent the respective resistances of the aggregate and the cement

paste. The resistance of the aggregate will dominate, producing a high value of resistance, R_T, and a high value of resistivity for the concrete sample.

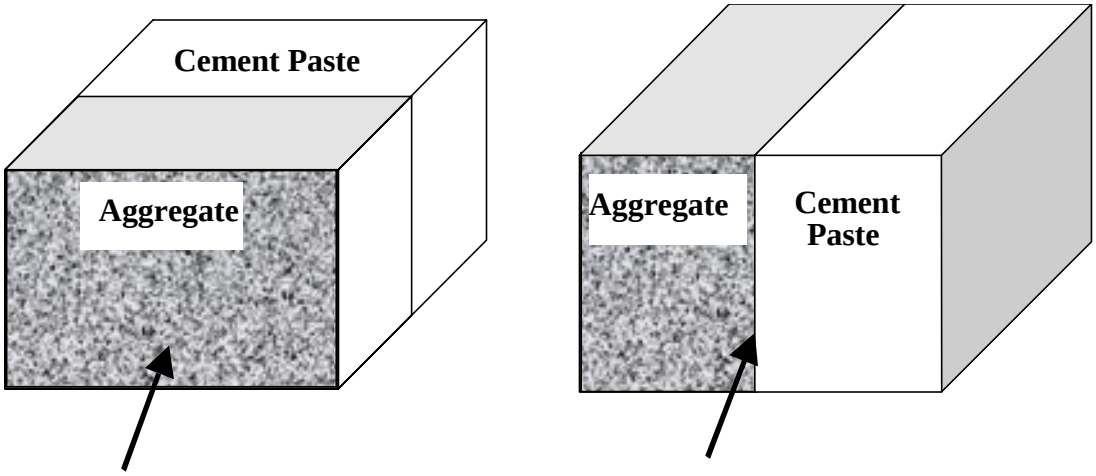

Model A

$$R_T = R_a + R_c$$

Model B

$$1/R_T = 1/R_a + 1/R_c$$

Figure 4.1. Resistivity as a function of the bulk volume distribution. Model A- high resistivity; Model B- low resistivity.

Model B assumes that the aggregate is displaced along the length of the conduction path. The electrical resistance of the aggregate and the cement paste are connected in parallel. "The cross-sectional area of these two components are proportional to the volume ratios of the aggregate and the cement paste (Wilson J G et al. 1985, pp. 80)." Since the resistivity of the cement paste is less than that of the aggregate, the resistance of the cement paste path will be smaller than that of the aggregate. For electrical resistances in parallel, the combined resistance, R_T, is less than the smaller singular resistance value; therefore the resistance of the cement paste will govern the resistivity of concrete.

Wilson states "In view of the packing characteristics of naturally occurring and crushed aggregates, continuous cement paste paths will always exist, rendering this second model [Model B] the relevant option (Wilson J G et al. 1985, pp. 80)." Since the current is initially carried by the cement pore system, it is useful to explore the resistivity behavior of cement paste.

4.2 RESISTIVITY OF CEMENT PASTES

The electrical conduction cement paste relies on ionic conduction through water-filled capillary pores. The resistivity of cement paste, in a saturated condition, depends on the relative volume proportions of the cement matrix and the free water. For conduction to occur, the water paths and the capillary pores must be continuous in the direction of conduction. The mobility of ions in the pore solution of hardened cement pastes is sensitive to the distribution and volume of saturated pores. The saturation level of the capillaries is dependent on the water content (Tashiro C et al. 1987).

Tashiro H. et al. 1987, investigated the dependence of electrical resistivity on the evaporable water content and the pore-size distribution in various cement pastes. The four cement pastes investigated were ordinary portland cement (OPC), alumina cement (AC) and ultra-rapid hardening cement (URHC). The rectangular 15 x 40 x 15-mm (0.6 x 1.6 x 0.6-in), test specimen had a w/cm ratio of 0.4 and were cured at 20°C in humid air. Two stainless steel electrodes of 6 x 25-mm (0.2 x 1-in) were embedded, 5 mm (0.2-in) apart, in cement. The molds were removed after one day of curing.

The specimens, at a fixed curing time, were placed in an oven at 60°C to evaporate the water. The samples were cooled to 20°C and the electrical resistance and weight were measured. Evaporable water content, at the time of the resistance measurements, was estimated from the difference in weight of the specimen's saturated and dry weight. Samples were placed in an oven at 100°C for 12 hours to remove any additional water. The electrical resistance was measured under an applied electric field with a frequency of 1.02 kHz. Pore size distributions were determined by mercury porosimeter. The measured range of pore size was 5 nm to 100 μm.

Results show that the log of the resistivity, log ρ, of cement pastes is proportional to reciprocal of the water content, w^{-1}. The electrical resistivity, ρ, of hardened cement paste is a function of the evaporable water content:

$$\rho = \rho_0 \exp\left(\frac{C}{w}\right) \qquad \textbf{Equation 4-1}$$

where the constant C is an intrinsic quality reflecting the microstructure of the capillary pores of the hydrated cement pastes

C increases with increasing curing time and approaches a constant value for OPC with a curing time of more than 28-days. The researchers regard C as a quantity associated with the microstructure of hardened cement paste and suggest characterization of hardened cement pastes with varying chemical compositions and curing times.

Hansson et al, 1983 studied the electrical resistivities of four different cements using both AC and DC measurements. The cements tested were: (1) Ordinary Portland Cement (OPC) paste, w/c = 0.50; (2) Sulfate Resistant Portland Cement (SRPC) paste, w/c = 0.26; (3) Blast Furnace Slag cement (BFSC) paste, w/c = 0.50; and (4) Dense Silica Fume (DSP) paste and mortar.

DC measurements were taken by applying cell voltages of 3.0, 4.5, 6.0, 7.5, and 9.0 V between two embedded electrodes and measuring the resulting current, I, as a voltage decrease across a small resistance, R_m. The current was allowed to decay to steady state conditions before the resultant current, I, was measured.

AC measurements were made on dense silica fume paste and mortar. A 500 Hz square wave voltage, with a small amplitude 10 mV peak to peak, was applied to the specimens and the maximum value of the resistance was measured.

Hansson found that the development of electrical resistivity in cement pastes is similar to the development of compressive strength. Results of the DC measurements are presented in Table 4-1. Twenty-day resistivities ranged from 14 Ωm for OPC to 2,000 Ωm for DSP paste. Resistivities, from AC measurements, for DSP mortar and paste at a frequency of 500 Hz were approximately 5 Ωm and 15 Ωm respectively at 200 days.

4.3 CONCRETE RESISTIVITY MEASUREMENT TECHNIQUES

There are a number of techniques use to measure resistivity. Resistivity can be measured using both AC and DC currents. The use of a DC current for measuring concrete resistivity results in polarization of the electrolyte and the formation of hydrogen and oxygen

at the electrodes (Hughes B P et al. 1985); (Millard S G et al. 1992) . Further explanation of this phenomenon follows.

Table 4-1. The DC Electrical Resistivities of Cements and Mortar after curing at 22C and 100% RH (Hansson I L H et al. 1983)

Specimen	w/c ratio	Resistivity (Ωm)	
		20-day	200-day
OPC	0.50	14	14
SRPC	0.26	37	53
BFSC	0.50	66	120
DSP	0.15	2,000	7,000
DSP, mortar	0.15	3,300	20,000

The flow of current is governed by the migration of ions in the pore water. The application of an electrical potential difference between two steel electrodes in contact with, or embedded in, the cement may results in the following electrochemical reactions (Hansson I L H et al. 1983):

$2H_2O + 2e^- = H_2 + 2OH^-$ **Equation 4-2**

$4OH^- = O_2 + 2H_2O + 4e^-$ **Equation 4-3**

$3Fe + 4H_20 = Fe_3O_4 + 8H^+ + 8e^-$ **Equation 4-4**

$2Fe + 3H_2O = Fe_2O_3 + 6H^+ + 6e^-$ **Equation 4-5**

Equations (4-2) and (4-3), which involve the dissociation of water, will be the dominant reactions in quality reinforced concrete due to the initial passivity of the steel reinforcing bars. In time these reactions may build up a layer of polarized material in the area surrounding the electrodes or the reinforcing steel in the case of reinforced concrete.

Several researchers have suggested the use of AC rather than DC currents, due to the electrochemical influences on DC measurements. One of the most commonly used technique for measuring concrete resistivity, using AC current, is the Wenner linear array (Figure 4.2). The technique was originally employed as a geophysical prospecting tool. Four equally spaced contacts are made with the concrete surface, and a small AC current, *I*, is passed between the outer contacts. The resultant potential difference between the two inner contacts *V* is measured. The resistivity is then calculated using equation (4.6).

$$\rho = 2\Pi a \frac{V}{I}$$ **Equation 4-6**

Where,

ρ = resistivity

I = a small AC current passed between outer contacts

V = Potential difference between inner contacts

a = Contact spacing between probes

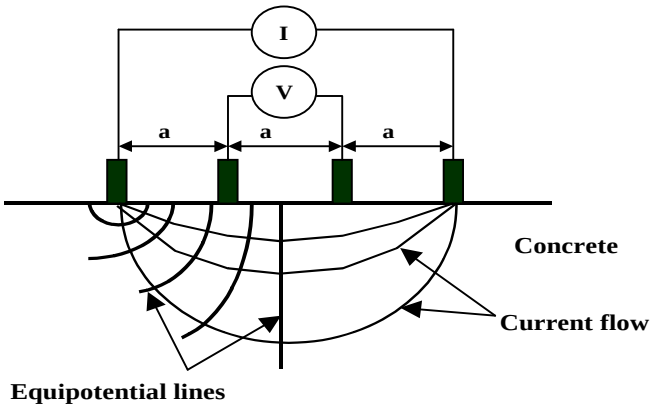

Figure 4.2 Wenner 4-point resistivity method.

There are a number of ways in which erroneous results are obtained when using this concrete resistivity measuring technique. Growers and Millard 1999 identified six sources of error in taking resistivity measurements. Errors may be due to the following influences: (1) Concrete geometry; (2) Concrete non-homogeneity; (3) Poor surface contact; (4) Surface layers of different resistivity from the bulk of the concrete; (5) The presence of reinforcing steel; (6) Changes in the ambient environment conditions (Growers K R et al. 1999). Table 4-2 presents some of the sources of error and recommended practices used to compensate for them.

One of the underlying assumptions in equation 4.6 is that the concrete specimen has infinite dimensions. For a large slab this assumption may hold true but there are cases in which the 4-point probe has been used on finite bodies as cores and cylinders. The theoretical basis for resistivity measurements on finite bodies is presented as follows (Morris W et al. 1996):

If *V'* and *I'* are the potential and current values obtained when applying the probe to a finite body, the apparent resistivity is given by:

$$\rho_{app} = 2\Pi a \frac{V'}{I'} \qquad \textbf{Equation 4-7}$$

When the probe is applied to a wide concrete slab with thickness >> the contact spacing, a, and there is no interference from the reinforcing steel, $\rho_{app} \approx \rho$ (Growers K R et al. 1999).

A constant cell correction *K* is needed for smaller bodies such as cylinders. *K* is defined as,

$$K = \frac{\rho_{app}}{\rho} \qquad \textbf{Equation 4-8}$$

where, *K* is a function of the inner-probe spacing and the geometry of the concrete body being tested. Morris et al. 1996 determined cell constant correction values experimentally for selected cases, and by means of finite element analysis to cover a wide range of situations. Empirical correlations between resistivity measurements with water filled concrete-test-molds and independent water resistivity measurements were used in the experimental method. Figure 4.3 (a) and (b) depicts the cell correction for the centered end and longitudinal cases.

The current distribution when using the Wenner probe tends to be representative of the concrete located roughly between the two center potential probes, extending into the concrete by a depth on the order of magnitude of the contact spacing (Morris W et al. 1996).

Table 4-2. Recommendations for use of 4-point Wenner array probe in practice.

Potential source of error	Recommended Practice
Concrete geometry	• Use a contact spacing less than or equal to one quarter of the concrete section thickness. • Resistivity measurements should be taken at a minimum distance of twice the contact spacing from the edge of the concrete specimen.
Concrete non-homogeneity	• Use a contact spacing of at least 1.5 times the maximum aggregate size of the concrete.
Poor surface contact	• Influence of surface contact area can be negated be using the four-contact resistivity method. To ensure good contact a high-conductivity gel may be used.
Differing resistivity	• If the presence of a low-resistivity surface layer is unavoidable, use a contact spacing not less than eight times the thickness of this layer.
Reinforcing steel	• Locate reinforcing bars and take resistivity measurements in a remote location. • If proximity to reinforcing bars is unavoidable, use a contact spacing less than or equal to two-thirds of the cover depth.
Ambient environmental conditions	• Measure at least 24-hr after rainfall • Use contact spacing of at least 4-cm where surface moisture effects are expected. • A temperature compensation of +1 kΩcm per 3°C decrease in temperature may be used to convert resistivity measurements to a standard temperature.

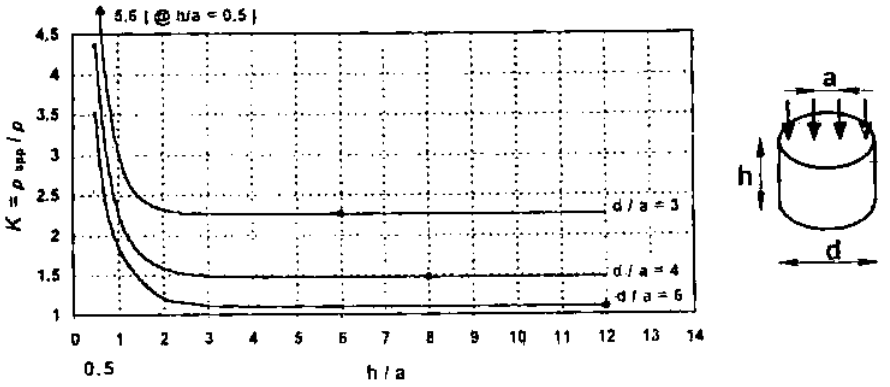

(a)

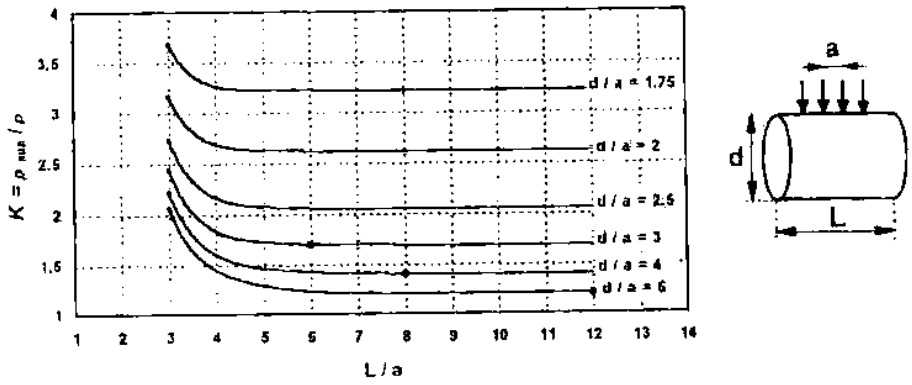

(b)

Figure 4.3. Cell correction factors as a function of d/a for and point of application (a) topical, (b) longitudinal (Morris W et al. 1996, pp. 1781 and 1783).

4.4 CONCRETE RESISTIVITY AND CONCRETE DURABILITY

Electrical properties of concrete are dependent on the amount of free water within the concrete, the type of cementitious materials, the degree of hydration, w/cm ratio and the proportion of aggregate present. These same factors play a large role in the development of strength and durability.

Several researchers have reported a linear relationship between resistivity and compressive strength (Rengaswamy N S et al. 1986); (Hughes B P et al. 1985); (Wilson J G et al. 1985). Rengaswamy et al., 1986 used 100-mm (3.94-in) concrete cubes having different mixture proportions by weight, with and without sodium chloride admixture.

Consolidation was achieved using a table vibrator. Samples were cured in distilled water. The cubes were removed from the water and the surface was air dried for 10 minutes prior to resistivity measurements. The measurements were taken on all four faces of the cube. Resistivity and strength was found to increase with decreasing w/cm. The resistivity of concrete was also found to develop over time, similarly to the development of compressive strength, increasing with age.

Rengaswamy suggests that an estimate of in-place concrete strength may be obtained from in-situ resistivity measurements, given the mixture design and the corresponding multiplication factor (Table 4-3.). It also suggested that the porosity of concrete can be assessed by measurement of the resistivity in dry and saturated condition (Rengaswamy N S et al. 1986).

Table 4-3. Relationship between compressive strength and concrete resistivity of cube specimens (Rengaswamy N S et al. 1986).

Specimen No	Mix Proportions	w/c ratio	Resistivity, ρ on 28th day kΩ-cm	28-day compressive strength N/mm^2	Multiplication factor
1	1: 1: 1	0.40	5.51 ± 0.07	40.2 ± 2.2	7.31
2	1: 1: 1.5	0.35	9.86 ± 0.05	54.5 ± 3.5	5.53
3	1: 1.35: 1.65	0.37	8.24 ± 0.32	46.5 ± 2.5	5.64
4	1: 1:14: 1.86	0.35	9.54 ± 0.42	48.0 ± 4.0	5.03
5	1: 1.71: 2.09	0.50	8.04 ± 0.26	31.5 ± 1.1	3.92
6	1: 1: 2	0.54	6.01 ± 0.58	24.7 ± 3.5	4.11
7	1: 1.5: 3	0.60	7.84 ± 1.44	25.4 ± 2.8	3.24
8	1: 2: 4	0.60	9.30 ± 0.80	28.7 ± 1.7	3.09
9	1: 4: 8	0.50	15.92 ± 1.06	6.45 ± 0.25	0.41

Hughes et al., 1985 measured the electrical resistivity using both DC and AC sine-wave current (10V and 100 Hz) of twelve concrete mixtures. Three 150-mm (5.9-in) cubes were cast in plastic molds for each mixture. There were two brass plates on opposing ends of the each plastic mold, serving as electrodes during the first 24-hr. Specimens were covered with polyethylene for 24-hr at room temperature prior to demolding. Specimens were demolded after 24-hrs and placed in 23° C water to cure. Fluid cement paste with 0.5 w/cm

was used as the contact interface between the concrete specimens and the electrodes after specimen were demolded.

The concrete resistivity was found to increase gradually during the initial 8 to 10 hr. after casting, with a rapid rate of increase after the initially setting of the concrete. The results from 7-day and 28-day resistivity measurements are presented in Table 4-4. The rate of increase was observed to be greater from 1-7-day compared to the increase rate from 7 to 28-days. The electrical resistivity of concrete was found to be inversely proportional to the w/cm ratio and to increase with decreasing cement content.

Table 4-4. Concrete mixture proportions and hardened concrete electrical resistivities using AC and DC measurements (Hughes et al., 1985).

Mix	Cement content kg/m^3 – (lb/yd^3)	Cement paste volume fraction	Proportions by weight				Resistivity – DC (Ωm)		Resistivity – AC (Ωm)	
			Gravel	Sand	Cement	Water	7-day	28-day	7-day	28-day
1	400 (674)	0.287	3.08	1.54	1.00	0.40	60.2	77.5	54.9	70.7
2	400 (674)	0.307	3.00	1.50	1.00	0.45	45.0	58.6	41.6	53.0
3	400 (674)	0.327	2.92	1.46	1.00	0.50	42.0	54.6	39.4	48.6
4	400 (674)	0.347	2.82	1.41	1.00	0.55	35.7	43.5	30.9	37.9
5	350 (590)	0.268	3.62	1.81	1.00	0.45	56.3	64.0	50.3	59.6
6	350 (590)	0.286	3.53	1.76	1.00	0.50	49.7	58.9	42.9	5038
7	350 (590)	0.303	3.44	1.72	1.00	0.50	41.2	46.5	38.8	43.9
8	350 (590)	0.321	3.36	1.68	1.00	0.55	36.7	43.3	32.7	37.4
9	300 (506)	0.245	4.36	2.18	1.00	0.60	58.8	66.9	50.5	57.3
10	300 (506)	0.260	4.20	2.10	1.00	0.50	50.0	58.0	45.8	52.1
11	300 (506)	0.275	4.18	2.09	1.00	0.60	41.0	50.3	37.5	43.7
12	300 (506)	0.290	4.10	2.05	1.00	0.65	38.6	43.6	34.0	38.6

4.4.1 Concrete Resistivity and Chloride Ion Penetrability

Several researchers have reported a relationship between electrical resistivity and strength, water content, total charge passed (ASTM C 1202-97), and porosity (Hughes B P et al. 1985); (Rengaswamy N S et al. 1986); (Tashiro C et al. 1987); (Wilson J G et al. 1985). However, until recently there was no quantification of this relationship. Two researchers

have made an attempt to quantify the inner-relationship between the electrical resistivity of concrete and ASTM C 1202 results (Clear, K, 2000; Wee T. H., et al. 2000).

Figure 4.4 presents the quantification of the relationship between electrical resistivity and total charge passed as proposed by Clear (2000). Saturated concrete resistivity of 4-inch by 8-inch cylinders were determined using the Wenner array operating mode. AC resistance and the specimen temperature were also measured. The measured resistance was converted to a resistance at standard temperature 23 C (73 F) using the FHWA Time-to-Corrosion temperature adjustment relationship (Equation 4-9). An experimentally determined constant, 12.68, was used to convert the resistance at 73 F (R_{73}) to resistivity.

$$R_{73} = R_T \, e^{2883((1/295.78)-(1/T))} \qquad \textbf{Equation 4-9}$$

where T = the concrete temperature in degree K

The relationship between ASTM C1202 Charge Passes vs. Saturated Cylinder Resistivity is expressed in Equation 4-10.

$$y = 10^7 x^{-0.9602} \qquad \textbf{Equation 4-10}$$

where

y = Charge passed, in coulombs, and

x = the 100 x 200-mm (4 x 8-in) Saturated Concrete Cylinder Resistivity at 23 F in kΩ-cm.

Wee et. al (2000) investigated the permeability properties of silica fume concrete and slag cement concrete. The relationship between resistivity and total charge passed proposed by Wee is expressed in equations 4-11 and 4-12 for silica fume and slag cement concrete respectively (Figure 4.5).

$$y = 7864e^{-0.079x} \qquad \textbf{Equation 4-11}$$

$$y = 5986.1e^{-0.1136x} \qquad \textbf{Equation 4-12}$$

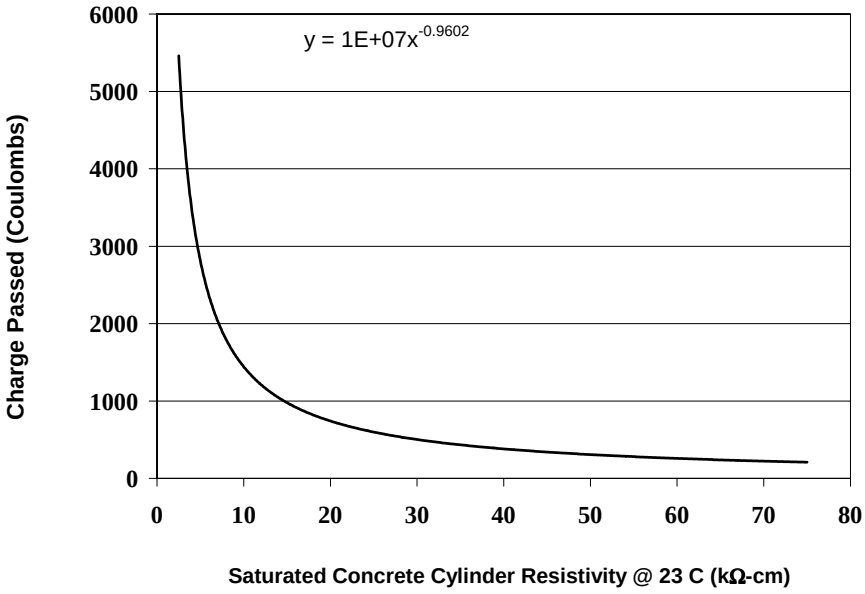

Figure 4.4. Relationship between resistivity and ASTM C 1202 as proposed by Clear (2000).

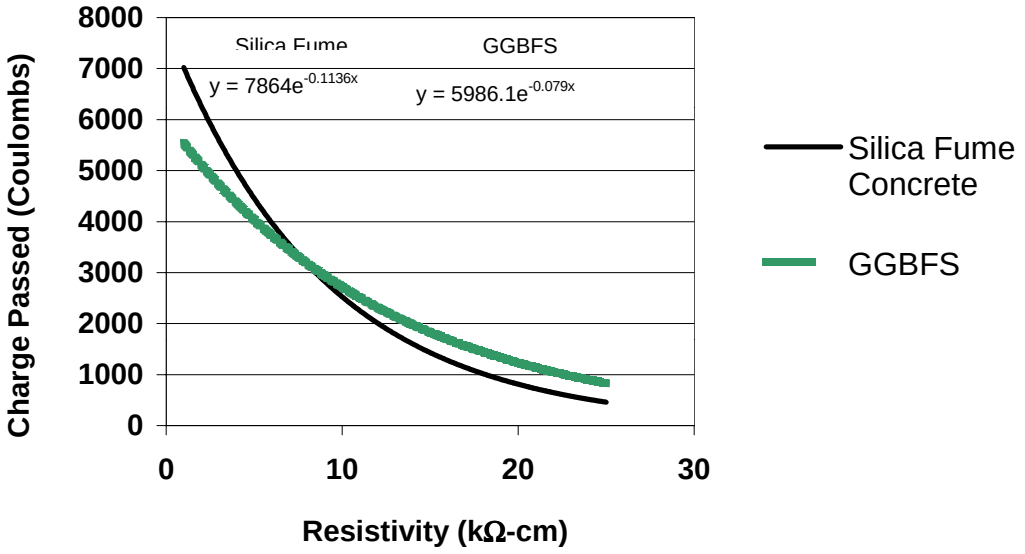

Figure 4.5. Relationship between resistivity and ASTM C 1202 as proposed by Wee et al. (2000).

CHAPTER 5. METHODS AND MATERIALS

5.1 RESEARCH SCOPE AND OBJECTIVES

The primary objective of this investigation is to evaluate the effectiveness of in-place testing methods in assessing the present quality of concrete as determined by ASTM C 1202-97, the standard laboratory test method. The secondary objective is to investigate the effect of initial moist curing period on the development of strength and long-term permeability.

This investigation included a laboratory and a field phase. The laboratory phase of this study investigated in-place permeability properties of six HPC bridge deck mixtures representative of those used in the Commonwealth of Virginia. In-place permeability test methods included electrical resistivity and the surface air flow (SAF) measurements. Permeation properties were assessed in the laboratory using ASTM C 1202-97. The field phase of this research used the previously described test methods to assess the permeation properties of a newly constructed concrete bridge deck element. The following sections present the methods and the materials used in this research program.

5.2 CONCRETE MIXTURES

The concrete mixtures used in the laboratory portion of this research represent a broad range of class 35 (A4) bridge deck mixtures used in the Commonwealth of Virginia. The three aggregate types used in the laboratory study were gravel (G), limestone (LS), and diabase (D). Diabase, the least familiar of the three, consists of augite and plagioclase with smaller amounts of quartz, potassium feldspar, biotite and opaque minerals (USGS).

A VDOT class 55 concrete was used in the field phase of this project. Table 5-1 presents the general VDOT specifications for class 35 and class 55 hydraulic cement concrete. The coarse aggregates and their respective fine aggregates used for the laboratory and field phase of this research meet VDOT Road and Bridge 1997 Specifications requirements. The aggregate properties for the laboratory mixtures are presented in Appendix A. The mixture proportions for the laboratory and field mixtures are presented in Appendix A.

Table 5-1. VDOT Requirements for Class 35 (A4), and 55 (A5) Hydraulic Cement Concrete.

Concrete Class	Specified Compressive Strength at 28-days (f'_c) (Mpa)	ASTM C 33 Aggregate Size No.	Nominal Max. Aggregate Size (mm)	Min. Cement Content (kg/ cu m)	Max w/c ratio	Slump (mm)	Air Content (%)
55 (A5)	55	57 or 68	25/19	375	0.40	0-175	4 ½ ± 1 ½
35 (A4)	28	57	25	375	0.45	50-175	5 ½ ± 1 ½

VDOT has proposed a special provision on low permeability concrete elements using ASTM C 1202-97. The provision on low permeability requires that the specimen be tested at 28-days after moist curing for 1 week at room temperature followed by three weeks at 38 C. The elevated temperature curing accelerates pore refinement and gives an indication of 6-month coulombs values at 28 days. The special provision requires a 28-day accelerated cure total charge passed value of 1,500 coulombs or less for prestressed concrete, 2,500 coulombs or less for bridge decks and 3,500 coulombs or less for the substructure (Ozyildirim 1998). The provision also states that moist curing be applied for a minimum of 7-days and until 70 percent of the minimum 28-day compressive strength is obtained. High performance, for the concrete mixtures used in this research, is defined as having a 28-day, accelerated cure total charged passed of 2,500 coulombs or less.

5.3 LABORATORY EXPERIMENTAL DESIGN

5.3.1 Test Specimen

The test specimens consisted of two concrete slabs having dimensions of 280 x 280 x 102-mm (11 x 11 x 4-in) and twenty-five 102 x 204-mm (4 x 8-in) cylinders per concrete mixture. Slab specimens were placed and remained in the formwork throughout the testing period. All test specimens were prepared in accordance with ASTM C 192-95.

The two types of curing regimes used in this study were standard moist curing and simulated field curing. Standard moist cure consisted of curing cylinder specimens in a saturated limewater bath. Specimens were left in the saturated limewater until the time of testing, or further conditioning. The simulated field-curing regime used wet burlap and

plastic sheeting for 3 and 7 days respectively and was applied to slabs and cylinders. One slab per mixture underwent the 3-day simulated field cure and the other slab underwent the 7-day simulated field cure. Each slab had a set of 8 companion test cylinders that underwent the same curing conditions. Table 5-2 presents the curing designation and description for each curing regime.

Table 5-2. Curing designations, descriptions and number of test specimens per mix.

Curing designation	Abbreviation	Description
3-day simulated field cure	3B	Specimens were cured for 3-days under wet burlap and plastic sheeting, then allowed to cure in laboratory environment for 4-days before being placed outdoors.
7-day simulated field cure	7B	Specimens were cured for 7-days under wet burlap and plastic sheeting before being placed outdoors.
Standard curing	W	Specimens were cured continuously in limewater after initial 24-hr moist cure period until time of testing, or further conditioning.
Accelerated cure	A	Specimens were continuously cured in limewater for 7 days and then allowed to cure in 38 C water bath for 21-days prior to testing.

Test specimens were cast and allowed to achieve initial set before application of the wet burlap and plastic sheeting. The control cylinders were moved into the saturated limewater bath after initial 24-hour moist curing under wet burlap and plastic sheeting. The remaining specimens were cured for 3 and 7 days respectively under wet burlap and plastic sheeting in the laboratory environment. The simulated field-cured specimens were sprayed with water daily to ensure idea moisture conditions for hydration. All simulated field cured specimens were placed outdoors at the age of 7 days.

Cylinder specimens were labeled according to aggregate, additive materials, Microsilica (MS), Ground Granulated Blast-furnace Slag (SG), and Fly Ash (FA), and the initial curing condition, type of testing and age at time of testing. Slab specimens were labeled in accordance with aggregate type, pozzolanic material, and initial curing conditions. A cylinder specimen containing Diabase aggregate with Ground Granulated Blast-furnace Slag, with an initial curing of 3 days wet burlap and plastic sheeting tested for chloride ion penetrability (P) at 28-days would be labeled DSG-3B28P. The corresponding slab specimen would be labeled DSG-3B.

5.3.2 Specimen Testing

Slabs were tested on finished surface using the SAF at 28 and 91 days, and 4-point electrical resistivity measurements at 1, 3, 7, 14, 28 and 91 days. Compressive strength (CS) tests were conducted at 7 and 28 days. Chloride ion penetrability tests were performed at 7, 28, and 91 days. The Virginia Transportation Research Council (VTRC) conducted all chloride ion penetrability tests. All other tests were conducted at Virginia Tech facilities. Electrical resistivity measurements were taken on cylinder specimens at 7, 14, 28 and 91 days. Table 5-3 presents the laboratory-testing matrix.

5.3.3 Test Methods

Hardened concrete properties were assessed using chloride ion penetrability (P), concrete compressive strength (CS), electrical resistivity and relative permeability (SAF). Compressive strength testing was conducted in accordance with ASTM C 39-96. All compressive strength cylinders were capped with sulfur in accordance with ASTM C 617-94. There is no standard test method for electrical resistivity. The test method that governs the SAF meter is AASHTO Designation: TP26-94. The chloride ion penetrability was performed in accordance to ASTM C 1202-97. A brief summary of the testing procedures follows.

ASTM C 1202-97

All chloride penetrability specimens were sent to the Virginia Transportation Research Council (VTRC) for testing. Two 2-in (50-mm) samples were cut from each

specified test cylinder. The first sample contained one finished and one cut surface, the other sample both surfaces were exposed (or cut). The sides of the test specimens were coated with epoxy. The specimens were then vacuum saturated for 3 hours in distilled water. The samples were left in the water bath for at least 18 hours prior to time of testing.

Table 5-3. Testing matrix.

Test Specimen	Laboratory Testing
Slabs 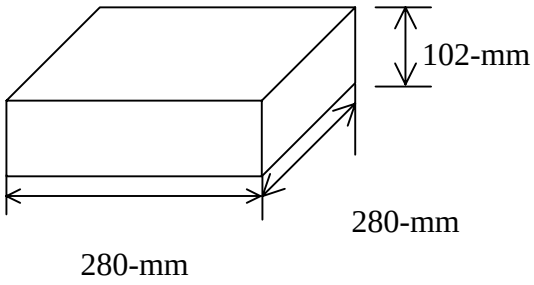 	▪ **4-pont electrical resistivity** *1, 3, 7, 14 and 91-day testing* ▪ **SAF** *28 and 91 testing*
Cylinders 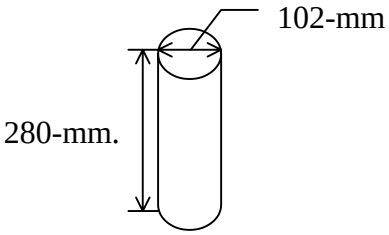 	▪ **4-point electrical resistivity** *7, 14, 28 and 91-day testing* ▪ **ASTM C 1202-97** *7, 28 and 91-day testing* ▪ **Compressive Strength ASTM C39** *7 and 28 days*

Once the specimen was conditioned for testing, one end was immersed in a sodium chloride solution and the other in a sodium hydroxide solution. A 60 V potential was maintained across both ends. The amount of current passing through the test specimen was measured for 6 hours. The plot of current versus time was integrated, which yields the total charge passed. The total charge passed, in coulombs, gives an indication of the chloride permeability of the specimen.

AASHTO Designation: TP-26-94 Standard Test Method for Determining the Relative Permeability of Concrete by Surface Air Flow.

This test method describes the procedure for determining the rate of air flow out of the surface of a concrete element under vacuum pressure. The SAF device used in this study

is manufactured by the Texas Research Institute. This packaged system was used for all SAF investigations. The general testing procedure is as follows:

The concrete test surface is cleaned of all excess debris. Special attention is given to locating cracks or surface irregularities that may prevent the vacuum from obtaining a good seal. The vacuum plate is placed against a steel plate and the flow is observed to check if there is any system leakage. The testing standard calls for spot drying of the concrete surface in order to reduce the effects of moisture content, if the concrete element has received a significant amount of moisture 24 hours prior to testing.

The vacuum plate is placed on the test site. The power switch is turned on and the initial pressure recorded. The vacuum pump is switched on, and the pressure is then monitored, until the pressure level has stabilized, and the air-flow reading is then recorded.

The following should be noted in reference to surface air flow measurements:

- Spot drying was not used in this research plan because care was taken to remove the test specimens from the outdoor environment 24 hours prior to testing.
- During testing vacuum grease was placed along the face of the foam gasket to ensure no leakage occurred between the vacuum face plate and the concrete surface, ensuring an adequate air seal.

Electrical Resistivity

Electrical resistivity measurements were taken on both slabs and cylinder specimens. A Nelson Model 400 4-pin soil resistance meter was configured to measure concrete resistivity. Four equally spaced water saturated wood contact points were placed on the concrete surface. The water saturated wood contact spacing was set at 50-mm (2-in). The slabs were tested on the finished surface. The cylinders were tested longitudinally along it height on the cast surface.

5.4 FIELD INVESTIGATION

A section of the Wilson Creek Bridge project in Montgomery County Virginia was used to assess the effectiveness of in-place test methods in assessing the permeation

properties on a concrete element under construction. The specified minimum 28-day concrete strength for the Wilson Creek Bridge project was 55 Mpa (8000 psi).

5.4.1 Test specimens

Construction personnel cast test specimens, mini-slabs and cylinders, on-site, during the placement of deck sections A and B. The mini-slabs and test cylinders were 280 x 406 x 102-mm (11 x 16 x 4-in) and 102 x 204-mm (4 x 8-in) respectively. A total of four test mini-slabs were cast on-site, two for each test section. A set of test cylinders was cast for standard permeability and strength testing. Two mini-slabs, one from each deck section, underwent the same curing and environmental conditions as the deck test sections. The deck section was cured for two-days under a wet burlap blanket (2B). The remaining specimens were transported to the Virginia Tech laboratory for testing.

5.4.2 Test methods

Field prepared slab specimens that were transported to the Virginia Tech facility were tested at 7, 14, 28, 42 and 91-days using electrical resistivity. SAF air flow measurements were performed at 28 and 91-days. Slab specimens that were left in the field were tested at the same time deck testing occurred. Permeation properties were measured on bridge deck section A at 14, 42 and 28-days. Section B was tested at 42 and 91-days. Field test ages were weather and construction constraint dependent. The as-built element was allowed to dry at least 48-hrs after significant rainfall.

CHAPTER 6. PRESENTATION OF RESULTS

6.1 INTRODUCTION

This section presents the results from the experimental research plan. The results are presented as laboratory and field results. Laboratory mixtures are referred to as Plain Portland Cement Concrete (PPCC) and High-performance Portland Cement Concrete (HPCC) mixtures. The PPCC mixtures are identified by aggregate type (e.g. LS identifies the limestone mixture). The HPCC mixtures are identified by aggregate type and type of supplementary cementitious materials (e.g. DMS identifies the diabase with microsilica mixture). The field mixture is designated as bridge mix (BM).

6.2 LABORATORY INVESTIGATION

The in-place permeability of six laboratory bridge deck mixtures used in the Commonwealth of Virginia was assessed using electrical resistivity, surface air flow, and ASTM C 1202-97. Compressive strength measurements were taken at 7 and 28-days for all mixtures. Concrete mixture proportions are presented in Appendix A. Information on the test specimens and curing conditions were presented in Section 5, Methods and Materials.

6.2.1 Compressive Strength

Compressive strength results for 7 and 28-days are presented in Table 6-1, individual measurements are presented in Appendix B. The seven-day results are for a single test cylinder under standard curing conditions, 7W. The 28-day compressive strength results are an average of two test specimen for each curing condition 3B, 7B and 28W.

6.2.1.1 Plain Portland Cement Concrete (PPCC) Mixtures

6.2.1.1.1 Seven-day Compressive Strength Results

The seven-day compressive strength values were 28, 33, and 40-Mpa (4060, 4850 and 5770-psi) respectively for mixtures G, LS, and D. The results differ according to aggregate

type, the highest strength exhibited by mixture D (diabase) followed by LS (limestone) and G (gravel).

Table 6-1.Compressive strength for laboratory mixtures at 7 and 28-days[1]

		Compressive Strength, Mpa					
Curing Condition	**Test Age (days)**	**G**	**LS**	**D**	**DSG**	**DFA**	**DMS**
7W	7	28	33	40	29	28	38
28W	28	36	43	48	45	39	42
3B	28	36	42	40	38	36	46
7B	28	37	45	46	42	37	46

[1] 7-day values are for a single cylinder, 28-day values are an average of two cylinders.
***1Mpa ≅ 145 psi**

6.2.1.1.2 Twenty-eight day Compressive Strength Results

The 28-day compressive strength results for PPCC mixtures, cured under standard conditions, were 36, 43, and 48-Mpa (5290, 6280 and 6900-psi) for mixtures G, LS and D respectively. The 28-day compressive strengths differ according to aggregate type similarly to 7-day results.

The 28-day compressive strength results for PPCC specimen under 3B curing conditions were 36, 42 and 40-Mpa (5290, 6090 and 5790-psi) for mixtures G, LS, and D respectively. Twenty-eight day compressive strength results for PPCC mixtures, cured under 7B curing conditions, were 37, 45, and 46-Mpa (5370, 6540 and 6720-psi) for G, LS and D mixtures respectively. All PPCC mixtures, under all curing conditions, achieved the minimum specified 28-day compressive strength of 28 Mpa (4000-psi).

6.2.1.2 High-performance Portland Cement Concrete (HPCC) Mixtures

6.2.1.2.1 Seven-day Compressive Strength Results

The seven-day compressive strength results for HPCC mixtures were 29, 28, and 38-Mpa (4220, 4020 and 5570-psi) for mixtures DSG, DFA and DMS. The results differ according to the type of supplementary cementious material with mixture DMS exhibiting

the highest strength followed by DSG and DFA. The DMS mixture achieved the minimum specified 28-day compressive strength of 28 Mpa (4000-psi) at 7-days.

6.2.1.2.2 Twenty-eight day Compressive Strength Results

Twenty-eight day compressive strength results for HPCC mixtures, under standard curing conditions, were 45, 39, and 42-Mpa (6460, 5590 and 6160-psi) differing according to additive type, with DMS achieving the highest compressive strength followed by DSG and DFA. All of the HPCC mixtures under standard conditions achieved the minimum specified 28-day strength of 28Mpa (4000 psi).

HPCC mixtures under the 7B curing regime achieved higher 28-day strengths as compared to specimens under 3B curing. Although increased strength is achieved with additional initial simulated curing period, all HPCC specimens achieved the specified minimum 28-day compressive strength under 3B curing conditions.

6.2.2 Chloride Ion Penetrability Test (ASTM C 1202-97)

Chloride ion penetrability test were conducted on cylinder specimens for each concrete mixture at 7, 28 and 91 days. A total of two 2-inch test specimens per concrete cylinder were cut from the top four inches of concrete. The chloride ion penetrability results for specimens containing the top two inches of cylinder specimens are presented in this section because it is representative of the cover concrete. Results of total charge passed and initial current for all test specimens are presented in Appendix C. Table 6-2 presents the average ASTM C 1202-97 results for the top surface.

Twenty-eight day results for specimens undergoing the elevated temperature cure, were used to evaluate the effectiveness of all concrete mixtures in attaining high performance status. High-performance as defined be VDOT permeability provision is concrete having a total charge passed of less then 2,500 coulombs at 28 days, for specimen undergoing accelerated temperature cure.

Table 6-2. ASTM C 1202-97 results for laboratory specimens, top finished surface.

Curing Condition	Test Age (days)	Total Charge Passed, Coulombs					
		G	LS	D	DSG	DFA	DMS
3W	7	5276	8703	7889	4295	8482	4704
7W	7	5200	5894	6311	3855	8487	4777
28W	28	3860	3332	3684	2199	4796	2166
3B	28	4237	3717	4626	2485	3989	1892
7B	28	3765	3890	3746	2356	3306	1735
91W	91	2919	2185	3164	1526	1166	1023
3B	91	3323	2621	2055	2073	1119	1165
7B	91	2961	2635	2306	1547	1336	1234
28WA[1]	28	3767	2325	2543	1238	839	979

Results are an average of two test specimen unless otherwise noted
[1] Specimen were cured in accelerated temperature water bath after 7 days initial moist curing (7W), only one sample per result.

6.2.2.1 Plain Portland Cement Concrete (PPCC) Mixtures

6.2.2.1.1 Seven-day Chloride Ion Penetrability Results

The seven-day total charged passed for PPCC mixtures range from 5200 coulombs to 8700 coulombs for 3W and 5200 to 6300 coulombs for 7W specimens. Although the total charge passed for 7W specimens are lower than 3W specimens, both sets of specimens achieve a penetrability rating of *high*.

6.2.2.1.2 Twenty-eight day Chloride Ion Penetrability Results

The 28-day penetrability results for all PPCC mixtures, cured at standard conditions, are within the 2000 – 4000 coulomb range, indicating no apparent difference in penetrability with respect to aggregate type.

The penetrability values at 28-days for PPCC mixtures cured under the 3B and 7B regimes obtained total charge values of approximately 4,000 coulombs. A 28-day penetrability rating of *high* was achieved for mixtures G and D under 3B curing conditions. Mixture LS, under 3B curing conditions, achieved a penetrability rating of moderate at 28-

days. All PPCC mixtures cured under 7B conditions achieved a penetrability rating of moderate.

6.2.2.1.3 Elevated Temperature Cured 28-day Chloride Ion Penetrability Results

The elevated temperature results for PPCC mixtures are 3767, 2325 and 2543 coulombs respectively for G, LS, and D. Mixtures LS and D may be considered high performance concrete in terms of low permeability, having obtained a penetrability value of approximately 2500 coulombs or less.

6.2.2.1.4 Ninety-one day Results

The 91-day penetrability results, under standard curing conditions, were approximately 2920, 2190 and 3160 coulombs respectively for mixtures G, LS and D. All PPCC mixtures under standard curing conditions at 91 days were classified as *moderately permeable* according to ASTM C 1202-97. There is no difference in penetrability rating at 91 days with respect to aggregate type or simulated field curing conditions.

6.2.2.2 High-performance Portland Cement Concrete (HPCC) Mixtures

6.2.2.2.1 Seven-day Chloride Ion Penetrability Results

The seven-day penetrability results approximately ranged from 4000 to 8500 coulombs for both 3W and 7W specimens. The penetrability rating for all HPCC mixtures at seven-days is *high* having a total charge passed greater than 4,000 coulombs, the exception being DSG-7W. Specimen DSG-7W achieved a total charge passed on 3855-coloumbs and a penetrability rating of moderate.

The addition of slag and microsilica produces lower penetrability results at 7 days for both initial curing regimes compared to results for the mixture D. The addition of fly ash had no relative affect on the 7-day penetrability results as compared to mixture D.

6.2.2.2.2 Twenty-eight day Chloride Ion Penetrability Results

The 28-day penetrability results for HPCC mixtures under standard curing conditions are 2199, 4796 and 2166 coulombs for DSG, DFA, and DMS, respectively. Mixtures DSG and DMS reach the desired high performance total charge passed of less than 2,500 coulombs at 28-days under standard conditions.

The 28-day penetrability results for HPCC mixtures are not significantly different with respect to simulated field curing regimes. Mixtures DSG and DMS achieved a 28-day total charge passed of less than 2,500 coulombs for both simulated field curing regimes.

6.2.2.2.3 Elevated Temperature Cured 28-day Chloride Ion Penetrability Results

The elevated temperature cured results for HPCC mixtures were 1240, 840 and 980 coulombs for DSG, DFA and DMS, respectively. All HPCC mixtures obtained an accelerated cured chloride penetrability result of 1,200 coulombs or less, significantly lower than the 2,500 coulombs needed for HPC classification.

6.2.2.2.4 Ninety-one day Chloride Ion Penetrability Results

The 91-day penetrability results for HPCC mixtures, under standard curing conditions, were 1526, 1170 and 1023 coulombs for DSG, DFA and DMS, respectively. The DFA mixture obtained a lower penetrability result for all curing regimes. No significant difference is observed in the 91-day chloride penetrability results with respect to simulated field-curing period, the exception being mixture DSG. The difference in mixture DSG, with respect to simulated field curing regimes, resulted in a change in the ASTM C 1202-97 penetrability rating from *moderate* for 3B to *low* for 7B.

6.2.3 Electrical Resistivity

Electrical resistivity measurements were taken on both slabs and cylinders, using the Wenner 4-point array method. The slabs were tested on the finished surface at 1, 3, 7, 14, 28 and 91 days. The cylinder specimens were tested longitudinally along its height on the cast

surface. Cylinder specimens cured under standard conditions (W) were tested at 7, 14, 28 and 91-days. Simulated field cured specimens, 3B and 7B were tested at 14, 28 and 91-days.

6.2.3.1 Slab Specimens

Tables 6-3 and 6-4 present resistivity results for slab specimens for PPCC and HPCC mixtures respectively. Individual resistivity measurements along with summary statistics tables, and graphs are presented in Appendix D. One-way Analysis of Variance was performed at the 95% confidence level to determine for each individual curing regime the effect of aggregate type for PPCC specimens and supplementary cementitious material type for HPCC mixtures.

6.2.3.1.1 Plain Portland Cement Concrete (PPCC) Mixtures

Figures 6.1, 6.2 and 6.3 present electrical resistivity vs. time PPCC slab specimens for G, LS and D respectively. The error bars represent the 95 % confidence limits for 3B and 7B resistivity results, respectively.

The 1-day resistivity for all PPCC mixtures was less than 10 kΩ-cm. The influence of aggregate type on resistivity measurements is observed as early as 3 days, with LS exhibiting a resistivity value significantly higher than D and G for both curing regimes.

Seven-day results are the first test time where curing regimes are significantly different. No significant difference was observed, at the 95% confidence level, for 7-day resistivity measurements, in regard to differing curing regimes for PPCC mixtures. The 14-day resistivity results for PPCC slab specimens ranged from 8 to 14 kΩ-cm for both simulated field curing regimes. No significant difference was observed, at the 95% confidence level, for 14-day resistivity measurements, in regard to differing curing regimes for PPCC mixtures.

The 28-day resistivity results ranged from 14 kΩ-cm to 48 kΩ-cm. The 28-day resistivity values were slightly higher than the 14-day results, the exception being mixture D. Significant differences, at the 95% confidence level, were observed in the resistivity results for mixtures D and LS with respect to curing conditions.

The 91-day results range from 19 kΩ-cm to 25 kΩ-cm. The 91-day resistivity measurements indicate no significant difference in regard to curing regime for all PPCC mixtures. The 91-day resistivity results indicate differences, with respect to aggregate type, that are on the order of magnitude of 3 to 5 kΩ-cm.

Table 6-3. Electrical resistivity for PPCC slab specimens.[1]

	1-day		3-day		7-day		14-day		28-day		91-day	
	3B	7B	3B	7B	3B	7B	3B	7B	3B	7B	3B	7B
G	7.15^{a}	6.30^{b}	7.18^{c}	7.26^{e}	9.35^{g}	13.02^{i}	9.62^{k}	9.78^{m}	14.19^{o}	14.81^{r}	21.68^{t}	23.07^{u}
LS	5.96^{a}	4.32^{b}	38.68^{d}	54.00^{f}	21.16^{h}	27.46^{j}	14.28^{l}	14.86^{n}	17.94^{p}	20.54^{r}	25.39^{u}	27.42^{v}
D	5.63^{a}	5.80^{b}	12.66^{c}	18.53^{e}	14.08^{g}	13.59^{i}	10.77^{kl}	16.24^{n}	15.51^{q}	47.95^{s}	19.93^{t}	21.83^{u}
p-value	0.197	0.109	0.002	0.004	0.000	0.000	0.002	0.000	0.000	0.000	0.001	0.001

[1] For a given age and curing condition resistivity results with identical letter notation shared are not statistically different.

Table 6-4. Electrical resistivity for HPCC slab specimens.[1]

	1-day		3-day		7-day		14-day		28-day		91-day	
	3B	7B	3B	7B	3B	7B	3B	7B	3B	7B	3B	7B
DSG	21.53^{a}	25.79^{c}	20.74^{e}	43.41^{h}	15.02^{j}	15.87^{l}	18.08^{m}	21.64^{o}	27.67^{p}	30.55^{r}	53.26^{u}	48.21^{w}
DFA	13.08^{ab}	7.26^{d}	40.75^{f}	46.52^{h}	6.86^{k}	10.08^{l}	14.44^{m}	14.99^{o}	18.00^{q}	19.02^{s}	57.30^{u}	52.27^{w}
DMS	5.12^{a}	7.20^{d}	7.73^{g}	7.11^{i}	15.36^{j}	13.72^{l}	18.31^{m}	18.82^{o}	25.74^{p}	25.37^{t}	29.08^{v}	31.29^{x}
p-value	0.000	0.000	0.000	0.000	0.001	0.880	0.006	0.203	0.000	0.000	0.000	0.000

[1] For a given age and curing condition resistivity results with identical letter notation shared are not statistically different.

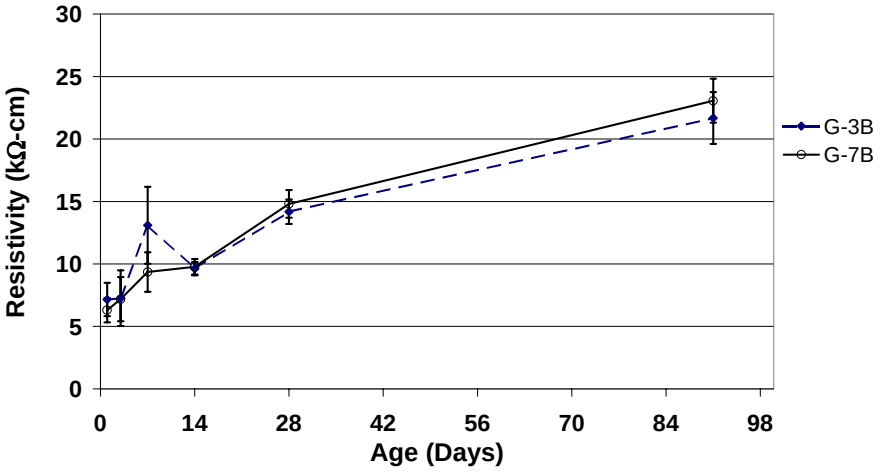

Figure 6.1. Electrical resistivity vs. age, Gravel (G) slab specimens.

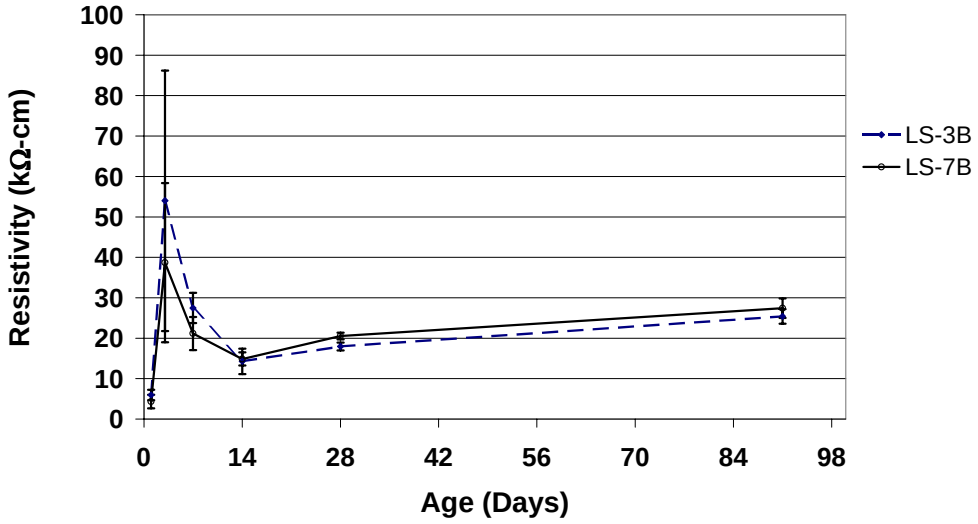

Figure 6.2. Electrical resistivity vs. age, Limestone (LS) slab specimens.

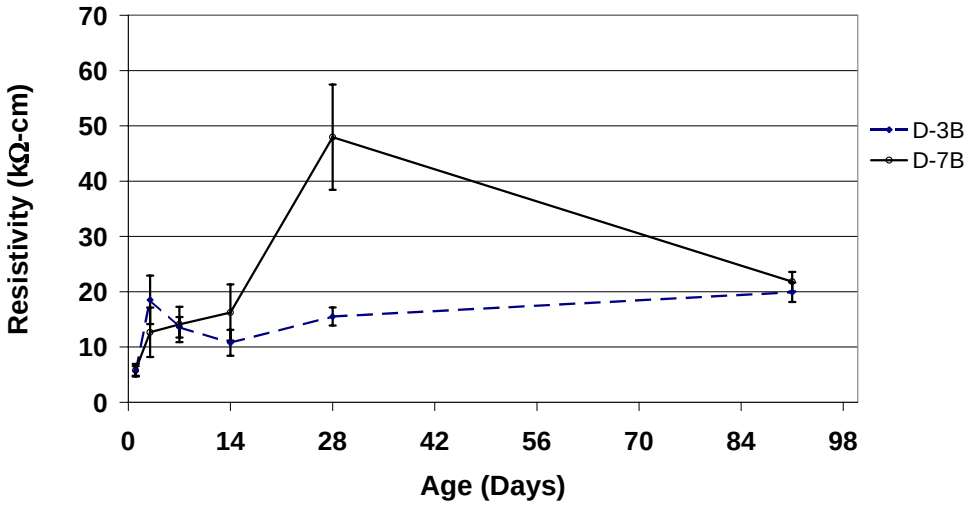

Figure 6.3. Electrical resistivity vs. age, Diabase (D) slab specimen.

6.2.3.1.2 High-performance Portland Cement Concrete (HPCC) Mixtures

Figures 6.4, 6.5 and 6.7 present electrical resistivity vs. time for HPCC mixtures DSG, DFA, and DMS. The error bars on resistivity plots represent the 95% confidence limits for 3B and 7B resistivity results, respectively.

The 1-day resistivity results for HPCC range from 4 kΩ-cm to 24 kΩ-cm with DSG exhibiting the highest value. The influence of additive type on resistivity measurements is observed as early as 1 day, with resistivity values of 4, 10 and 24 kΩ-cm for DMS, DFA and DSG respectively. At 3 days DFA achieves the highest resistivity followed by DSG and DMS.

The seven-day resistivity results ranged from 6 to 15 kΩ-cm and 10 to 16 kΩ-cm respectively, for 3B and 7B specimens. No significant difference was observed at the 95% confidence level between seven-day resistivity results for mixtures DSG and DMS in regard to curing regimes and supplementary cementitious material type. The resistivity result for mixture DFA was significantly lower as compared to other HPCC mixtures.

The fourteen-day resistivity results for HPCC slab specimens ranged from 14 to 18 kΩ-cm for both simulated field curing regimes. No significant difference was observed, at the 95% confidence level, for 14-day resistivity measurements, in regard to differing curing regimes and supplementary cementitious materials.

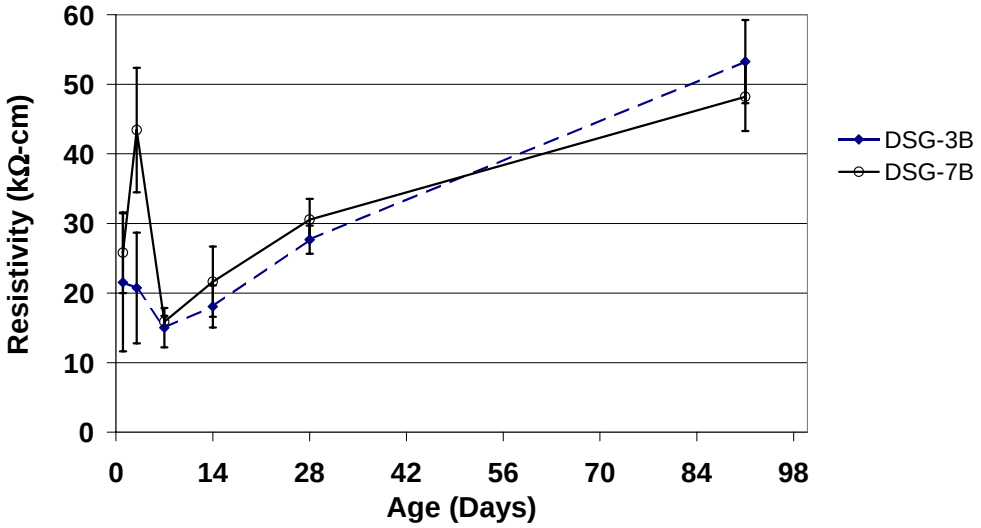

Figure 6.4. Electrical resistivity vs. age, Diabase Slag (DSG) slab specimens.

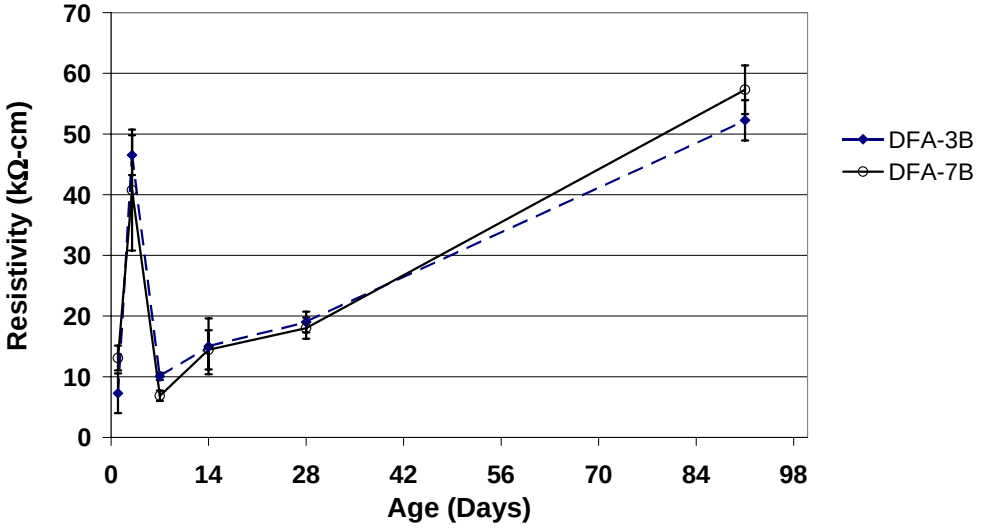

Figure 6.5. Electrical resistivity vs. age, Diabase Fly Ash (DFA) slab specimens.

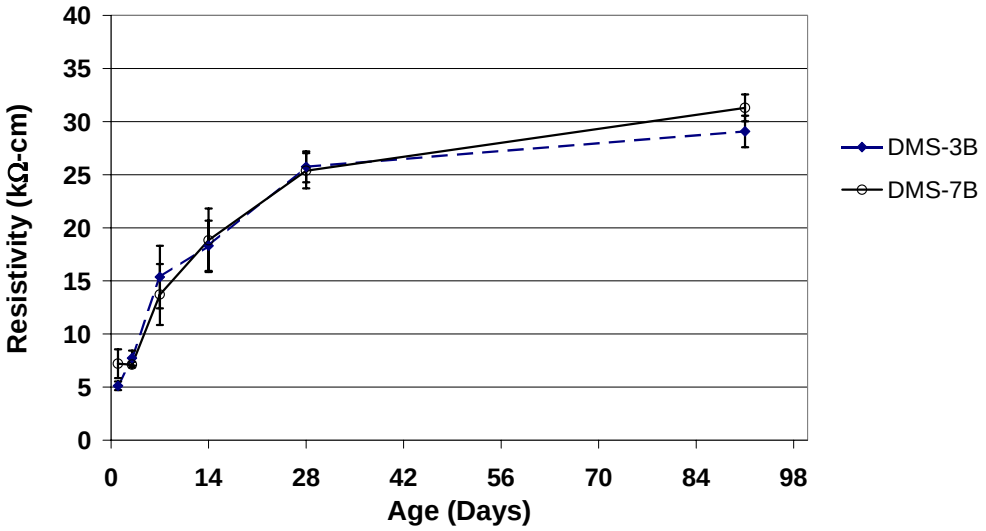

Figure 6.6. Electrical resistivity vs. age, Diabase Microsilica (DMS) slab specimens.

The 28-day resistivity results range from 18 kΩ-cm to 27 kΩ-cm. No significant difference was observed in HPCC specimen, at the 95% confidence level, for 28-day resistivity measurements, in regard to differing curing regimes. The 28-day resistivity results for mixture DSG and DMS are statistically the equivalent. Mixture DFA achieves a resistivity result significantly lower than other HPCC mixtures.

No significant difference was observed, at the 95% confidence level, for 91-day resistivity measurements, in regard to differing curing regimes. The 91-day resistivity results were 48.21, 52.27 and 31.29- kΩ-cm respectively for HPCC mixtures DSG, DFA and DMS. No statistical difference is observed for 91-day results for mixture DSG and DFA. The 91-day resistivity for mixture DMS is significantly lower than the other HPCC mixtures.

6.2.3.2 Cylinder specimens

Table 6-5 and 6-6 present the average resistivity results respectively for PPCC and HPCC cylinder specimens. Individual resistivity measurements along with summary statistics tables, and graphs are presented in Appendix D. One-way Analysis of Variance was performed at the 95% confidence level to determine for each individual curing regime the effect of aggregate type for PPCC specimens and supplementary cementitious material type for HPCC mixtures.

Table 6-5. Electrical resistivity for PPCC cylinder specimens.[1]

	7-day	14-day			28-day			91-day		
	W	**W**	**3B**	**7B**	**W**	**3B**	**7B**	**W**	**3B**	**7B**
Gravel	12.70^{a}	15.59^{b}	12.23^{d}	13.58^{f}	15.29^{h}	15.96^{k}	16.31^{n}	19.17^{q}	21.29^{t}	21.18^{v}
Limestone	21.16^{b}	19.70^{c}	19.78^{e}	17.43^{g}	26.98^{i}	24.55^{l}	30.05^{o}	26.32^{r}	30.89^{u}	28.61^{w}
Diabase	14.08^{a}	15.98^{b}	12.04^{d}	15.63^{fg}	21.64^{j}	19.92^{m}	22.13^{p}	20.91^{s}	22.57^{t}	21.41^{v}
p-value	0.000	0.000	0.000	0.000	0.000	0.000	0.000	0.000	0.000	0.000

[1] For a given age and curing condition resistivity results with identical letter notation shared are not statistically different.

Table 6-6. Electrical resistivity for HPCC cylinder specimens.[1]

	7-day	14-day			28-day			91-day		
	W	**W**	**3B**	**7B**	**W**	**3B**	**7B**	**W**	**3B**	**7B**
DSG	15.87^{a}	26.55^{d}	30.99^{f}	29.06^{i}	39.71^{k}	38.87^{m}	39.55^{p}	46.26^{s}	60.37^{v}	60.49^{y}
DFA	10.08^{b}	18.56^{e}	13.67^{g}	19.06^{j}	42.45^{k}	22.48^{n}	24.58^{q}	49.45^{t}	78.41^{w}	69.94^{z}
DMS	12.78^{c}	18.07^{e}	20.63^{h}	20.25^{j}	33.19^{l}	50.86^{o}	48.59^{r}	53.37^{u}	49.48^{x}	53.88^{A}
p-value	0.000	0.000	0.000	0.000	0.000	0.000	0.000	0.000	0.000	0.000

[1] For a given age and curing condition resistivity results with identical letter notation shared are not statistically different.

6.2.3.2.1 Plain Portland Cement Concrete (PPCC) Mixtures

Figure 6.7 presents the electrical resistivity with time for PPCC slab specimens under standard curing conditions. The seven-day resistivity is 12.70, 21.16, and 14.07-kΩ-cm for mixtures G, LS, and D respectively. At the 95% confidence level there is no significant difference in seven-day cylinder resistivity for mixtures D and G. Mixture LS exhibits the highest early age resistivity. At fourteen days the resistivity results for cylinder specimens D and G statistically equivalent, while mixture LS continues to achieve a significantly higher resistivity.

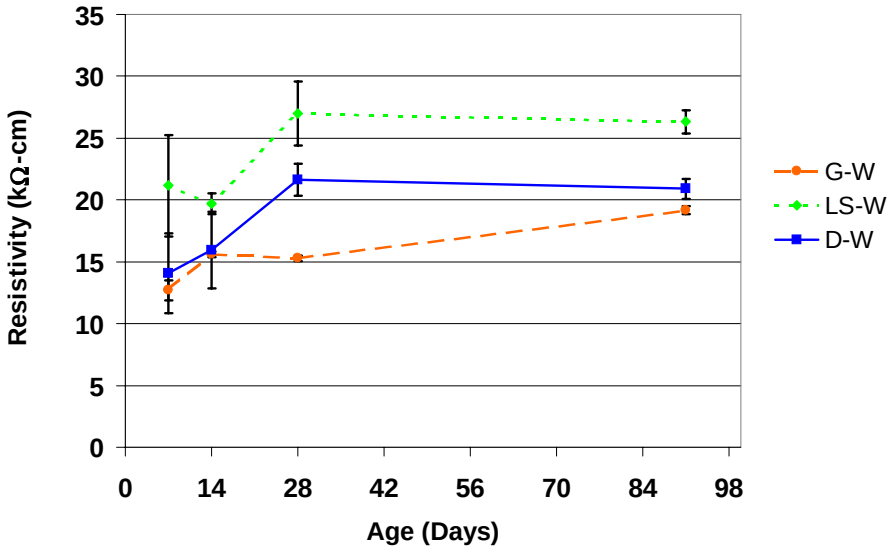

Figure 6.7. Electrical Resistivity with age, PPCC mixtures under standard curing.

A significant difference is observed at the 95% confidence level in the 28 and 91-day resistivity results, with respect to aggregate type. The 28-day resistivity results were 15.28, 26.98, and 21.64-kΩ-cm respectively for mixtures G, LS and D. The 91-day resistivity values were 19.18, 26.32-kΩ-cm and 20.91 respectively for mixtures G, LS, and D.

Figure 6.8 presents the electrical resistivity with age for Gravel cylinder specimens under curing conditions W, 3B, and 7B. No difference is observed between electrical resistivity results, with regard to simulated field curing regimes in PPCC mixtures at all ages. Mixtures LS and D achieve resistivity results similar to mixture G, in respect to simulated

curing regimes. Figures similar to Figure 6.8 are presented in Appendix D for all PPCC cylinder specimens.

6.2.3.2.2 High-Performance Portland Cement Concrete (HPCC) Mixtures

Electrical resistivity with time for HPCC and mixture D cylinder specimens, under standard curing conditions is presented in Figure 6.9. The 7-day resistivity results for HPCC specimens range from 10 to 16-kΩ-cm. The 14-day range of resistivity results for HPCC is 19 to 27-kΩ-cm which is significantly higher than 7-day results.

The 28-day resistivity is 39.71, 42.45, and 33.19-kΩ-cm for mixtures DSG, DFA and DMS. The 91-day range of resistivity values is 46 to 54-kΩ-cm. The resistivity of HPCC mixtures at 28 and 91-days are higher compared to mixture D.

Figure 6.10 presents the electrical resistivity with age for DSG cylinder specimens under curing conditions W, 3B, and 7B. No difference is observed between electrical resistivity results, with regard to simulated field curing regimes in DSG at all ages. Mixtures DFA and DMS exhibit behavior similar to DSG with respect to simulated curing regimes. Figures for resistivity with age for all HPCC mixtures are presented in Appendix D.

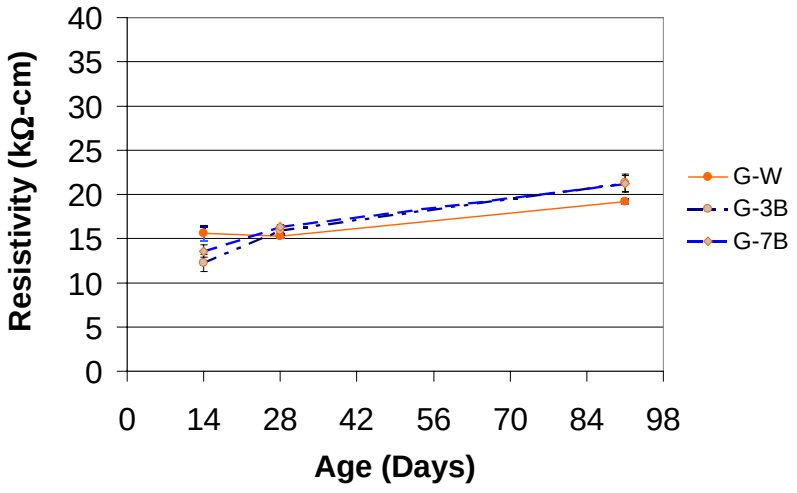

Figure 6.8. Resistivity with age for Gravel cylinder specimens.

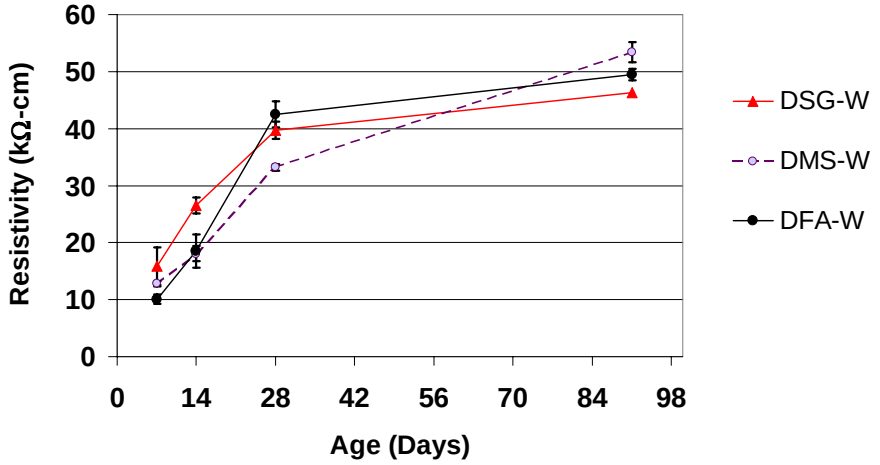

Figure 6.9. Electrical Resistivity with age, HPCC mixtures under standard curing.

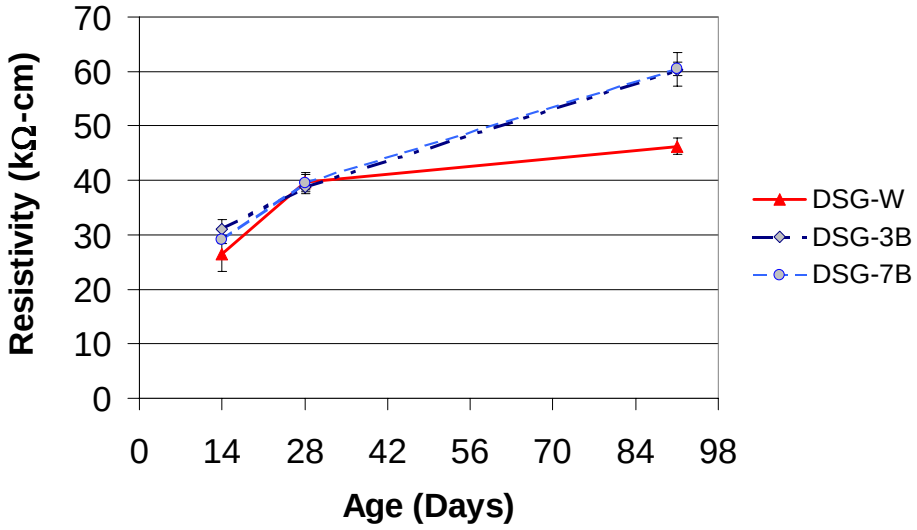

Figure 6.10. Resistivity with age for Diabase –Slag Cement(DSG) cylinder specimens.

6.2.4 Surface Air Flow

Surface air flow measurements were taken on the finished surface at 28 and 91 days for PPCC slab specimens. Testing of HPCC mixtures were conducted only at 91 days. Table 6-7 presents SAF data for all laboratory mixtures, which is an average of 10 measurements. No significant difference is observed with respect to simulated field curing regimes for PPCC and HPCC mixtures. Mixtures G and D, at 28 days, are rated as having a

low relative permeability, while mixture LS is rated as moderately permeable. All mixtures achieve a rating of low at 91 days.

Table 6-7. Surface Air Flow (ml/minute) for laboratory mixtures.[1]

	Surface Air Flow (ml/minute)			
	28-day		91-day	
	3B	7B	3B	7B
G	15	17	22	26
LS	35	40	26	30
D	14	28	26	29
DSG	X	X	24	23
DFA	X	X	22	29
DMS	X	X	28	25

[1]Results are an average of 10 measurements.

6.3 FIELD INVESTIGATION

Electrical resistivity, surface air flow, and chloride ion penetrability tests were used to assess the permeation properties of a section of the Wilson creek bridge and corresponding laboratory samples. Resistivity measurements were taken on laboratory slab specimens at 7, 14, 28, 42 and 91 days. The deck sections and the corresponding field cured test specimen were tested on 14, 42 and 91 days using SAF, resistivity and ASTM 1202-97. The compressive strength was measured at 7 and 28 days.

6.3.1 Compressive Strength

Compressive strength results for field mixtures are presented in Table 6-8. The results are an average of two moist cured cylinders, per section. Individual compressive strength results are presented in Appendix A. The 7-day compressive strength for sections A and B is approximately 48 Mpa (7000 psi). The 28-day compressive strength results are 62 Mpa (8990 psi) and 59 Mpa (8550 psi) for specimens from sections A and B respectively, both meeting the minimum specified 28-day compressive strength of 55 Mpa (8000 psi).

Table 6-8.Compressive strength for Wilson Creek Bridge mixtures at 7 and 28-days[1]

Section	Test Age (days)	Compressive Strength (Mpa)
BM-A	7	48
BM-B	7	48
BM-A	28	62
BM-B	28	59

Presented results are an average of two cylinders
***1 psi ≅ 0.00689 Mpa**

6.3.2 ASTM C 1202-97

Chloride ion penetrability results are presented in Table 6-9. The 7-day penetrability results for cylinder specimens corresponding to deck sections A and B achieve a penetrability rating of *moderate*, and are both below the specified accelerated cured HPCC penetrability criteria of total charge passed of less than 2,500 coulombs. The variation between batches is observed to be insignificant, not resulting in a change in penetrability rating. The 28-day results are 1879 and 1541 coulombs for BM-A and BM-B respectively. The 42-day measurements are 1232 and 918 coulombs for BM-A and BM-B respectively.

Table 6-9. ASTM C 1202-97 results for field specimens, top finished surface.

Section	Test Age (days)	Total Charge Passed, Coulombs
BM-A	7	2397
BM-B	7	2202
BM-A	28[1]	1879
BM-B	28[1]	1541
BM-A	42	1232
BM-B	42	918

[1]Presented results are an average of two moist cured cylinders

6.3.3 Electrical Resistivity

Electrical resistivity results for bridge deck sections, laboratory cured slabs, field cured slab specimen are presented in Table 6.10. The laboratory cured slabs were cast at the jobsite, moist cured under wet burlap and plastic sheeting until 2-days of age, after which they were placed in an outdoor environment. Field cured slabs were cast at the jobsite and

underwent same environmental and curing conditions as the bridge deck. Small variations are observed between results taken on the bridge deck and both set of slab specimens. The nature of the relationships for field specimens with the bridge deck will be explored in Chapter 7 of this dissertation.

6.3.4 Surface Air Flow

Surface Air Flow measurements were taken on laboratory slabs and deck sections. Table 6-11 presents the SAF results for the field cast specimens and deck sections. In all cases the SAF measurements results in a classification of low relative permeability.

Table 6-10. Electrical resistivity, Field cast specimens and Deck

		Resistivity (kΩ-cm)				
		Test Age (Days)				
Test Regimen	Curing Regime	7	14	28	42	91
Laboratory slabs						
A	2B	22.34	18.66	14.22	26.41	26.98
B	2B	22.92	22.04	25.04	28.89	25.28
Field Slabs						
A	2B	X	16.32	X	20.15	24.29
B	2B	X	18.38	X	19.66	24.15
Deck Sections						
A	2B	X	21.29	X	18.87	30.18
B	2B	X	X	X	18.95	31.26

***2B – Initial moist cure period of two-days under wet burlap blanket (Deck specimens) or wet-burlap and plastic sheeting (Laboratory specimens).**

Table 6-11. Surface Air Flow, Field cast specimens and Deck

Test Regimen	14	28	42	91
Laboratory slabs				
A	X	24	X	27
B	X	21	X	23
Deck Sections				
A	28	X	20	26
B	X	X	14	26

CHAPTER 7. ANALYSIS AND DISCUSSION

This section presents the discussion of results from the experimental research plan presented in Chapter 6. Statistical analyses were performed to assess the significance of the relationships for the following:

- Total charge passed and initial current (ASTM C 1202-97)
- 3B resistivity and 7B resistivity
- Slab and cylinder resistivity
- Slab resistivity and ASTM C-1202-97 (Total Charge and Initial current)
- Surface Air Flow and ASTM C-1202-97

7.1 CONCRETE COMPRESSIVE STRENGTH

Figure 7.1 presents the compressive strength results of PPCC and HPCC mixtures cured under standard conditions. The compressive strength for PPCC mixtures at seven and 28 days vary according to aggregate type. The highest compressive strength is achieved by mixture D followed by mixtures LS and G for both seven and 28 days.

Generally the compressive strength increases with decreasing w/c ratio. The w/c ratio for mixtures G, LS, and D are 0.42, 0.45, and 0.43 respectively. The shape and surface texture of the aggregate play an important role in the development of compressive strength. The compressive strength is influenced by the interlocking mechanical bond between the cement paste and the aggregate. Aggregates with rough surfaces generally result in a stronger mechanical bond, yielding higher compressive strength. The gravel used in mixture G is a rounded smooth surface aggregate with one or two crushed surfaces, which may account for lower compressive strength results as compared to other PPCC specimens. All PPCC mixtures cured under standard conditions achieved the minimum specified 28-day compressive strength of 28 Mpa (4000 psi).

The compressive strength for HPCC mixtures at seven and 28 days vary according to type of supplementary cementitious material. The seven-day compressive strengths for mixtures DFA and DSG are considerably lower than the compressive strength for mixture DMS. The high early age strength achieved with the addition of micro-silica may be

attributed to its finer particle size, resulting in an increased hydration rate. The addition of ground granulated blast furnace slag and fly ash slow the hydration reactions, resulting in lower compressive strengths at early ages.

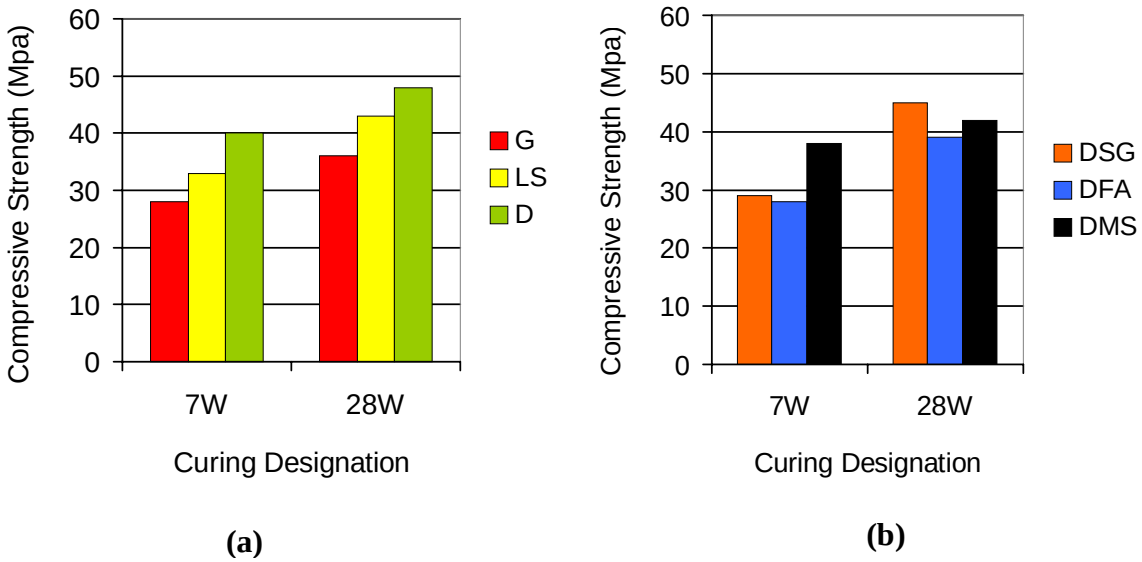

Figure 7.1. Compressive strength for (a) PPCC and (b) HPCC laboratory mixtures under standard conditions.

The 28-day compressive strength for mixtures DMS and DFA are not considerably different. Mixture DSG achieves a higher compressive strength as compared to the other HPCC mixtures. Although the hydration reactions are slowed with the addition of slag and fly ash, similar compressive strengths are observed at 28-days for all HPCC mixtures. All HPCC mixtures cured under standard conditions achieved the minimum specified 28-day compressive strength of 28 Mpa (4000 psi).

Figure 7.2 presents 28-day compressive strength results for all laboratory mixtures under simulated field curing conditions. The 28-day compressive strength for 7B specimens is slightly higher than 3B specimen for all mixtures, with the exception of mixture DMS. The minimum specified 28-day compressive strength was achieved by all simulated field cured mixtures. There was no 28-day compressive strength benefit associated with increasing initial moist curing time from 3-day to 7-days.

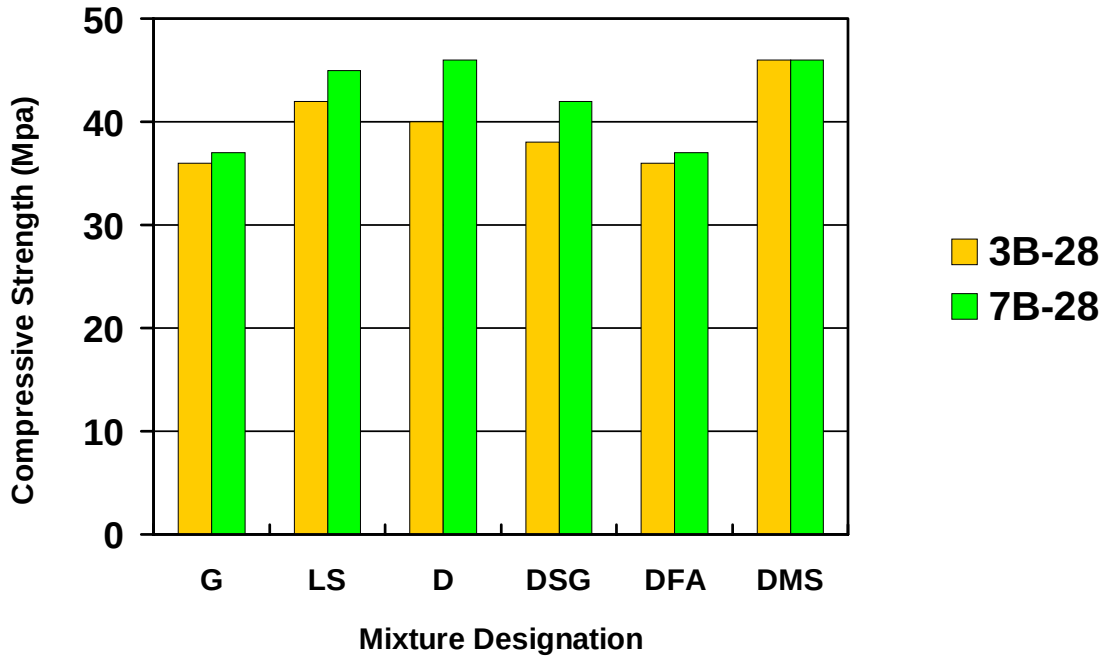

Figure 7.2. Compressive strength for PPCC and HPCC laboratory mixtures, under simulated field cure conditions.

The relatively small differences in 28-day compressive strength results in regard to differing curing regimes should be expected. The test specimens were moist cured for 3 and 7 days respectively, and were placed outdoors until time of testing. It should also be noted that the compressive strength test specimens were left in their molds until time of testing. Moisture was only liberated through the top surface of the concrete (cover concrete). The core concrete was insulated from the excessive loss of moisture by the molds and the cover concrete. Even after the moist curing is removed, the core concrete, under these test conditions, should have enough moisture available for sufficient pore system development at 28 days. The differences in 3B and 7B compressive strength results may be attributed to the curing condition of the core concrete. If compressive strength specimens were tested immediately after the initial moist curing period, the specimens cured for 7 days should achieve a higher compressive strength as compared to the 3-day cured specimens. The increase is strength would be a function of both initial moist curing time and age.

7.2 CHLORIDE ION PENETRABILITY (ASTM C 1202-97)

Figure 7.3 presents total charge passed at 7, 28 and 91 days for PPCC and HPCC specimens cured under standard conditions. At early ages the concrete pore solution and pore structure are dynamically changing. The characteristics of the pore system in concrete is a controlling factor in permeability measures. The instability of the pore system at early ages may cause high penetrability results. The penetrability results for PPCC and HPCC mixtures decrease with increasing age as the pore system becomes more stable.

Penetrability results for all standard cured PPCC mixtures are not considerably different within a given age. The penetrability ratings for seven, 28, and 91 days are respectively *high*, *moderate, and moderate*.

The effect of supplementary cementious material type is apparent as early as 7 days. DFA achieves a penetrability rating considerably higher than mixtures DSG and DMS. Mixture DMS and DSG are classified as having high and *moderate* penetrability ratings. At 28 days, there is no significant difference in penetrability results for mixtures DMS and DSG both achieving charge passed criterion for HPC classification. Mixture DFA continues to achieve a penetrability rating of *high* at 28 days. .

At 28-days there is a considerable decrease in the chloride ion penetrability value when comparing DSG and DMS to mixture D. The decrease indicates that at 28 days the use of slag or micro-silica gives an added benefit in terms of penetrability. Although mixtures D, DSG, and DMS are all classified as having a *moderate* chloride penetrability according to ASTM C 1202-97, the HPCC mixtures reach the desired high performance criteria of less than 2,500 coulombs. The fly ash had a negative effect on the 28-day penetrability results, yielding a value of 4800 compared with 3700 for mixture D. Penetrability rating for all HPCC mixtures at 91 days is *low*, indicating the long-term penetrability benefits associated with the use of slag, fly ash and micro-silica

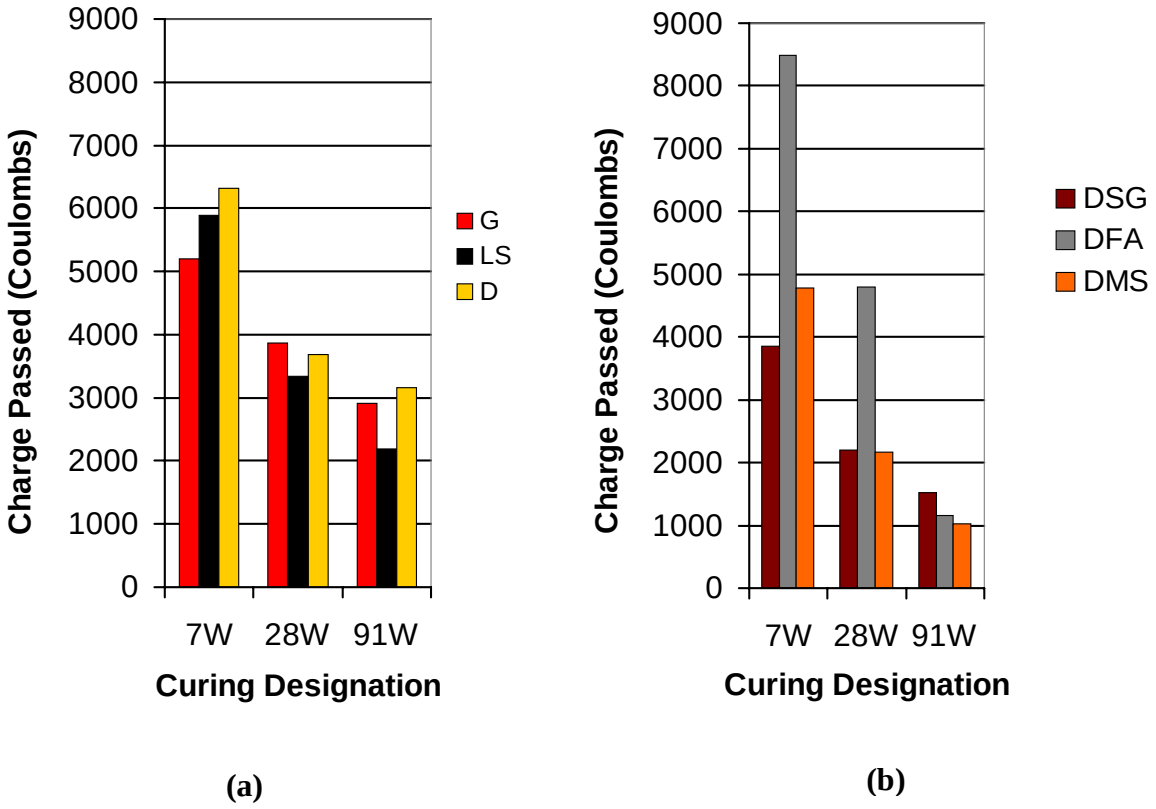

Figure 7.3. Charge passed at 7, 28 and 91 days for (a) PPCC and (b) HPCC specimens under standard curing conditions.

Figures 7.4 and 7.5 present total charge passed for all laboratory mixtures and curing conditions at 28 and 91 days, respectively. The penetrability result for standard cure specimens should represent the minimum theoretical charge passed. For a given concrete mixture at a given test age standard cured specimens should achieve lower penetrability results as compared to simulated field cured specimens. The standard cured PPCC specimens achieved lower penetrability results compared to simulated field cured PPCC specimens at 28 and 91 days, with the exception of mixture D at 91 days. There is not a considerable difference in penetrability results for PPCC 3B and 7B specimens. The additional four-days of curing time yield little long-term penetrability benefits for PPCC specimens.

The standard cured HPCC specimens achieve a lower penetrability results compared to simulated field cured HPCC specimens at 28-days for mixture DSG and at 91 days for

mixtures DSG and DMS. There is not a considerable difference in long-term penetrability results for HPCC 3B and 7B specimens.

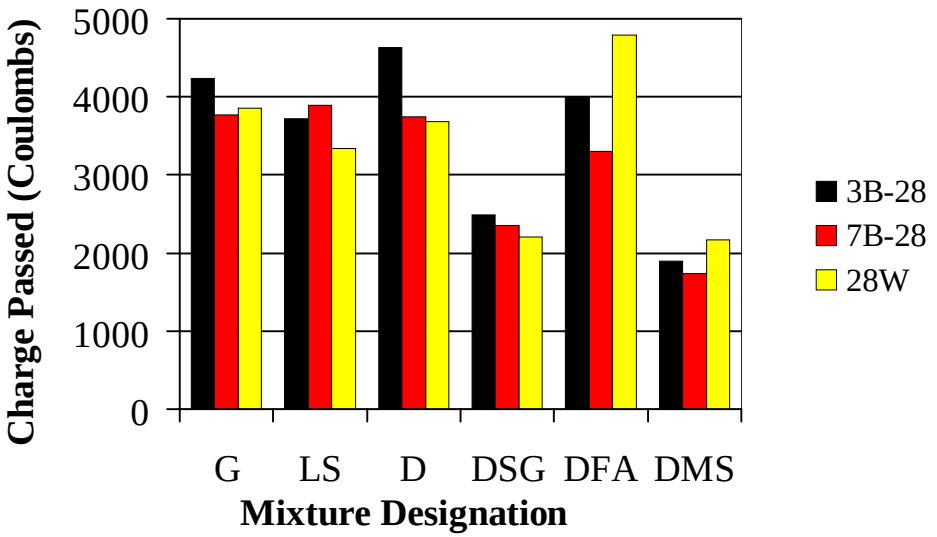

Figure 7.4. Charge Passed for laboratory mixtures at 28-days.

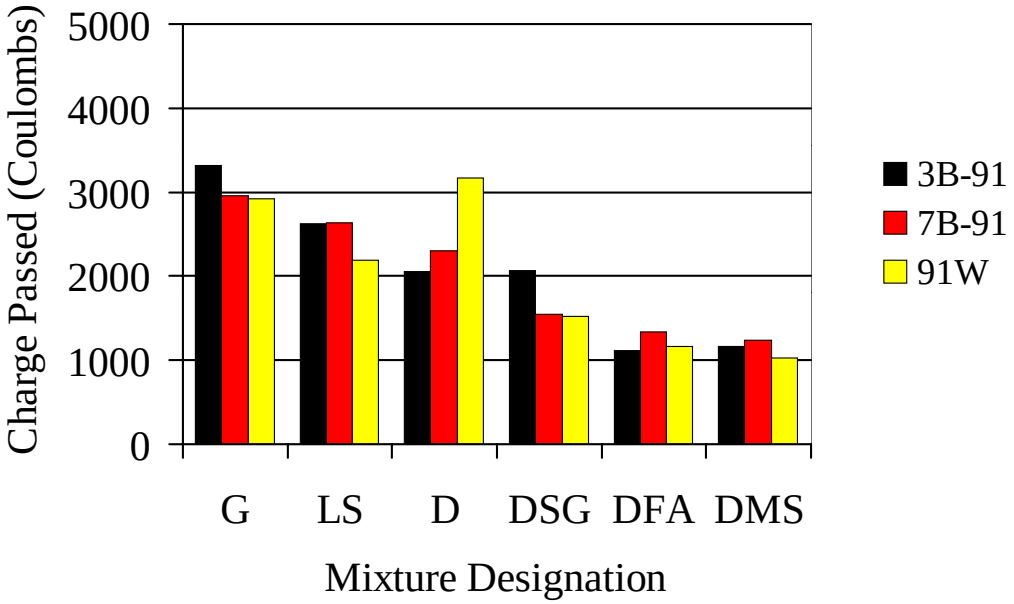

Figure 7.5. Charge Passed for laboratory mixtures at 91-days.

7.2.1 Charge Passed and Initial Current

Several researchers have expressed concerns about the ability of ASTM C 1202-97 to assess the penetrability properties of concretes containing supplementary cementitious materials due to the changes that occur in the pore structure and pore solution during the 6-hr test period. The use of the initial current (mA) reading that is produced, as an output, at the beginning of the test has been promoted as an option in characterizing permeability properties of concrete (Feldman et al., 1999). All references to initial current in this analysis correspond to current output taken within the first 10 minutes of the ASTM C 1202-97 test. The scatter diagram, regression equation, with the 95 % confidence band (CB) and the 95% prediction band (PB) for total charge passed and the initial current is presented in Figure 7.6.

The relationship between initial current and charge passed is well defined for all laboratory mixtures used in this study. A high correlation coefficient (R^2) of 92.5 % is achieved. Some differences between total charge passed and initial current should be expected since the Initial current is an instantaneous measure taken at a specific time ($t \leq 10$ min) and total charge passed is the integration of current measurements over time. However, these results indicate that the initial current may be an effective method for assessing chloride ion penetrability properties of concrete in significantly less time than the current testing standard while achieving similar precision. As illustrated, the results indicate that at the 95% confidence level the charge passed will range from approximately 2000 to 4000 coulombs for an initial charge of less than 100 mA. The strong correlation observed between charge passed and initial current may also indicate that the changes that occur in the pore system of concrete containing supplementary cementitious materials has a negligible effect on the penetrability results.

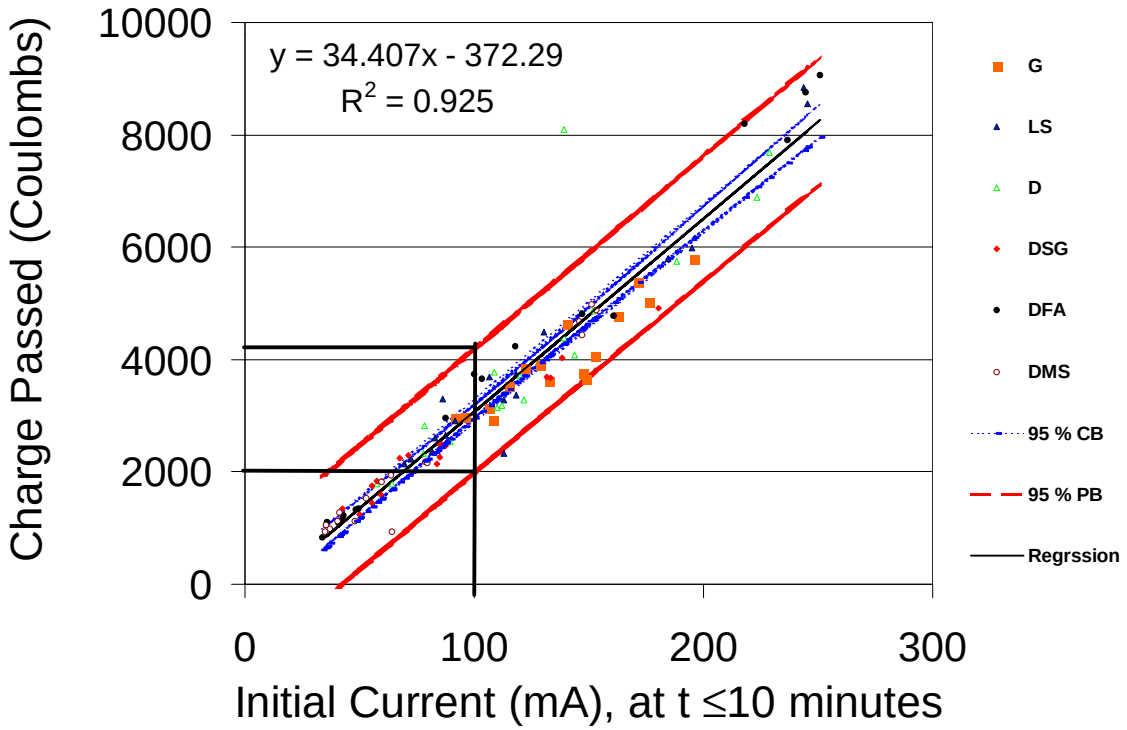

Figure 7.6. Initial current vs. charge passed for all laboratory mixtures.

7.3 ELECTRICAL RESISTIVITY

7.3.1 Variability in Resistivity Measurements

A large amount of variability is observed with early age resistivity measurements. Polder (2000) states that "considerable scatter is present in most sets of resistivity measurements, even if they concern data from laboratory cast specimens from the same mix and exposed identically." No replicate specimens were cast for this experimental plan, but at the ages of one and three-days the conditions for 3B and 7B slab specimens are identical. Table 7-1 presents results from one-way ANOVA tests performed on one and three-day resistivity results for all laboratory slab specimens to determine if the variability between specimens is greater than the variability within a specimen.

All test were performed at the 0.05 significance level, therefore any comparison with a p-value > 0.05 indicates that the variability between slab specimens is not significantly larger then the variability with slab specimens. Analysis results indicate that the variability

within a specimen and between specimens were comparable for nine of the twelve tests performed. These results establishes the underlying basis of comparison of the various mixtures used in this study with replicated specimens. Since few differences in the within slab and between slab variability were observed, within slab variability was used as a surrogate for the between slab estimate of variance.

Electrical resistivity measurements are affected by the pore structure and the pore solution. During the early stages of hydration the pore system is very dynamic and somewhat unstable. The stability of the pore system increases with increasing time, therefore the variability of resistivity measurements within a specimen should decrease with time.

The coefficient of variation (CV) is a normalized measure of the variability within a sample. Figure 7.7 presents the CV over time for 3B PPCC slab specimens. Coefficient of variations of 20 to 25 % are normal for resistivity measurements taken on concrete specimens (Polder R., 2000). The variability during early ages is initially high but steadily decreases with time as the pore system becomes more stable. The behavior of the CV shown for 3B PPCC is typical of all laboratory slab specimens tested in this study. The CV converges to the "normal" range at 28 days for both PPCC and HPCC mixtures, with the exception of mixture D.

Figure 7.8 presents the CV behavior of 7B slab specimens containing diabase aggregate including HPCC mixtures. The CV of HPCC specimens is extremely volatile before 28-days of age. In all but one case, the variability of mixtures containing diabase begin to stabilize at 28-days, following the general trend for PPCC mixtures. Mixture D exhibits an increased rate of variability at 28 days when compared to all other mixtures. The increased variability at 28 days of age is not expected and may be accounted for by some experimental error. Although the exact nature of the error is not known, the trend for CV of resistivity results is well defined by the other five concrete mixtures used in this study, therefore the 28-day resistivity results for mixture D have been omitted from all subsequent analysis.

Table 7-1. One-way ANOVA results for all laboratory mixtures at 1 and 3-days, testing for differences in between and within slab variability.

Mixture Designation	P-value Age (day)	
	1	3
G	0.324	0.954
LS	0.146	0.435
D	0.857	0.080
DSG	0.475	0.001
DFA	0.007	0.292
DMS	0.006	0.111

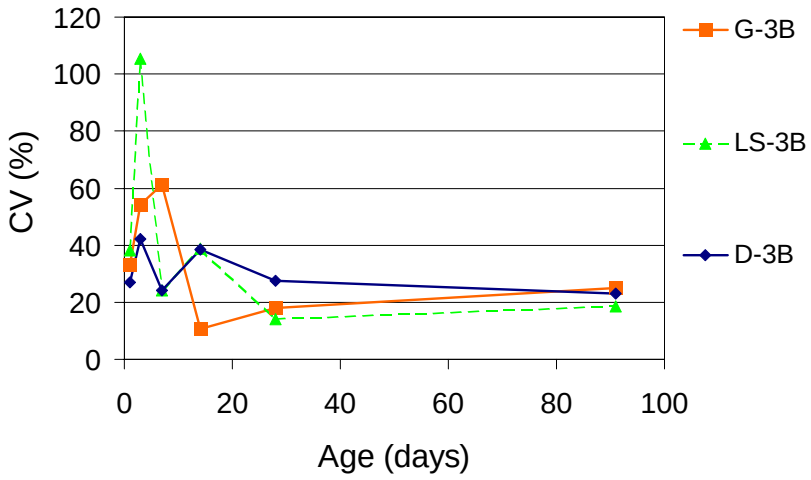

Figure 7.7. Coefficient of variation over time for 3B PPCC Slab specimens.

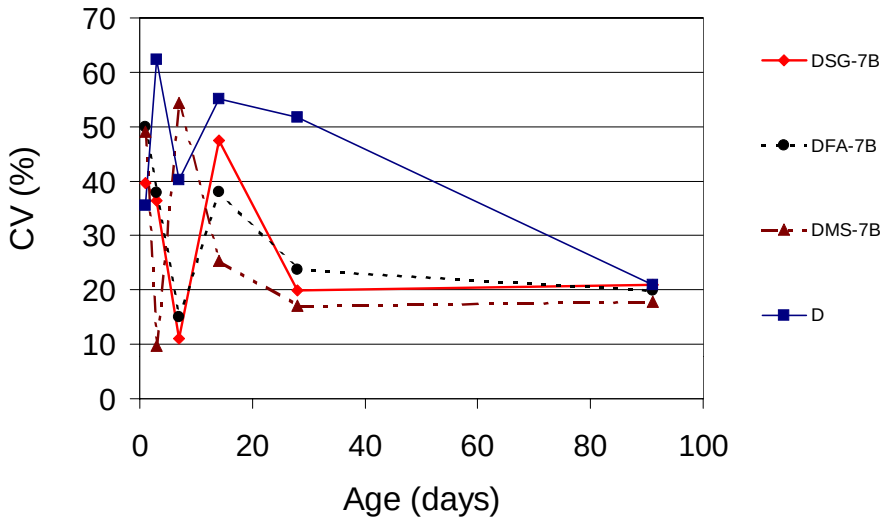

Figure 7.8. Coefficient of variation over time for 7B HPCC and D Slab specimens.

Because of the more uniform and smooth surface properties of the cylinders, the variability within cylinder specimens is expected to be lower when compared to slab specimens. The CV range for PPCC cylinder specimens at 91 days is four to ten percent and five to sixteen percent respectively for standard and simulated field cured conditions. The CV range for HPCC cylinder specimens is five to 9 percent and eight to thirteen percent, respectively for standard and simulated field cured specimens.

7.3.2 Comparison of 3B and 7B Resistivity Results

Results from compressive strength and ASTM C 1202-97 indicate that there is little to no difference in results obtained from 3B and 7B specimens. Figures 7.9 and 7.10 present the relationship between 3B and 7B resistivity results respectively for slab and cylinder specimens. Linear regression analysis was performed to quantify the nature of the relationship between 3B and 7B specimens. The relationship between 3B and 7B resistivity measurements should be close to one-to-one if there is no difference in resistivity results with respect to curing regimes.

A high correlation coefficient (R^2) of greater then 90% is achieved between 3B and 7B resistivity results for both slabs and cylinders. Formal statistical analysis was performed to determine whether the slope of the regression line can be equated to 1. A paired t-test was used at a significance level of 0.05 (0.025 for two-tailed test). Table 7-2 presents the results

of paired t-test analysis, which indicate that slopes presented for 3B, and 7B relationships are statistically equivalent to one. There is no statistical difference at the 5% significance level between resistivity results obtained from 3B and 7B specimens.

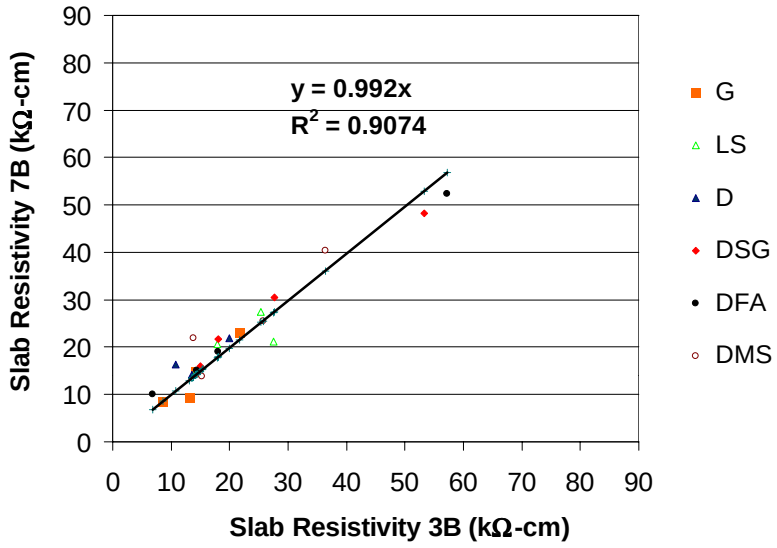

Figure 7.9. Relationship between 3B and 7B slab resistivity.

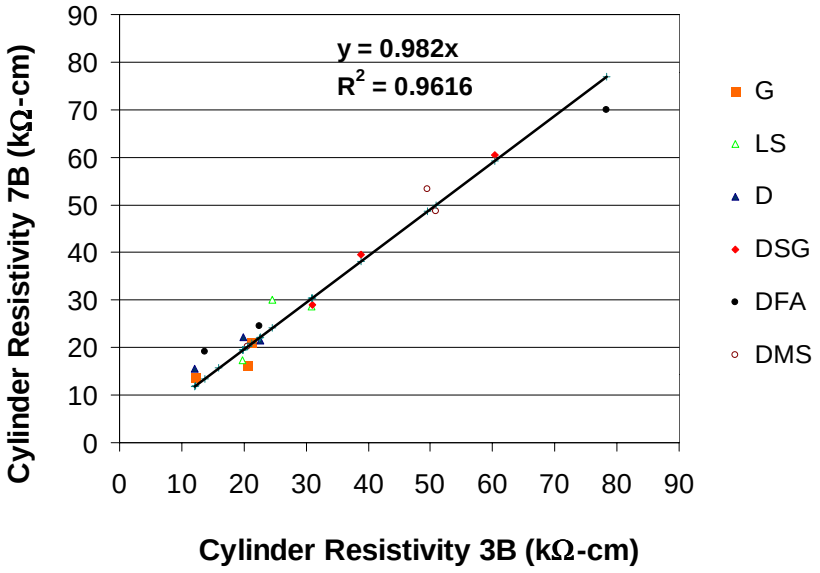

Figure 7.10. Relationship between 3B and 7B cylinder resistivity.

Table 7-2. t-test analysis for 3B and 7B resistivity relationships.

Specimen	Slope (β_1)	Standard Deviation	DF	$\lvert t_{obs} \rvert$	$t_{0.025, DF}$	$\beta_1 \approx 1$
Slab	0.992	0.0296	22	0.257	2.0739	Yes
Cylinder	0.982	0.0221	17	0.816	2.1098	Yes

7.3.3 Relationship Between Slab and Cylinder Resistivity

The relationship of resistivity results between slab and cylinder specimen is of great interest. The resistivity of concrete is believed to be a geometry independent material property. Theoretically, if a one-to-one relationship exists, resistivity measurements taken from cylinder specimens could give a direct indication of the in-place electrical properties.

Figure 7.11 presents the relationship between slab and cylinder resistivity. A correlation coefficient of 89 % is observed. The relationship between cylinder and slab resistivity is not one-to-one. Resistivity results for cylinder specimens are slightly higher than results obtained for slab specimens. The difference in resistivity results between slabs and cylinders may be a function of the testing surface texture and testing orientation.

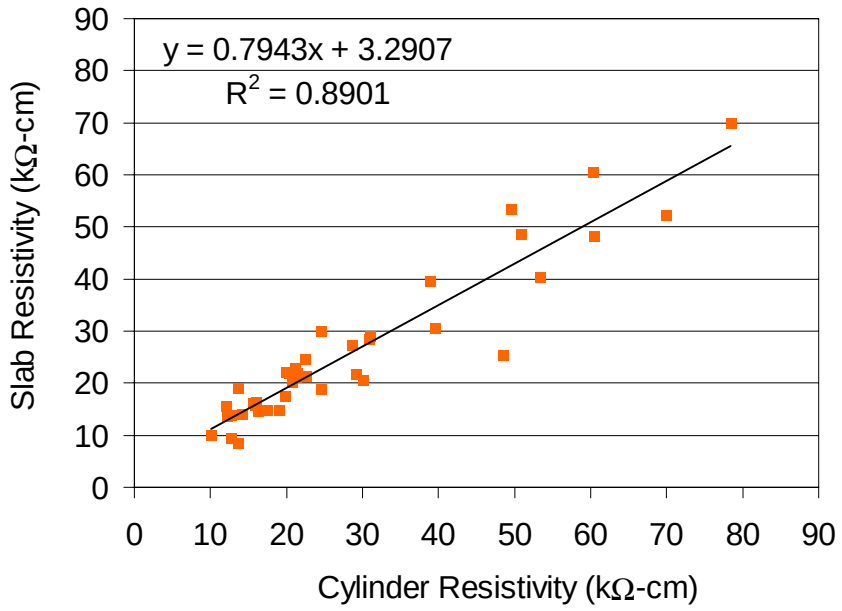

Figure 7.11. Relationship between slab and cylinder resistivity

Slab specimens were tested on the finished surface while cylinder specimens were tested on the cast surface along its height. The difference in test surface texture properties of

slabs and cylinders may have an affect of the contact resistance between the electrodes and the concrete surface, which affects the resistivity measurement.

In this experimental plan the slabs and cylinders were left in forms and molds respectively until time of testing. Moisture was allowed to leave through the top surface of the concrete in both cases. The moisture gradient may be different for each test orientation (see Figure 7.12). The cylinder test orientation is perpendicular to the moisture movement and the slab orientation is the same direction as the movement of moisture. It is well known that the moisture content affects the electrical properties of concrete. The slab specimens may encounter a more uniform moisture distribution as compared to the cylinder specimens where testing may be across varying moisture levels.

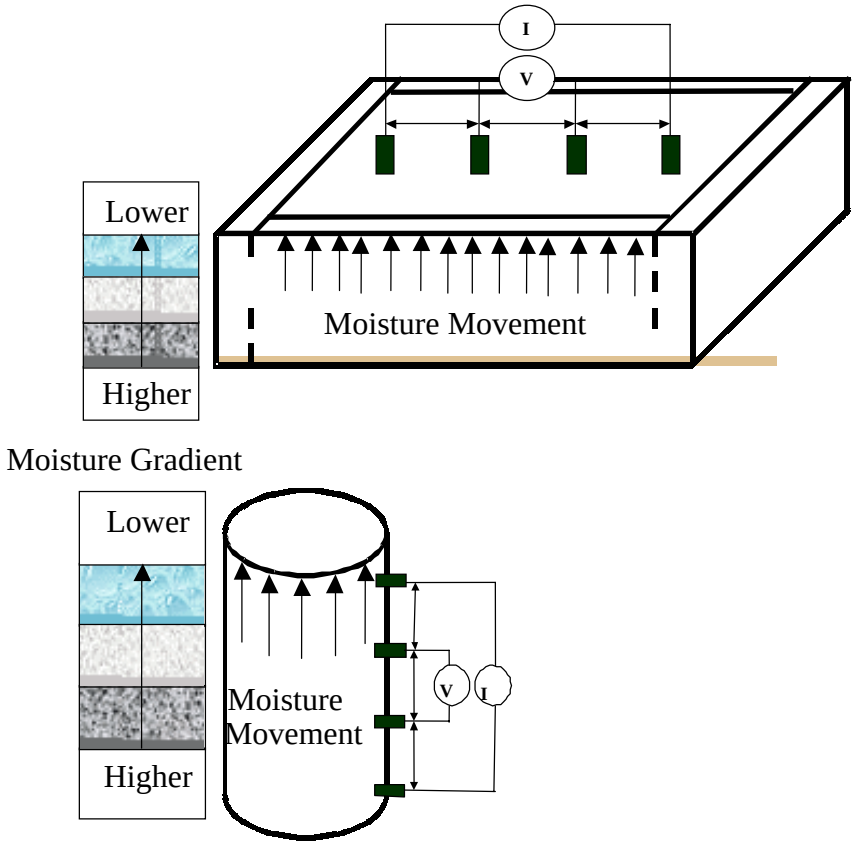

Figure 7.12. Theoretical moisture movement and testing orientation.

7.4 RESISTIVITY AND CHLORIDE ION PENETRABILITY

The relationship between electrical resistivity and ASTM C 1202-97 measures, total charge passed and initial current was investigated using regression analysis. Slab resistivity

measurement condition and testing orientation is approximately equal to field conditions. Therefore this portion of the analysis uses only slab resistivity results. The relationship between 3B and 7B resistivities was discussed earlier and was found to consistent with a one-one relationship, therefore for each ASTM C 1202-97 measure there are two resistivity values presented, one for 3B the other corresponding to 7B. ASTM C 1202 measures correspond to continuous moist cured specimens.

7.4.1 Plain Portland Cement Concrete Mixtures (PPCC)

Figures 7.13 and 7.14 present the scatter diagrams for slab resistivity and ASTM C 1202-97 measures. As illustrated, there appears to be a poor relationship between the seven-day measurements. This maybe the result of the higher variability of these early-age measurements, see Figure 7.7. Figures 7.15 and 7.16 present scatter diagram for 28 & 91-day slab resistivity measurements, total charge passed and initial current, respectively.

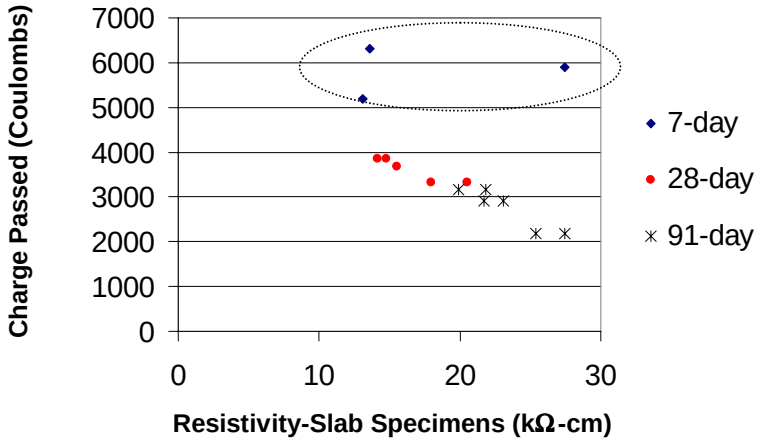

Figure 7.13. Slab resistivity vs. total charge passed for PPCC specimens.

An inverse linear relationship was found to describe the behavior of slab-resistivity and ASTM C 1202-97 measures for PPCC specimens at 28 and 91 days. Correlation coefficients of 93% and 84% were observed respectively, for the relationship between resistivity and charge passed and resistivity and initial current. The relationship between total charge passed and resistivity appears to be a stronger relationship than between total charge passed and initial current for PPCC measurements. The range of charge passed and

initial current are 2000 to 4000 coulombs and 100 to 150 mA, respectively, over an approximately 15 kΩ-cm resistivity range.

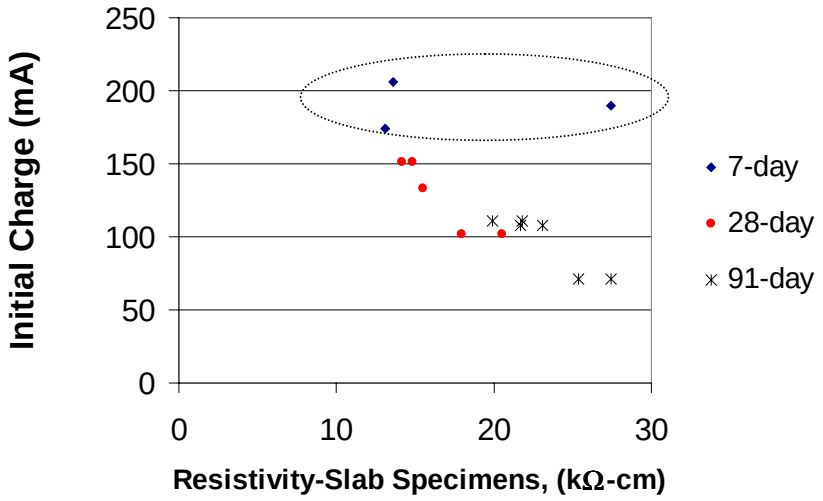

Figure 7.14. Slab resistivity vs. Initial current for PPCC specimens

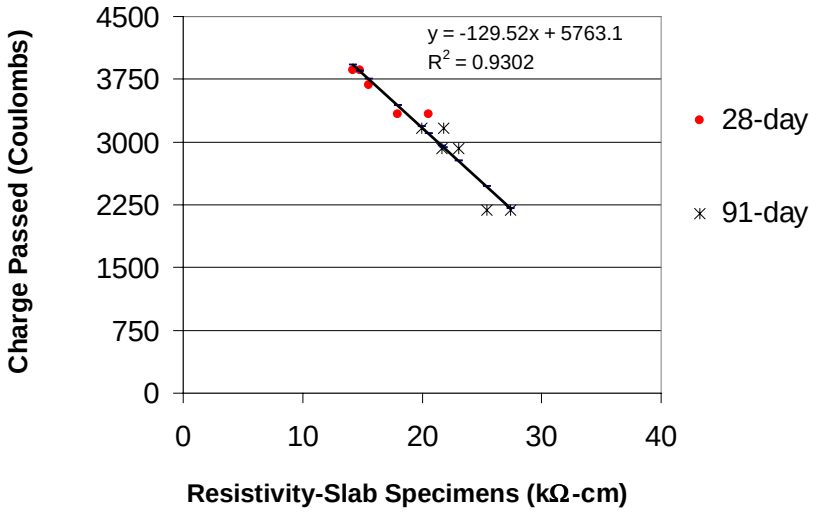

Figure 7.15. Slab resistivity vs. total charge passed for PPCC specimens (28 &91-days)

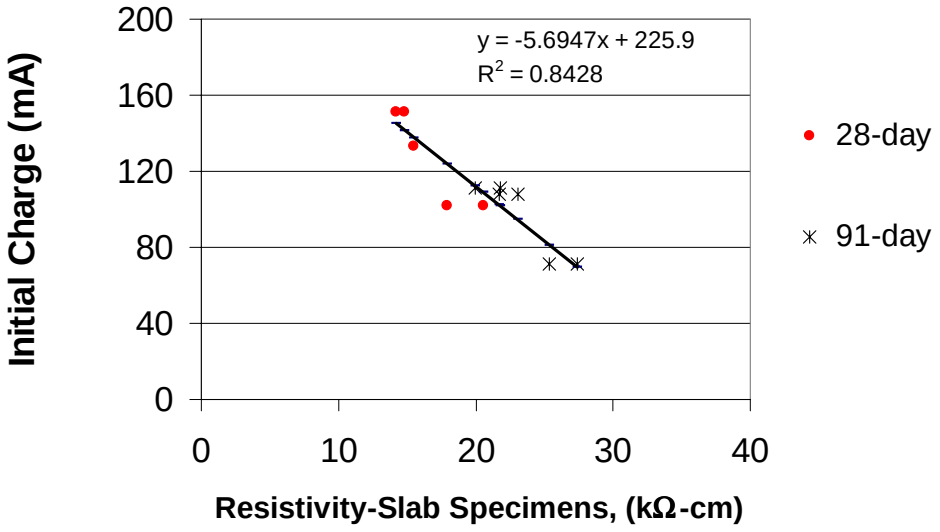

Figure 7.16. Slab resistivity vs. initial current for PPCC specimens (28 &91-days)

7.4.2 High-Performance Portland Cement Concrete Mixtures

The relationship between slab resistivity and ASTM C 1202-97 measures for HPCC was investigated using regression analysis and is presented in Figures 7.17 and 7.18. An inverse power function was found to best describe the relationship between slab resistivity and ASTM C 1202-97 measures for HPCC specimen, similar in form to the relationship proposed by Clear (2000).

As illustrated, the relationship between seven-day HPCC measurements and ASTM C 1202-97 measures is in agreement with later-age measurements. HPCC specimens may have a more well defined pore system at early ages. A correlation coefficient of approximately 89% was observed for both relationships.

The respective relationships between electrical resistivity and ASTM C 1202-97 measures cover a broader range as compared to the PPCC relationships. Resistivity values range from 5 to 60 kΩ-cm for HPCC relationships compared to 15 to 28 kΩ-cm for PPCC. The charge passed and initial current range for HPCC relationships are 1,000 to 10,000 coulombs and 45 to 350 mA, respectively.

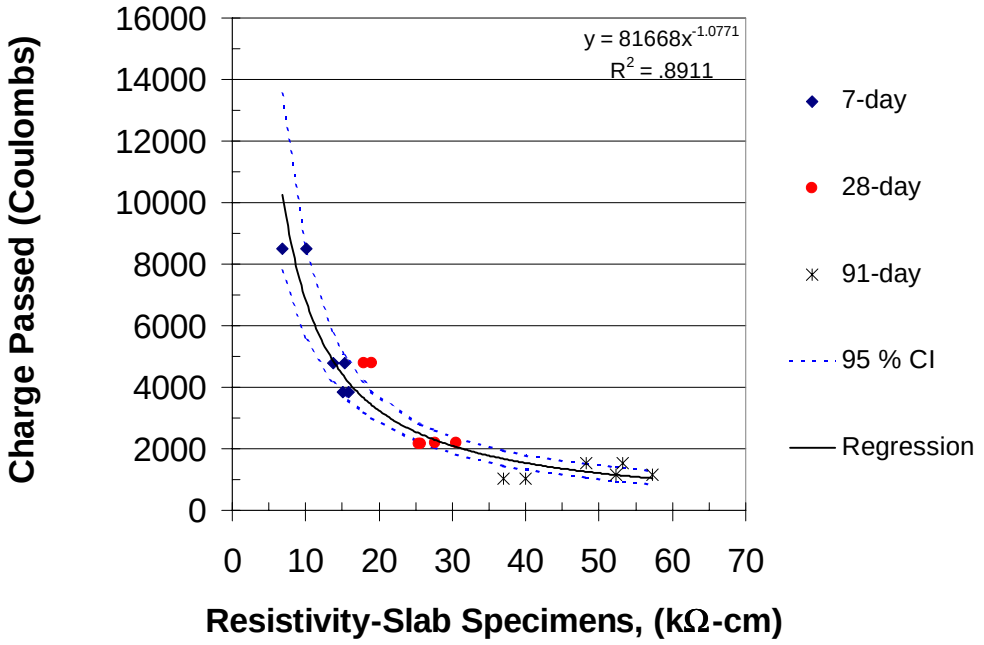

Figure 7.17. Resistivity-slab specimens and charge passed for HPCC mixtures

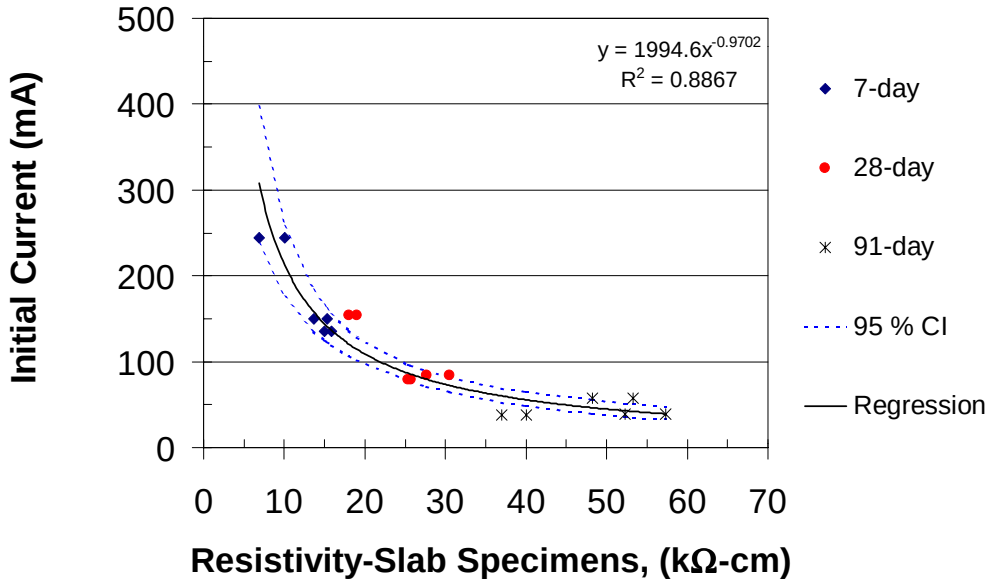

Figure 7.18. Resistivity-slab specimens and initial current for HPCC mixtures.

The broader range provided with the HPCC relationships may cover the in-place penetrability indication of a wider range of concretes. The inverse power model was used to assess the relationship between resistivity and ASTM C 1202 measures for all concretes used in the laboratory portion of this study and is presented in the next section.

7.4.3 Resistivity and Chloride Penetrability for HPCC & PPCC Mixtures Combined

The scatter diagrams and fitted regression curve with 95% confidence limits for slab resistivity and ASTM C 1202-97 measures for combined PPCC and HPCC mixtures are presented in Figures 7.19 and 7.20. The seven-day measurements from PPCC specimens are excluded from this analysis due to the higher variability of these specimens, Figure 7.7. The regression analysis follows an inverse power series similar to the relationship found for HPCC specimens.

The combined model has a correlation coefficient (R^2) of 88% for resistivity and both ASTM 1202-97 measures, respectively. The range of values produced from using the combined mixtures is similar to the range produced using only HPCC mixtures. The strength of the relationships established using the combined resistivities is slightly weaker than the HPCC relationship. However the combined model may be is able to assess the in-place permeation properties of both HPCC and PPCC concretes.

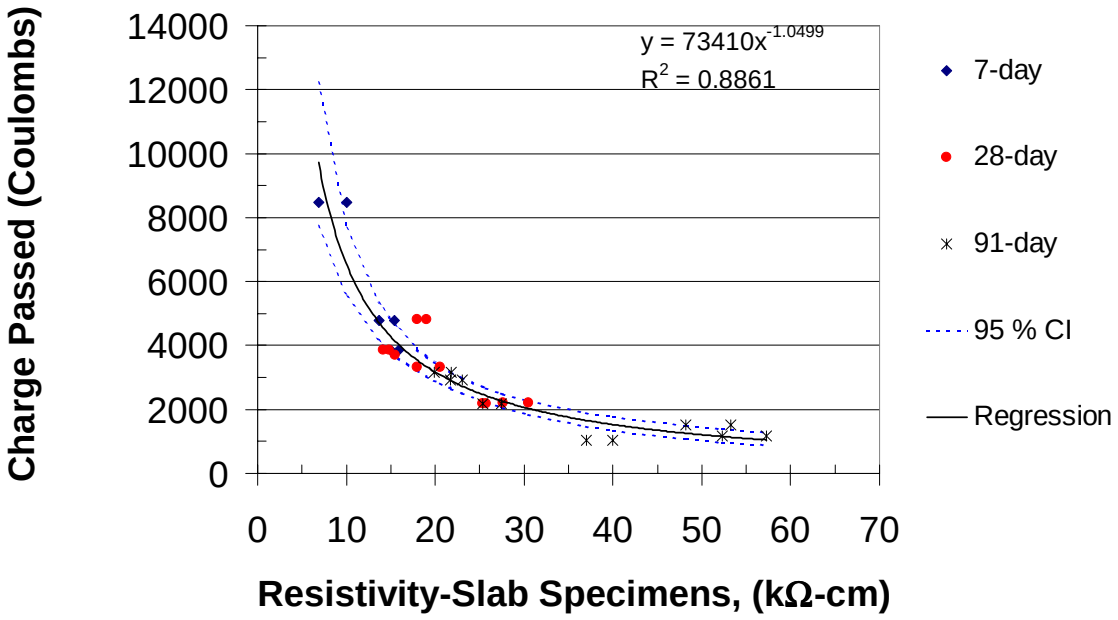

Figure 7.19 Resistivity and charge passed HPCC and PPCC mixtures.

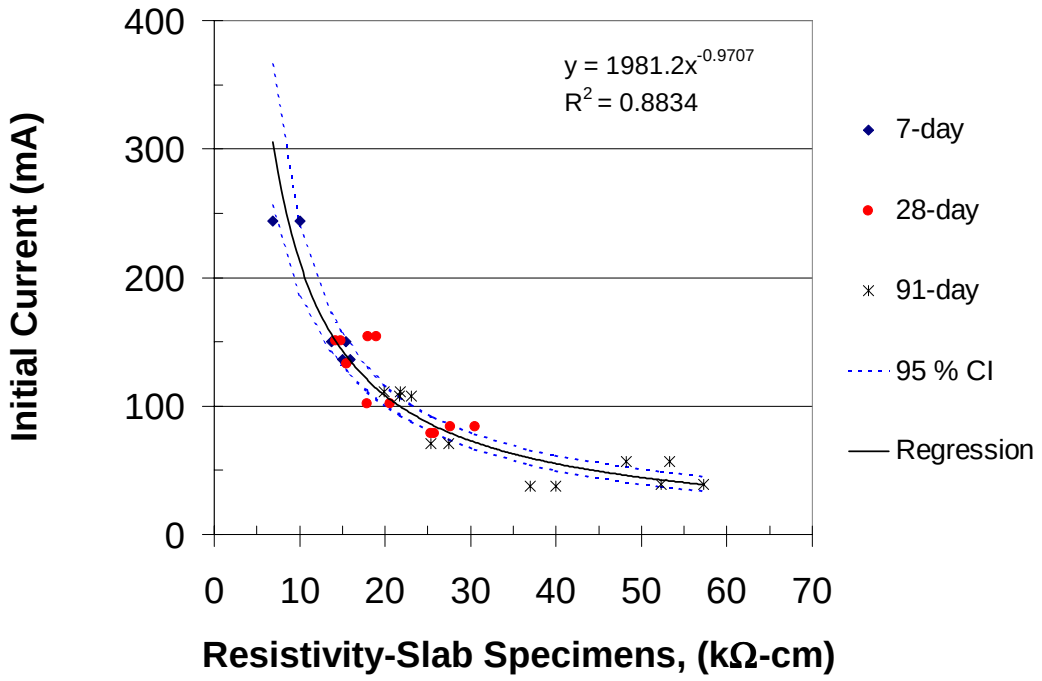

Figure 7.20 Resistivity and initial current HPCC and PPCC mixtures.

7.4.4 Resistivity and Chloride Penetrability for Total Charge Passed of Under 4000

The maximum specified range of penetrability values that correspond to current bridge deck mixtures should not exceed 4,000 coulombs, which is the upper limit of a moderate chloride ion penetrability rating. Figures 7.21 and 7.22 present the scatter diagrams with the 95 % confidence interval for regression analysis for slab resistivity and ASTM C 1202-97 measures for all specimens that have a charge passed of under 4000.

A coefficient of correlation of approximately 86% was achieved for describing the resistivity relationship with charge passed and initial current. The range of values covered are slightly smaller to the range covered by the HPCC models but is larger than the range proposed using only PPCC data. The range of values used in this model may represent typical values desired in the field. This relationship takes into account the level of maturity in the concrete pore system with an upper total charge passed (coulomb) limit.

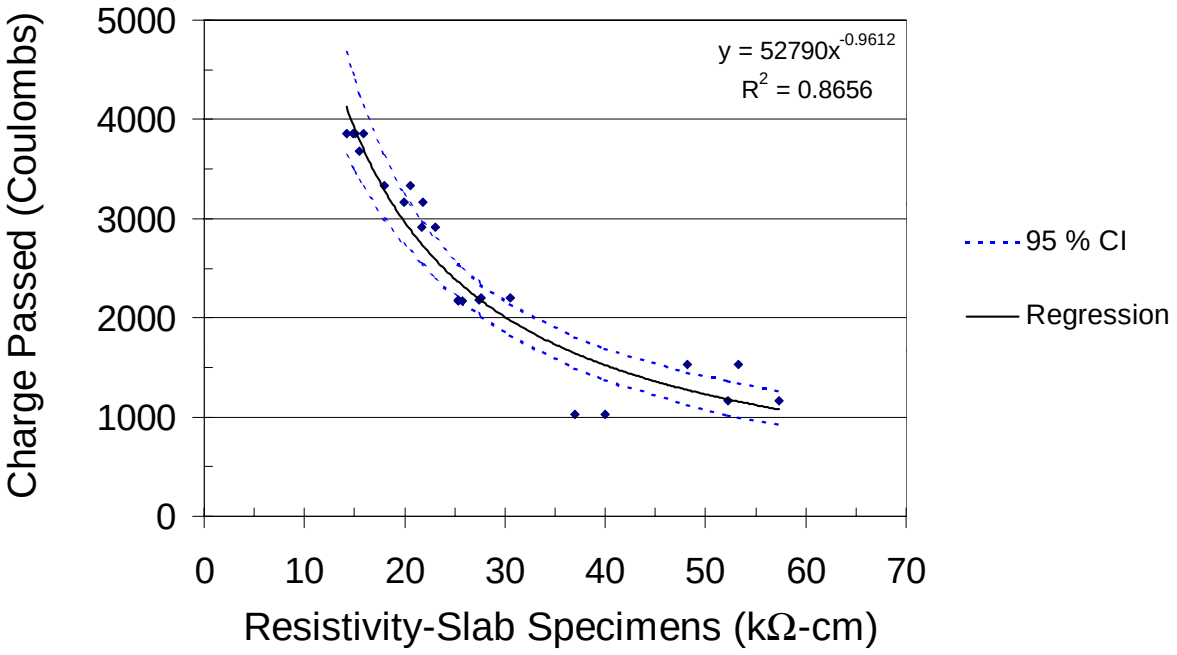

Figure 7.21 Resistivity and charge passed for mixtures under 4000 coulombs.

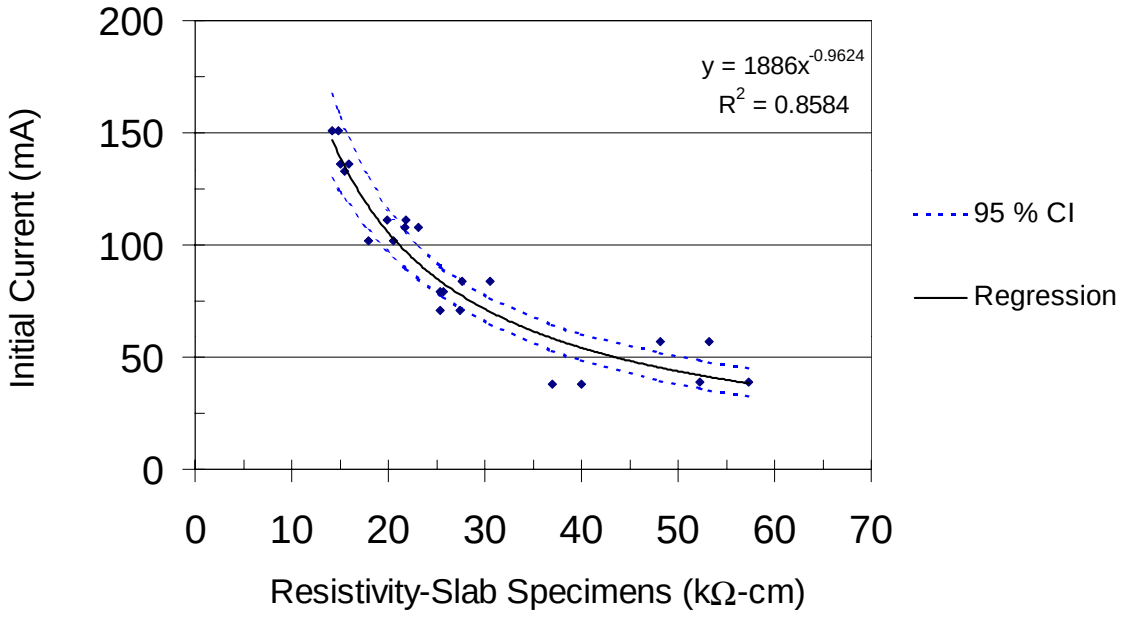

Figure 7.22 Resistivity and Initial current for mixtures under 4000 coulombs.

The inverse power relationship between resistivity and ASTM 1202 measures, charge passed and initial current are not surprising. As stated in Chapter 4 the electrical resistivity is the reciprocal of conductivity. Therefore the relationship between these electrical properties

is expected to resemble the form of 1/x. The slope coefficients for the HPCC, the combined and the under 4000-coulmbs model are all equivalent to –1, which confirms the underlying current-to-potential relationship defined by Ohms law (V = IR).

7.5 SURFACE AIR FLOW

Surface air flow (SAF) measurements were taken on the finished surface at 28 and 91-days for PPCC slab specimens. Testing of HPCC mixtures were conducted at 91-days. Figure 7.23 presents 28 and 91-day SAF results for PPCC specimens under 3B and 7B curing regimes. Mixture LS achieves the highest air flow at 28 and 91-days. Low permeable concrete is classified as having an air flow of less than 30 ml/minute. All PPCC mixtures achieve a relative permeability rating of low, with the exception of mixture LS. The differing curing regimes have no affect on the relative permeability rating due to the broad range of permeability classifications associated with this test method. All SAF results for HPCC specimens were below 30 ml/minute and thus have a relative permeability rating of *low*.

A good seal between the concrete surface and the vacuum plate in needed to insure correct relative permeability results. Difficulties in attaining a proper seal were encountered during the initial stages on this investigation. Vacuum grease was placed along the face of the foam gasket to ensure no leakage occurred between the vacuum face plate and the concrete surface, ensuring an adequate air seal (Chapter 5.3.3). Some system leakage, on the order of 1 to 5 ml/minute was observed even after the application of the vacuum seal. The test method may yield to much influence to the characteristics of the testing surface to be used assess permeation properties in the field.

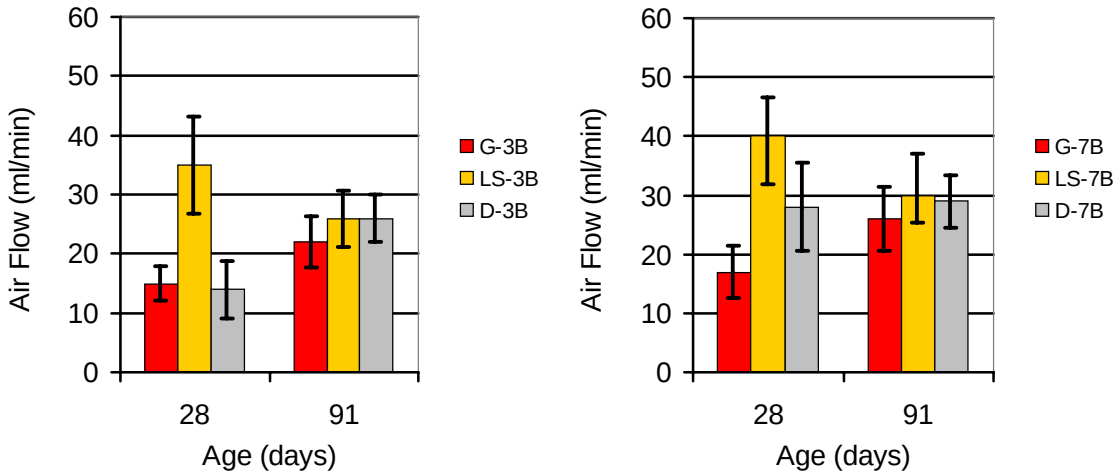

Figure 7.23. Surface Air Flow with time for PPCC specimens 3B and 7B

7.5.1 Surface Air Flow and ASTM C 1202-97

Although SAF and ASTM C 1202-97 determine permeation properties by different mechanisms, some level of agreement qualitatively is expected. As the concrete ages and the surface air flow may increase as moisture is released from the system, allowing air to flow through the larger void spaces. The SAF measurements are taken at 28 and 91 days of age, when the pore system is assumed to be relative stable, and little difference expected in results. The results from ASTM C 1202-97 indicate that the total charge decreases with age, and behave best when the pore system is well defined. Qualitatively, for a concrete with a well defined pore structure, the air flow should remain relatively constant and total charge is expected to decrease with time.

Figure 7.24 presents the scatter diagram for SAF and total charge passed. The total charge passed decreases as the air flow increases. This observation should occur at early ages, when large amounts of moisture is being liberated from the pore system, but should not be the case for well cured concretes with a well defined pore system. Surface air flow results classify all concrete as having low relative permeability, with the exception of mixture LS. The classification of these concretes by ASTM C 1202-97 is *moderate* and *low*. The SAF measurements may lack the sensitivity needed in order to correctly classify a broad range of concretes.

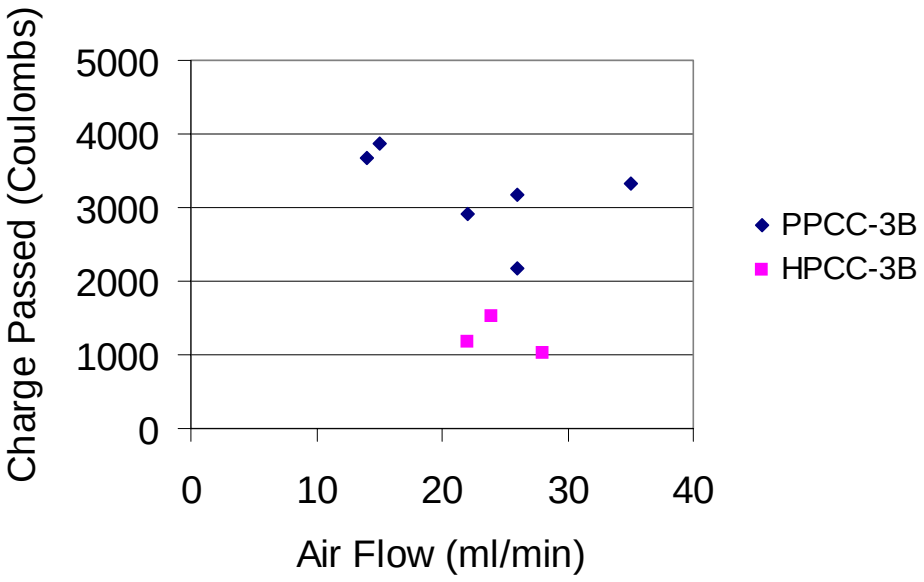

Figure 7.24. Air Flow and charge passed for 3B slab specimens.

7.6 FIELD INVESTIGATION

Electrical resistivity results, with 95 % confidence error bars, for bridge deck sections, laboratory cured slabs, and field cured slab specimen are presented in Figure 7.25. The test ages correspond to age of deck testing. Differences in resistivity results for lab slab and deck slabs may be do the different curing environment. The laboratory cured slabs were cast at the jobsite, moist cured under wet burlap and plastic sheeting for 2 days, after which they were placed in an outdoor environment. Field cured slabs were cast at the jobsite and underwent same environmental and curing conditions, two-days under a wet burlap blanket, as the bridge deck. After moist curing both sets of slabs were left in their respective environments. The deck slabs, which were placed on the bridge deck surface, were exposed to higher and more variable wind conditions as compared to the laboratory tested field cast specimens, which were outdoors but in relatively calm wind conditions. The exposure conditions could be responsible for the increases resistivity results for deck slabs at 42-days. Resistivity measurements are influenced by the moisture content, the drier the concrete the higher the resistivity.

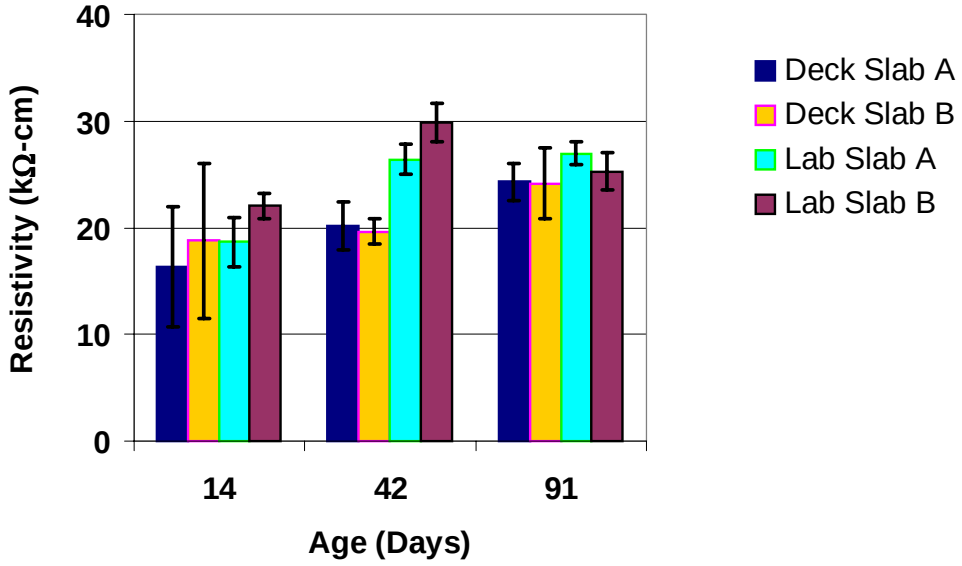

Figure 7.25. Electrical resistivity of field mixtures.

Since resistivity is a geometry independent material property, resistivity results taken from deck slabs and the corresponding deck sections should be similar. Figure 7.26 presents a comparison of deck sections and deck slabs, with 95 % confidence limits. The resistivity of the deck section and the laboratory tested field cured specimens are not significantly different at 14 and 91 day at the 95 % confidence level. A difference is observed at 42 days, where the laboratory tested specimens achieve a higher resistivity as compared to the deck sections. The 91-day deck section resistivity measurements were taken during windy conditions, which may have caused higher results. It is reasonable to assume that the resistivity measurements taken from the laboratory tested specimens are not significantly different from the as-built deck resistivities.

Figure 7.27 presents electrical resistivity with age for field cast laboratory specimens with 95 % error limits. The only significant difference in resistivity values is observed at 28 days. The resistivity result from slab A is significantly lower than slab B. The resistivities converge to similar values at 42 and 91 days. Results from laboratory tested field cast slab specimens were used to investigate the relationship between slab resistivity and total charge passed because of similar testing ages.

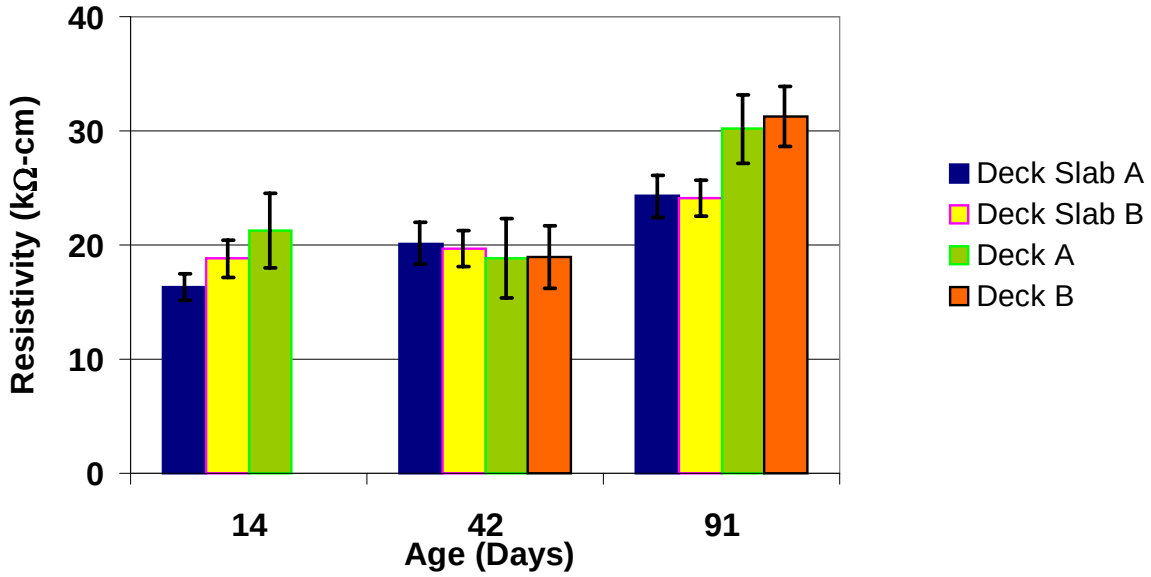

Figure 7.26. Resistivity of deck sections and deck slabs.

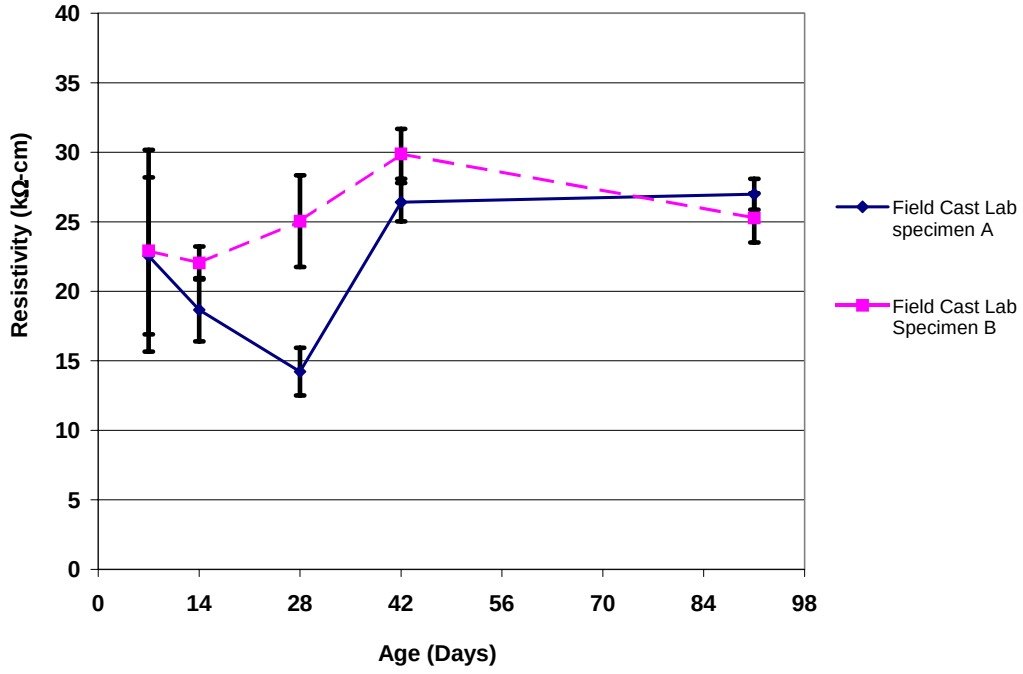

Figure 7.27. Electrical Resistivity with age for laboratory tested field cast specimens.

The scatter diagrams for electrical resistivity of field cast laboratory slab specimens and ASTM C 1202-97 measures are presented in Figures 7.28 and 7.29. An inverse power

series was used to describe the resistivity ASTM C 1202-97 measures in the laboratory portion of this research. The inverse power series does not appear to correlate well with the field mixtures, attaining correlation coefficients of 19 % and 22 % respectively or charge passed and initial current. The field mixture decreases in permeability over a very short range of resistivity values. Metakaolin was used as the supplementary cementitious material in the field mixtures. The form of the relationships, an inverse power function, found to describe laboratory specimens does not appear to describe the resistivity-charge passed relationship for this material.

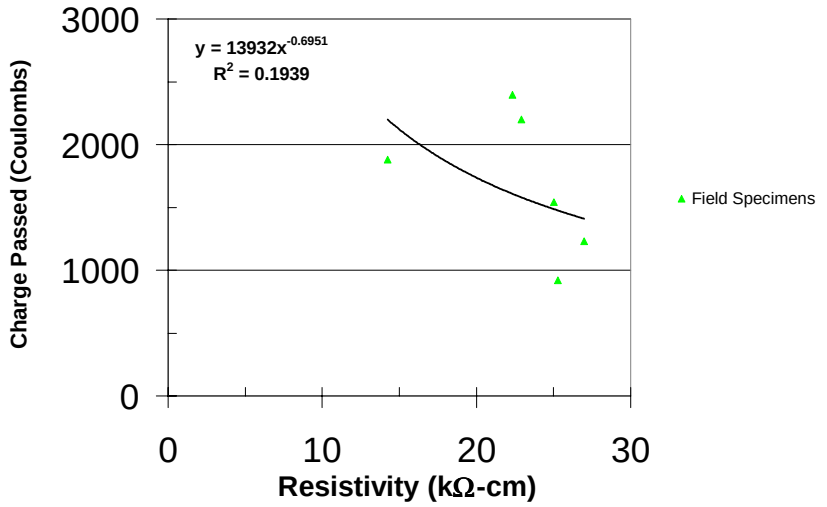

Figure 7.28. Slab resistivity and charge passed for field specimens

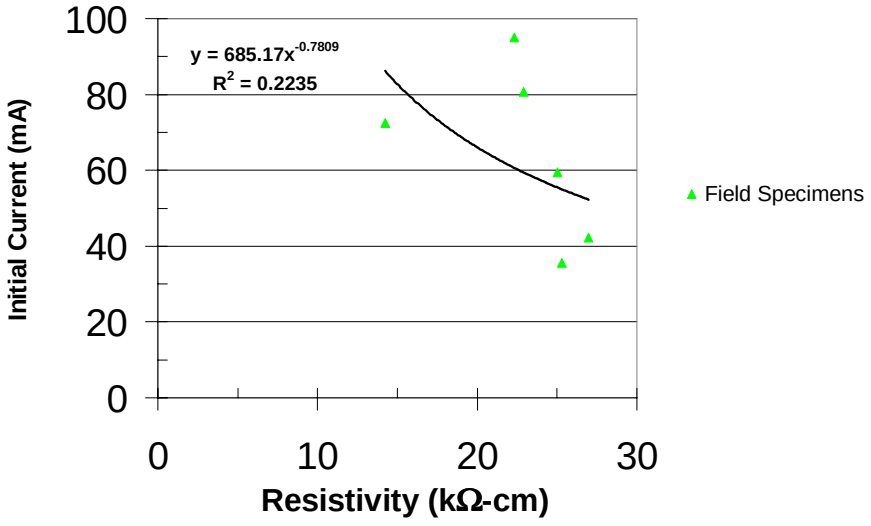

Figure 7.29. Slab resistivity and initial current for field specimens

Figure 7.30 presents that scatter diagram for SAF and total charge passed results. The SAF classifies the filed specimens as having a *low* relative permeability. The classification of field data by ASTM C 1202-97 ranges from *moderate* to *low*. As illustrated, the appears to be no quantitative relationship between total charge passed and SAF for the field mixtures.

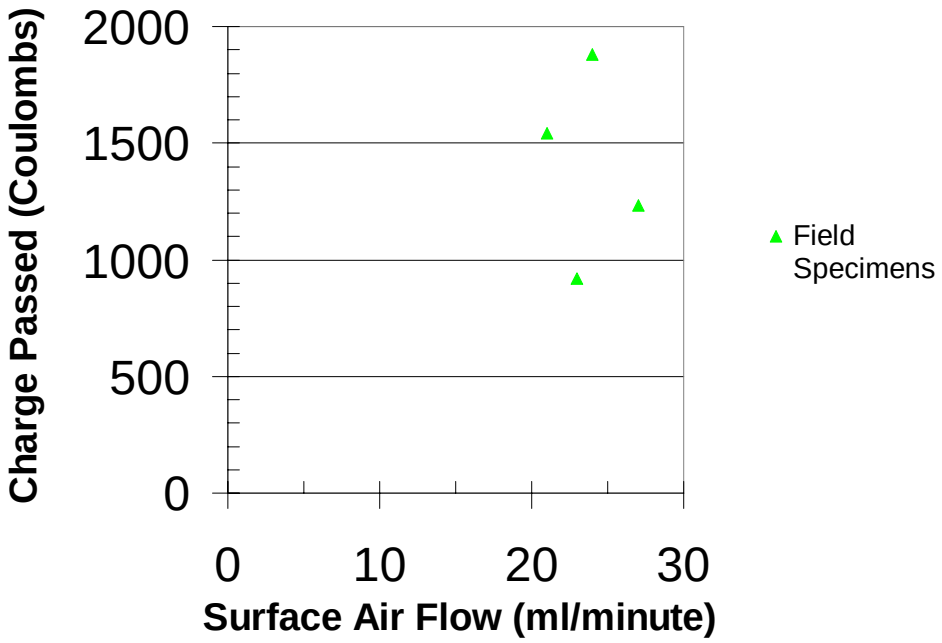

Figure 7.30. Surface air flow and charge passed for field specimens.

7.6.1 Model Prediction of Field Results

Although the field data does not follow the same form as the laboratory data, the laboratory established models may be able to predict field results. Inferences concerning the mean value of y, ASTM C 1202-97 measures, for a given setting of the independent variable, slab resistivity, can be made by constructing confidence intervals also known as confidence bands. For a given resistivity measurement the confidence interval indicates the range of expected mean values for passed charge and initial current. Prediction intervals, or bands, give an estimate of an expected value of a new observation of y, for a given value of x, the independent variable. For a given resistivity value, the prediction interval indicates a range

of expected charge passed and initial current values. Confidence and prediction intervals were determined, at a the 5% significance level, for regression models used to describe slab resistivity and ASTM C 1202-97 measures, respectively, for the model based on HPCC and PPCC results, and the under 4000 coulombs model.

Figures 7.31 and 7.32 present the scatter diagrams for field data with laboratory established regression models using combined HPCC and PPCC results for slab resistivity, charge passed and initial current. The 95% confidence and prediction intervals for the regression models are also presented. Approximately half of the field data lie within the 95% prediction band. If the field and laboratory data were consistent we would expect about 95% of the new observations to fall within the prediction band. The inability of the laboratory based models to predict the full range of field results may be a result of the type of mineral admixture used in the field mixture. The laboratory mixtures have a higher w/cm ratio as compared to the field mixture, which may also play a role in the predictive capabilities.

The maximum value of charge passed, and initial corresponding to the upper *moderate* penetrability limit is 4000 coulombs and approximately 100 mA, respectively. The 95 % prediction interval indicates a resistivity value of at least 25 kΩ-cm, and 30 kΩ-cm respectively, is needed to insure the in-place total charge passed and initial current are under the minimum desired value.

Figures 7.33 and 7.34 present the scatter diagrams for field data with laboratory established regression models based on a charge passed under 4000 coulombs for slab resistivity, charge passed and initial current. The 95% confidence and prediction intervals for the regression models are also presented. The majority of field data lie outside the 95% confidence interval for both the total charge passed and initial current based models. Only two of the six field data points lie within the 95% prediction band for the under 4000 charge passed models. The 95 % prediction intervals indicate a resistivity value of at least 20 kΩ-cm, and 30 kΩ-cm respectively, is needed to insure the in-place total charge passed and initial current are under the minimum desired value. In all cases the laboratory models consistently overestimate the field resistivity-total charge relationship.

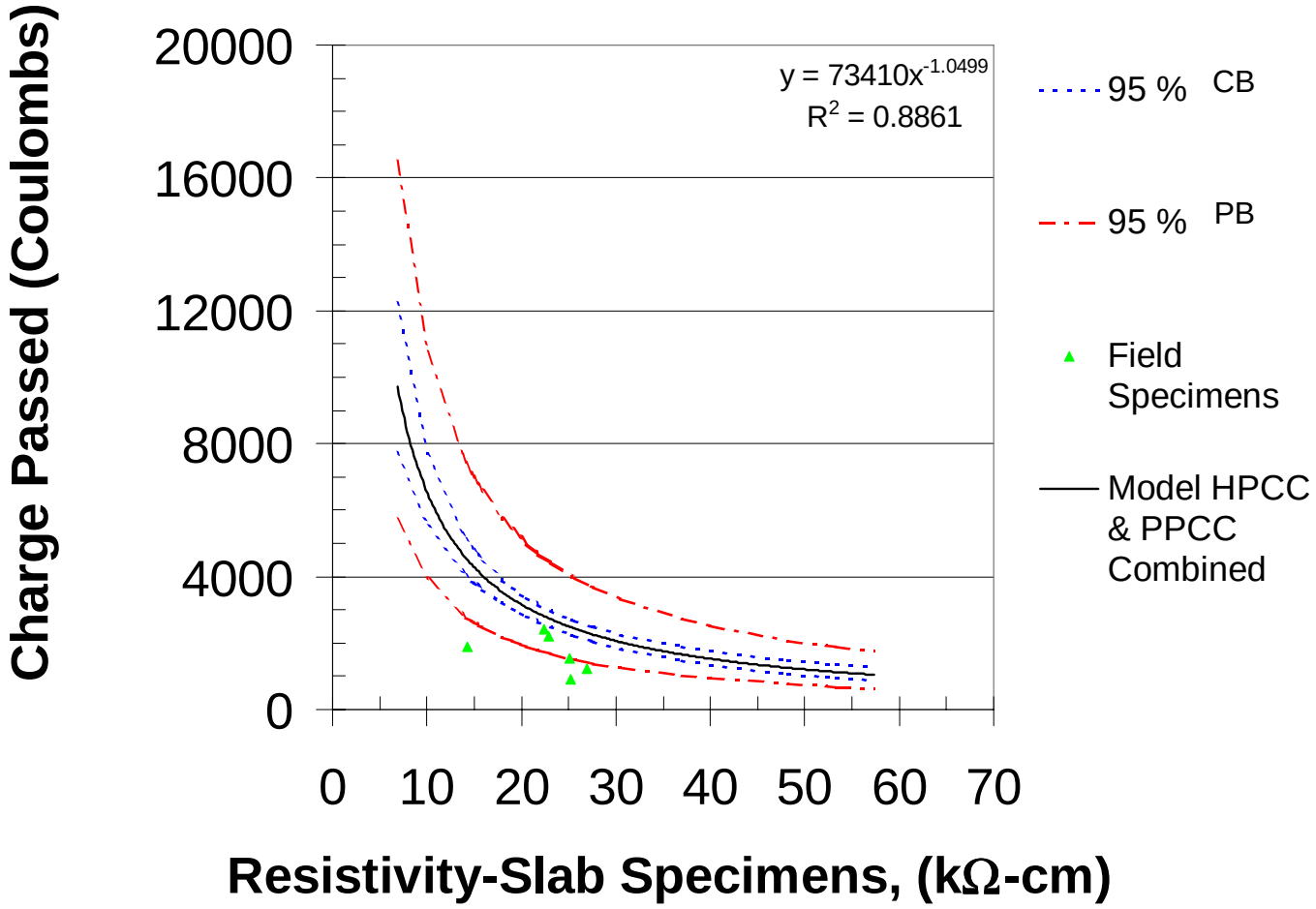

Figure 7.31. Slab resistivity and charge passed for field specimens compared with combined model (HPCC and PPCC).

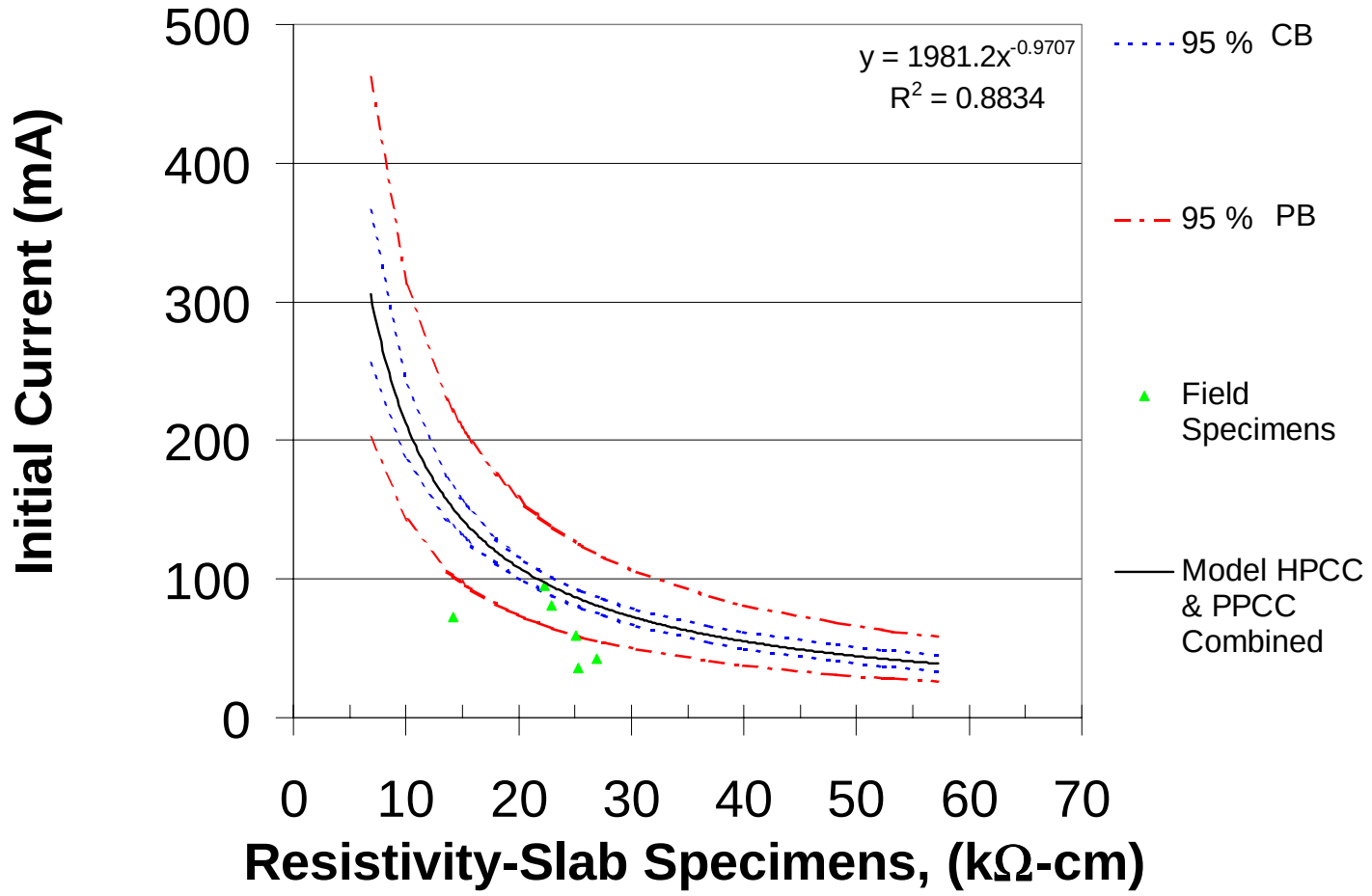

Figure 7.32. Slab resistivity and initial current for field specimens compared with combined model (HPCC and PPCC).

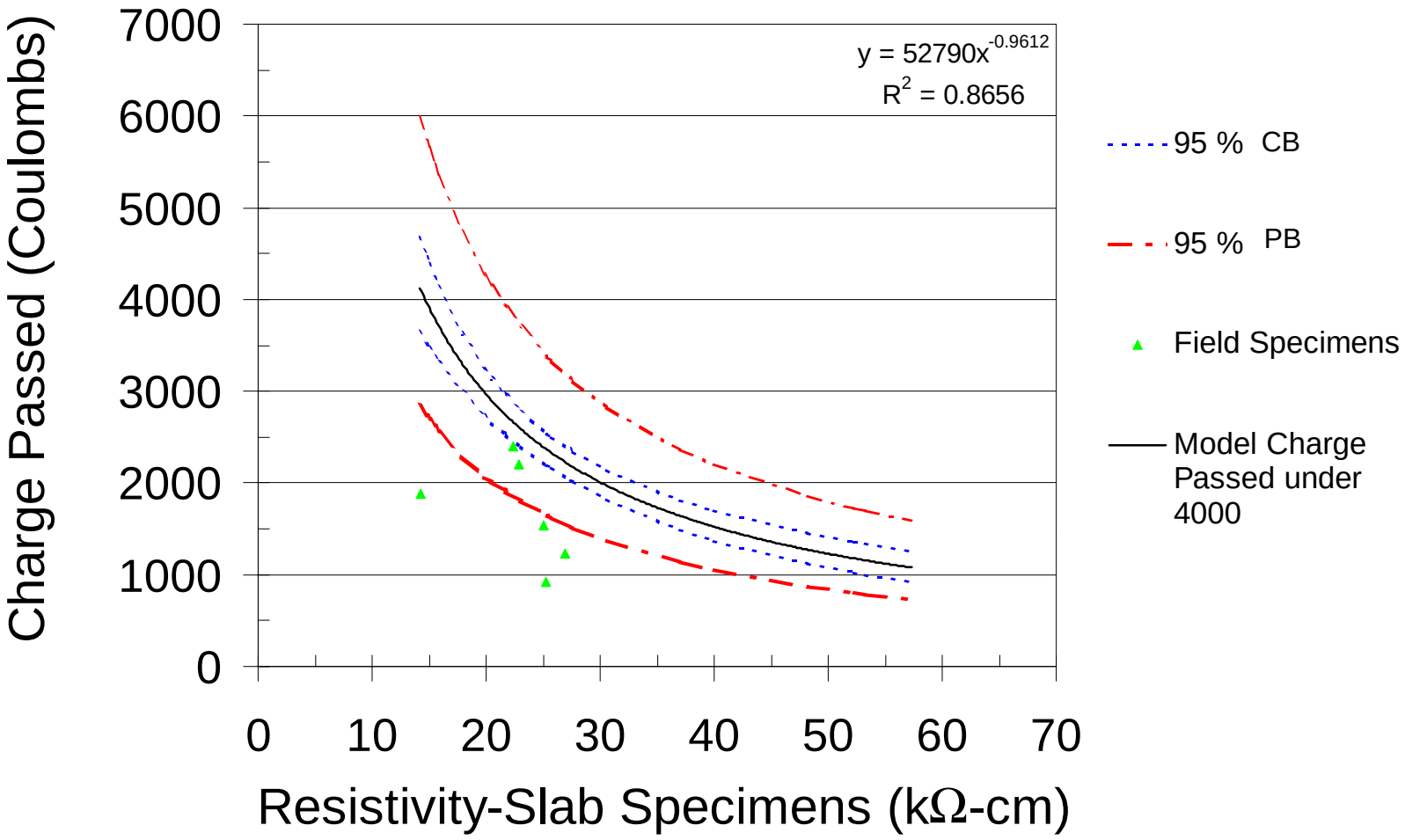

Figure 7.33. Slab resistivity and charge passed for field specimens compared with model for charge passed under 4000.

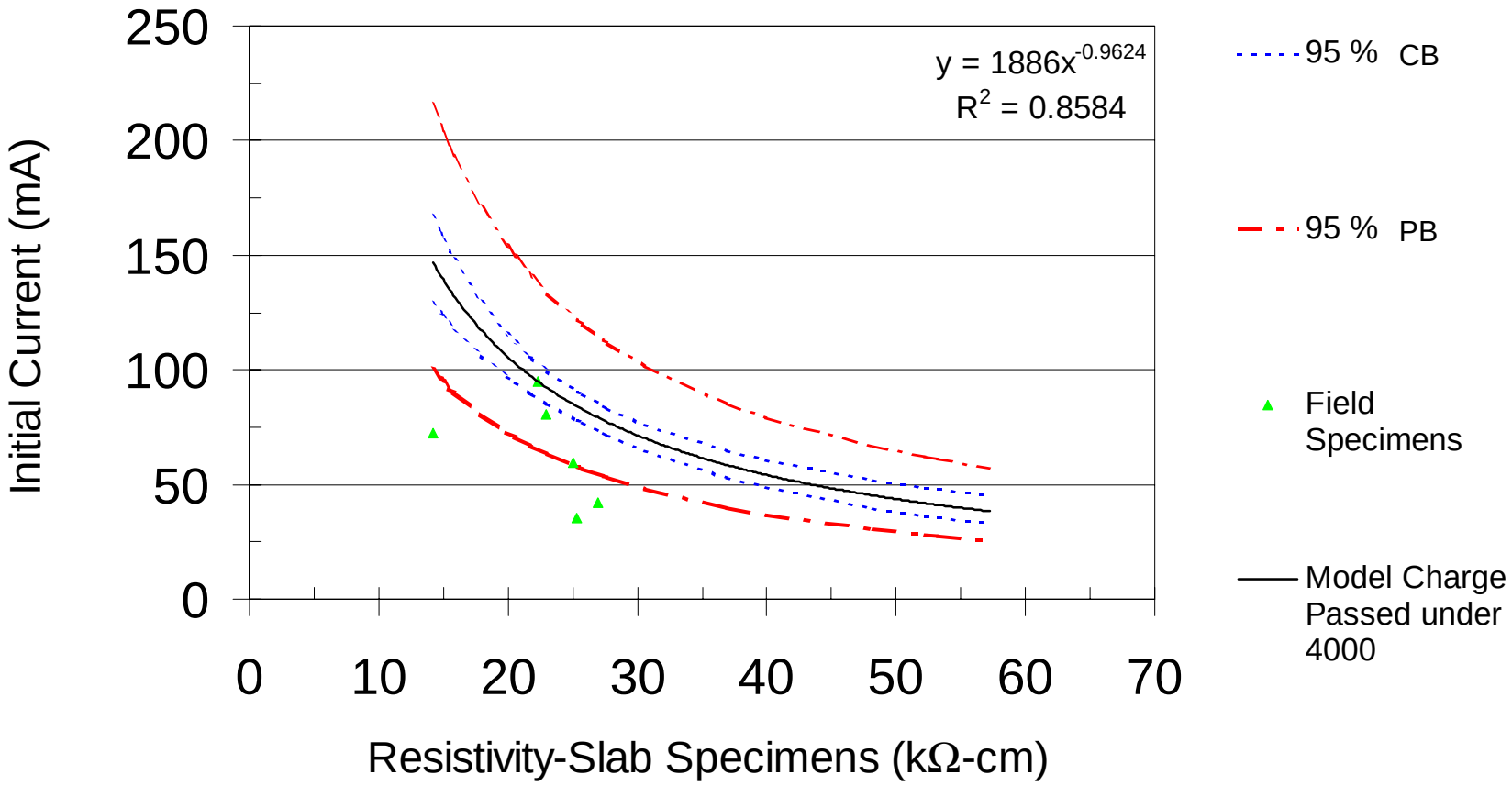

Figure 7.34. Slab resistivity and initial current for field specimens compared with model for charge passed under 4000.

CHAPTER 8. CONCLUSION AND RECOMMENDATIONS

8.1 SUMMARY

The primary objective of this study was to evaluate the effectiveness of in-place testing methods in assessing the present quality of concrete as determined by the standard permeation test method, ASTM C 1202-97. The secondary objective of this study was to investigate the effect of initial moist curing period on the development of strength and long-term permeability. This study investigated the in-place permeation properties of low permeability concrete bridge decks mixtures used in the Commonwealth of Virginia. Permeation properties were assessed in both the laboratory and in the field using 4-point Wenner array electrical resistivity, surface air flow (SAF), and chloride ion penetrability (ASTM C 1202-97).

The laboratory phase of this study investigated in-place permeability properties of six bridge deck mixtures representative of those used in the Commonwealth of Virginia. The three Plain Portland Cement Concrete (PPCC) laboratory mixtures contained aggregate types gravel (G), limestone (LS), and diabase (D), respectively. The remaining three concrete mixtures (HPCC) contained the diabase aggregate with supplementary cementitious materials: Microsilica (MS), Ground Granulated Blast-furnace Slag (SG), and Fly Ash (FA), respectively.

Laboratory test specimens consisted of two concrete slabs having dimensions of 280 x 280 x 102-mm (11 x 11 x 4-in) and twenty-six 102 x 204-mm (4 x 8-in) cylinders per concrete mixture. Thirteen cylinder specimens per concrete mixture underwent standard curing conditions in a saturated limewater bath. The simulated field-curing regime used wet burlap and plastic sheeting for 3 (3B) and 7 days (7B) respectively and was applied to slabs and cylinders.

Slab specimen were tested on finished surface using the SAF at 28 and 91 days, and 4-point electrical resistivity measurements at 1, 3, 7, 14, 28 and 91 days. Compressive strength (CS) tests were conducted at 7 and 28 days. Chloride ion penetrability tests were performed at 7, 28, and 91 days.

Statistical analyses were performed to assess the significance of the relationships for the following: Total charge passed and initial current (ASTM C 1202-97); 3B resistivity and 7B resistivity; Slab and cylinder resistivity; Slab resistivity and ASTM C-1202-97 (Total Charge and Initial current); and Surface Air Flow and ASTM C-1202-97.

The field portion of this research investigated the in-place permeation properties of a class 55 (A5) concrete mixture used for the Wilson Creek bridge project in Montgomery County Virginia. The field mixture used Metakaolin as a mineral admixture. Field cast specimens, test slabs and cylinders, were cast on-site during concrete bridge deck construction. The slab dimensions were 30.5 x 40.6 x 10.2 cm (12 x 16 x 4 in.), and the cylinders were 10.2 x 20.4 cm (4 x 8-in). In-situ SAF and resistivity measurements were taken on the bridge deck at 14, 42 and 91 days. In-place SAF and resistivity measurements on laboratory field cast slabs were taken at 7, 14, 42, 28 and 91-days. ASTM C 1202-97 specimens were prepared from field cast cylinders and tested at 7 and 28 and 42-days. The relationship between in-place permeation measures from field specimens was compared to laboratory data

8.2 CONCLUSIONS

1. No considerable differences were observed in 28-day compressive strength (Figure 7.2) and 28 and 91-day chloride ion penetrability (Figures 7.4 and 7.5) results in regard to differing curing regimes. All concrete mixtures used in the laboratory portion of this research exceeded the minimum specified compressive strength of 28 Mpa (4000-psi) under curing condition 3B, at 28 days. The electrical resistivity results confirm the previous conclusion in regard to differing curing regimes. There is no statistical difference at the 5% significance level between resistivity results obtained from 3B and 7B specimens (Figures 7.9 and 7.10).
2. A well defined relationship between initial current and charge passed was found for all laboratory mixtures used in this study (Figure 7.6). The initial current may be an effective method for assessing chloride ion penetrability properties of concrete in significantly less time than the current testing standard, while achieving similar precision. The results indicate an initial current of less than approximately 100 mA is needed to

achieve a total charge passed in the range of 2000 to 4000 coulombs. In order to be classified as a HPC, having a charge passed of less than 2500 coulombs, an initial current of less then 53 mA is recommended.

3. An inverse power function was found to describe the relationship between the electrical resistivity of concrete and ASTM C 1202-97 measures for all laboratory results. Regression analysis yielded models established from laboratory results for PPCC, HPCC, HPCC & PPCC combined, and under 4000 coulombs results (Figures 7.15 – 7.22). The combined HPCC & PPCC model and the model established for charge passed under 4000 coulombs are able to cover a wide range of concretes. In order to achieve a penetrability rating of under 4000 coulombs, the results indicate the in-place resistivity needs to be greater than 30 kΩ-cm. Two of the proposed regression models established from laboratory relationships were able to predict the full range of field results but only 30 to 50 % lie within the 95% prediction band (Figures 7.31 – 7.34). Electrical resistivity measurements may be able to give an indication of the present penetrability properties of as-built structures.

4. The SAF device lacked the sensitivity to describe the range of concretes used in this research (Figure 7.24). No quantitative relationship was found to exist between SAF and ASTM C 1202-97.

8.3 RECOMMENDATIONS FOR FUTURE RESEARCH

The use of electrical resistivity shows promise in assessing the in-place permeability properties of concrete elements. The inability of the laboratory based models to predict the full range of field results may be a related to the type of mineral admixture (Metakaolin) used in the field mixture. The laboratory mixtures have a higher w/cm ratio as compared to the field mixture, which may also play a role in the predictive capabilities. The following are suggestions for future research:

A. Correlation to Chloride Profiles from Ponding Tests

- Direct correlation of resistivity results with chloride profiles obtained from ponding tests.

A well defined relationship exists between electrical resistivity and ASTM C 1202-97 measures. The chloride ion penetrability test was originally correlated to chloride profiles obtained from ponding tests. The relationship between concrete resistivity and chloride profiles obtained from ponding test also needs investigation. This type of investigation may lead to direct correlation between concrete resistivity and level of in-place chloride contamination.

- Initial current and depth of chloride penetration from ponding tests

The testing standard, ASTM C 1202-97, requires a 6 hour time period in order to obtain the total charge passed. The initial current is an ASTM C 1202-97 output measured during the early stages of the test ($t < 30$ minutes). The underlying qualification of concretes by ASTM C 1202-97 is based on chloride profiles obtained from ponding tests. The ponding test-initial current relationship should be investigated. This investigation may provide a direct laboratory correlation between level of chloride resistance and initial charge, in significantly less time as compared to the current standard.

B. Investigation Into the Effects of Mixture Parameters on Concrete Resistivity

- Determine the effect of w/cm ratio on resistivity measurements

The electrical properties of concrete are dependent, in part, on the type of cementitious material, w/cm ratio and degree of hydration. The effect of mixture parameters such as w/cm ratio, water content, cement content, and other supplementary cementitious materials needs to be investigated. The penetrability properties of these concretes, weather based on total charge, initial current, or chloride profiles from ponding test should also be investigated. Findings from these investigations may produce different model coefficients (resistivity-penetrability models) based on mixture parameters and expand the predictive capacity of resistivity models.

C. Investigation on the effects of Initial Moist Curing Periods on Concrete Properties

- Effect of Initial Moist Curing Periods on Strength and Permeability

The effect of initial moist curing period on 28-day compressive strength and long-term permeability were investigated in the current study. The results indicate that increasing the initial moist curing time from 3 to 7 days has little effect on 28-day compressive strength or long-term permeability. The effect of initial moist curing times of 1, 3 and 7 day on concrete strength and permeability should be fully investigated. The effect of the amount cement on strength and permeability may also be of interest. This investigation should test parameters immediately at the end of initial moist curing period, when applicable, in addition to long-term testing (e.g. 28, 91, and 120 days) This investigation may lead to better understanding of affects of initial moist curing period on early-age and long-term parameters.

D. Field Investigations

- Field Investigation of As-Built Bridge Deck Structures

The laboratory established models were not consistent with the field data relationships. The laboratory based models consistently overestimated the field results. Additional research into the field application of in-place concrete resistivity measurements on as-built bridge deck elements is warranted. The investigation should include a variety of structures using similar mixture parameters to properly assess the variability in field measurements. The investigation should then move to quantify the relationship between resistivity and permeability for these mixtures, and compare the field relationship to laboratory established models. This methodology may also be extended to include deck elements cast using varying mixture parameters.

References

American Concrete Institute (2001), “Standard Practice for Curing Concrete (ACI 308-92).” ACI Manual of Concrete Practice, Part 2

Basheer PAM (1993). "Brief review of methods for measuring the permeation properties of concrete in-situ." Proceedings of the Institution of Civil Engineers, Structures and Buildings, 99(1), 74-83.

Berke, N. S., Pfeifer, D. W., and Weil T G (1988). "Protection Against Chloride-Induces Corrosion." Concrete International, 10(12), 45-55.

Clear K (2000). “Resistivity Charge-Passed and Apparent Chloride Diffusion Coefficient, Summary of Ken Clear’s Thoughts.”

Dhir R K, Byars EA, and Shaaban I G (1987). "Predicting Concrete Durability from its Absorption." American Concrete Institute, SP 145, 1177-1194.

Ewertson C and Petersson P E (1993). "Influence of curing conditions on the permeability and durability of concrete. Results from a field exposure test." Cement & Concrete Research, 23(3), 683-692.

Feldman Rolf F, Chan Gordon W, Brousseau Rejean J, and Tumidajski Peter J (1994). "Investigation of the rapid chloride permeability test." ACI Materials Journal, 91(3), 246-255.

Feldman R, Prudencio, Jr. L R, and Chan G (1999). “Rapid chloride permeability test of blended cement and other concretes” correlations between charge, initial current and conductivity.” Construction and Building Materials, 13, 149-154

FHWA (1997) *High Performance Concrete, State of The Art Report (1989 – 1994)*, Editors Zia, P., Ahmad, S., and Leming, M., FHWA-RD-97-030, U.S. Department of Transportation Federal Highway Administration, 1997

Figg J (1989). "Concrete Surface Permeability. Measurement and Meaning." Chemistry Industry (London), 21, 714-719.

Foster S W (1994). "High Performance Concrete, Stretching the Paradigm." Concrete International, 16(10), 33-34.

Goodspeed C H, Vanikar S, and Cook R A (1996). "High Performance Concrete Defined for Highway Structures." Concrete International, 18(2), 62-67.

Growers K R and Millard S G (1999). "Measurement of Concrete Resistivity for Assessment of Corrosion Severity of Steel Using Wenner Technique." ACI Materials Journal, 96(5), 536-541.

Hansson I L H and Hansson C M (1983). "ELECTRICAL RESISTIVITY MEASUREMENTS OF PORTLAND CEMENT BASED MATERIALS." Cement and Concrete Research, 13(5), 675-683.

Haque MN (1990). "Some Concretes Need 7 days Initial Curing." Concrete International, 42-46.

Hughes B P, Soleit A K O, and Brierley R W (1985). "New Technique For Determining The Electrical Resistivity of Concrete." Magazine of Concrete Research, 37(133), 243-248.

Khatri R P, Sirivivatn AV, and Gross W (1995). "Effect of different supplementary cementitious materials on mechanical properties of high performance concrete." Cement and Concrete Research, 25(1), 209-220.

Martys, N (1995). “Survey of Concrete Transport Properties and Their Measurement.” U S Department of Commerce, National Institute of Standards and Technology, NISTIR Report 5592

Marusin S L (1986). "MICROSTRUCTURE AND PORE CHARACTERISTICS OF CONCRETE CONTAINING CONDENSED SILICA FUME WITH A SUPERPLASTICIZER." Proceedings of the International Conference on Cement Microscopy 8th, 327-335.

Meletiou Constantine A, Tia Mang, and Bloomquist David (1992). "Development of a field permeability test apparatus and method for concrete." ACI Materials Journal, 89(1), 83-89.

Mehta K P (1990). Concrete Structure, Properties and Materials.

Millard S G and Growers K R (1992). "Resistivity assessment of in-situ concrete. The influence of conductive and resistive surface layers." Proceedings of the Institute of Civil Engineering and Structural Buildings, 94(4), 389-396.

Morris W, Moreno EI, and Sagues AA (1996). "Practical evaluation of resistivity of concrete in test cylinders using a Wenner array probe." Cement and Concrete Research, 26(12), 1779-1787.

Ozyildirim, C. (1998). " Permeability specifications for high-performance concrete decks." Transportation Research Record, 1610, 1-5.

Polder R B (2001). “Test methods for on site measurement of resistivity of concrete – a RILEM 7C—154 technical recommendation.” Construction and Building Materials 15, 125-131

Rasheeduzzafar A.S and Al-Saadoun, S. S. (1989). "Influence of Construction Practices on Concrete Durability." ACI Materials Journal, 86(6), 566-575.

Rengaswamy N S, Srinivasan S, Mahadeva Iyer Y, and Suresh Bapu R H (1986). "Non-Destructive Testing of Concrete by Electrical Resistivity Measurements." Indian Concrete Journal, 60(1), 23-27.

Roy D M, P W Brown, D Shi, and W May (1993). "Concrete Microstructure Porosity and Permeability." SHRP-C-628.

Russell H G (1999). "ACI Defines High Performance Concrete." Concrete International Technical Committee.

Saricimen H, Maslehuddin M, Al-Tayyib AJ, and Al-Mana AI (1995). "- Permeability and durability of plain and blended cement concretes cured in field and laboratory conditions." -ACI Materials Journal, 92(2), 111-116.

Schonlin K and Hilsdorf H (1987). “Evaluation of the effectiveness of curing of concrete structures.” Concrete Durability, Katharine and Bryant Mather International Conference, ACI-SP-100, 207-226.

Shi C, Stegemann JA, and Caldwell RJ (1998). "Effect of supplementary cementing materials on the specific conductivity of pore solution and its implications on the rapid chloride permeability test (AASHTO T277 and ASTM C1202) results." ACI Materials Journal, 95(4), 389-394.

Shilstone J M and Shilstone, Jr. J. (1993). "High Performance Concrete Mixtures for Durability." *High Performance Concrete in Severe Environments*, Edited by Zia, P, ACI-SP 140-14, 281-305.

Swamy RN (1996). "High Performance Durability Through Design." International Workshop on High Performance Concrete, ACI-SP 159-14, 209-230.

Tabor L J (1993). “Repair materials and techniques.” Durability of Concrete Structures, Investigation, repair, protection.” Edited by Geoff Mays, E & FN SPON, 99-100

Tashiro C, Ishida H, and Shimamura S (1987). "Dependence of the Electrical Resistivity on Evaporable Water Content in Hardened Cement Pastes." Journal of Material Science Letters, 6(12), 1379-1381.

The Concrete Society (1988). “Permeability testing of site concrete – a review of methods and experience.” Report of a Concrete Society working party, Concrete Society technical report no. 31

Torrent, R J (1992). “A two-chamber vacuum cell for measuring the coefficient of air permeability of the concrete on site.” Materials and Structure, 25, 358-365.

Wee T H, A K Suryavanshi, and S S Tin (2000). "Evaluation of Rapid Chloride Permeability Test (RCPT) Results for Concrete Containing Mineral Admixtures." ACI Materials Journal, 97(2), 221-232.

Whiting D (1983). “In-situ measurement of the permeability of concrete to chloride ions.” In-situ/Non-destructive testing of concrete, CANMET, ACI SP 82, 510-424.

Whiting D. and Cady P. D (1993) Condition Evaluation of Concrete Bridges Relative to Reinforcement Corrosion, Volume 7: Method for Field Evaluation of Concrete Permeability, Washington DC .

Wilson J G, Whittington H W, and Forde M C (1985). "Physical Interpretation of Microcomputer-Controlled Automatic Electrical Resistivity Measurements on Concrete." Non-Destructive Testing International, 18(2), 79-84.

VITA

James William Bryant, Jr. was born in Philadelphia, Pennsylvania in 1972. He attended Drexel University from 1990 to 1993 completing coursework toward a degree in Commerce and Engineering. In 1993 He transferred to North Carolina Agricultural and Technical State University, in Greensboro, NC, where he received a B. S. Degree in Civil Engineering. In 1996 James enrolled in the Civil and Environmental Engineering graduate program at Virginia Tech. He received his M. S. Degree in Civil and Environmental Engineering, with a concentration in Civil Infrastructure Systems in 1999. In 1999 he was selected as a National Science Foundation Graduate Research Trainee in Civil Infrastructure Systems. He will receive his Ph. D. in Civil and Environmental Engineering with a concentration in Construction Engineering & Management and Structural Materials. He has accepted an offer to work in private industry dealing with maintenance management of transportation infrastructure systems.